

Searches for anomalous interactions in rare kaon decays †

L G Landsberg

DOI: 10.1070/PU2006v049n08ABEH005836

Contents

| | |
|---|------------|
| 1. Introduction | 777 |
| 2. Lepton flavor violation in processes with charged leptons in the final states and kaon experiments | 779 |
| 3. Searches for new types of interactions in K-decays | 782 |
| 3.1 General remarks; 3.2 Lepton decays $K^+ \rightarrow l^+ \nu_l$; 3.3 Semileptonic decays $K^+ \rightarrow \pi^0 l^+ \nu_l$; 3.4 On certain mechanisms of anomalous interactions in K_{l3} - and K_{l2} -decays; 3.5 The decays $K^+ \rightarrow \pi^+ e^+ e^-$ and $K^+ \rightarrow \pi^+ \mu^+ \mu^-$; 3.6 Other data on anomalous scalar and tensor interactions | |
| 4. Direct nonconservation of CP-invariance in charged kaon decays | 793 |
| 4.1 Searches for CP-violation effects in the decays $K^\pm \rightarrow \pi^\pm \pi^+ \pi^-$ and $K^\pm \rightarrow \pi^\pm \pi^0 \pi^0$; 4.2 Searches for T-odd correlations in the decays $K^+ \rightarrow \pi^0 \mu^+ \nu_\mu$ and $K^+ \rightarrow \mu^+ \nu_\mu \gamma$ involving measurement of the transverse muon polarization $P_{\mu\perp}$; 4.3 Searches for T-odd correlations in the decay $K^+ \rightarrow \pi^0 \mu^+ \nu_\mu \gamma$ | |
| 5. Searches for new light particles produced in K-meson decays | 798 |
| 5.1 Decays of the type $K^+ \rightarrow \pi^+ + X$ and the limits on their branching fractions from the BNL E787 experiment; 5.2 Searches for light pseudoscalar goldstinos in K-decays with the ISTRA+ detector | |
| 6. Searches for the decay $K^+ \rightarrow \pi^+ + \gamma$ | 800 |
| 7. Experiments with ‘tagged’ π^0-mesons produced in K-decays | 801 |
| 7.1 Studies of the $\pi^0 \rightarrow e^+ e^-$ -decays in the KTeV experiment using $K_L^0 \rightarrow 3\pi^0$ -decays; 7.2 The upper limit on $BR(\pi^0 \rightarrow \nu\bar{\nu})$ from the BNL E949 experiment from an analysis of ‘tagged’ pions in the decay $K^+ \rightarrow \pi^+ \pi^0$; 7.3 Searches for decays $\pi^0 \rightarrow \mu^\pm e^\mp$ in the case of ‘tagged’ π^0 -mesons | |
| 8. Conclusion | 803 |
| 9. Appendices | 803 |
| 9.1 The IHEP superconducting separated channel of K^+ -mesons and the OKA detector; 9.2 Recent works | |
| References | 806 |

Abstract. Feasible searches for anomalous processes involving New Physics in rare decays of K-mesons are considered. Discussed are searches for lepton flavor nonconservation in kaon decays, searches for anomalous scalar, pseudoscalar, and tensor interactions, and searches for nonstandard processes violating T- (or CP-) invariance in the decays of charged K-mesons. Considered also are searches for new light particles (the P-sgoldstino) in kaon decays and studies involving ‘tagged’ π^0 -mesons produced in $K_L^0 \rightarrow 3\pi^0$ and $K^+ \rightarrow \pi^+ \pi^0$ decays, as well as a number of other phenomena. The prospects of future experiments in this field being carried out at new experimental facilities are discussed.

† The present review is the last work published by Leonid Grigor’evich Landsberg (1930–2005). Questions and comments concerning the article are to be addressed to the Editorial Board (e-mail: ufn@ufn.ru). (Editor’s comment.)

L G Landsberg State Scientific Center of Russian Federation ‘Institute for High Energy Physics’,
142281 Protvino, Moscow region, Russian Federation

Received 14 July 2005, revised 15 February 2006
Uspekhi Fizicheskikh Nauk **176** (8) 801–832 (2006)
Translated by G Pontecorvo; edited by A Radzig

1. Introduction

At present, high-energy physics is going through a very complicated, interesting, and important stage. Practically all available data are in agreement with the Standard Model (SM) which provides a good description of physical processes in the energy region up to several hundred gigaelectron-volts (GeV). At the same time, we know that owing to a number of internal contradictions the SM can only serve as a low-energy approximation to a more complete theory, and that with an increase in energy we are to expect an extremely rich region of new phenomena [the New Physics (NP)] such as, for example, the production of new heavy particles, additional dimensions of space, the substructure of quarks and leptons, and manifestations of novel types of interactions.

Let us recall the main aspects of the SM. The Standard Model involves three generations of fundamental fermions — quarks and leptons:

$$u, d, \nu_e, e \text{ (the first generation)}, \quad (1)$$

$$c, s, \nu_\mu, \mu \text{ (the second generation)}, \text{ and} \quad (2)$$

$$t, b, \nu_\tau, \tau \text{ (the third generation)}. \quad (3)$$

These fundamental families exhibit the same structure, but have significantly different masses.

Strong interactions between quarks are characterized by particular quantum numbers — quark flavors and colors — and are realized by exchanges of eight types of massless colored vector gluons. These interactions are described within the framework of the modern theory of strong processes — quantum chromodynamics (QCD), which at sufficiently small distances (smaller, than $1\text{--}2\text{ GeV}^{-1}$) makes it possible to carry out reliable perturbative calculations accounting for the main logarithmic and the next-to-leading order approximation. The color quantum numbers of quarks and gluons render them nonobservable in a free state (the concept of confinement). Strong interactions conserve quark flavors: in such processes, quarks cannot transform into quarks of other flavors and can only undergo rearrangement into various combinations, undergo pair ($q\bar{q}$) production, or annihilate via like pairs.

Electroweak interactions, in which both quarks and leptons are involved, are carried by the intermediate vector bosons W^\pm , Z and the photon γ . An important part in weak interactions should also apparently be played by the scalar Higgs bosons H_0 , predicted by the SM but which, however, have not yet been observed. As we shall see below, the weak interactions of charge currents, carried by the W^\pm -bosons, change the quark flavors.

Let us now consider in greater detail the electroweak interactions of fundamental fermions, $SU(2)_L \times U(1)$. The interaction Lagrangian contains left-handed quarks and leptons grouped into weak isospin doublets:

$$\begin{pmatrix} \nu_e \\ e^- \end{pmatrix}_L, \quad \begin{pmatrix} \nu_\mu \\ \mu^- \end{pmatrix}_L, \quad \begin{pmatrix} \nu_\tau \\ \tau^- \end{pmatrix}_L, \quad (4)$$

$$\begin{pmatrix} u \\ d' \end{pmatrix}_L, \quad \begin{pmatrix} c \\ s' \end{pmatrix}_L, \quad \begin{pmatrix} t \\ b' \end{pmatrix}_L, \quad (5)$$

and right-handed quark and lepton singlets, q_R and l_R , respectively. Left- and right-handed fermions can be represented as

$$\psi_L = \frac{1}{2}(1 - \gamma_5)\psi, \quad \psi_R = \frac{1}{2}(1 + \gamma_5)\psi. \quad (6)$$

Electroweak interactions between quarks and leptons are realized by exchanges of the heavy gauge intermediate bosons W^\pm and Z^0 and of massless photons. These interactions are described by the Lagrangian

$$L[SU(2)_L \times U(1)] = L_{CC} + L_{NC}. \quad (7)$$

The density L_{CC} of the Lagrangian is determined by the charged weak ($V-A$)-current:

$$L_{CC} = \frac{g}{2\sqrt{2}}(J_\mu^+ W^{-\mu} + J_\mu^- W^{+\mu}), \quad (8)$$

where

$$J_\mu^+ = \bar{u}\gamma_\mu(1 - \gamma_5)d' + \bar{c}\gamma_\mu(1 - \gamma_5)s' + \bar{t}\gamma_\mu(1 - \gamma_5)b' + \bar{\nu}_e\gamma_\mu(1 - \gamma_5)e + \bar{\nu}_\mu\gamma_\mu(1 - \gamma_5)\mu + \bar{\nu}_\tau\gamma_\mu(1 - \gamma_5)\tau. \quad (9)$$

These interactions are determined by the exchange of intermediate W^\pm -bosons and involve a change in quark flavors.

The density L_{NC} of the neutral current Lagrangian has the form

$$L_{NC} = e J_\mu^{\text{em}} A^\mu + \frac{g}{2\cos\vartheta_W} J_\mu^0 Z^\mu, \quad (10)$$

where J_μ^{em} is the vector electromagnetic current, and J_μ^0 represents the weak neutral current with $(V-A)$ - and $(V+A)$ -components:

$$J_\mu^{\text{em}} = \sum_f Q_f \bar{f}\gamma_\mu f, \quad J_\mu^0 = \sum_f \bar{f}\gamma_\mu(v_f - a_f\gamma_5)f. \quad (11)$$

Here, $v_f = T_3^f - 2Q_f\sin^2\vartheta_W$ and $a_f = T_3^f$ are the respective coefficients of the vector and axial components of the neutral weak current; $\sin^2\vartheta_W = 0.23147 \pm 0.00016$ is the sine squared of the Weinberg angle; $g^2/8M_W^2 = G_F/\sqrt{2}$ is the Fermi weak interaction coupling constant, while Q_f and T_3^f are the electric charge and the third component of the weak isospin of the fermion f .

The expressions of the weak quark charged currents contain transformed components of the ‘down’ quarks d' , s' , and b' , determined via the Cabibbo–Kobayashi–Maskawa unitary quark mixing matrix V_{CKM} :

$$\begin{pmatrix} d' \\ s' \\ b' \end{pmatrix} = V_{\text{CKM}} \begin{pmatrix} d \\ s \\ b \end{pmatrix} = \begin{pmatrix} V_{ud} & V_{us} & V_{ub} \\ V_{cd} & V_{cs} & V_{cb} \\ V_{td} & V_{ts} & V_{tb} \end{pmatrix} \begin{pmatrix} d \\ s \\ b \end{pmatrix}. \quad (12)$$

The quark mixing matrix depends on the three mixing angles ϑ_{12} , ϑ_{13} , ϑ_{23} ($s_{ij} = \sin\vartheta_{ij}$; $c_{ij} = \cos\vartheta_{ij}$) of the quark generations, and on the nontrivial phase δ determining CP-violation in quark processes.

Thus, the SM provides a detailed description of processes taking place in the quark sector, of quark mixing, and of the change in quark flavors in weak decays.

At the same time, the situation in the lepton sector of the SM remained different for a long time. Leptons of the three different generations were characterized by the lepton flavors L_e , L_μ , and L_τ . The weak interactions of leptons were described by the SM Lagrangian in which the neutrinos were considered massless particles, and lepton flavors were assumed to be conserved.

It must be noted that the conservation of lepton flavors was not due to some new global gauge symmetries such as $U(1)$, as happens, for example, with the conservation of electric charge, which is caused by the gauge symmetry of electromagnetic interactions. Therefore, the issue of possible lepton flavor nonconservation always remained open. Of great interest also was the issue of total lepton charge conservation:

$$L = L_e + L_\mu + L_\tau.$$

Here, first of all, the possibility of observing such processes as the double neutrinoless β -decay $(Z, A) \rightarrow (Z+2, A) + 2e^-$, the decays $K^+ \rightarrow \pi^- l^+ l^+$, or neutrinoless muon conversion into electrons of opposite sign, $\mu^- + (Z, A) \rightarrow e^+ + (Z-2, A)$, is intended.

One of the most important recent achievements in elementary particle physics has turned out to be the direct observation of neutrino oscillations in experiments with atmospheric and solar neutrinos [1, 2], at reactors [3] and, possibly, at an accelerator [4]. The hypothesis of neutrino oscillations was first put forward by B Pontecorvo in 1957 [5] (see also the review [6], in which the evolution of ideas concerning neutrino oscillations is discussed). The observation of neutrino oscillations signifies that neutrinos of different fundamental generations have different masses, and that lepton flavors are not rigorously conserved quantum numbers. Therefore, neutrinos mix with each

other and transform into each other. The observation of neutrino oscillations brought to an end the perennial searches for these effects and opened a new direction in the studies of neutrino physics and of the properties of lepton flavors.

Although neutrino oscillations do not fit into the general SM picture, their actual observation did not result in the necessity of revising the fundamental properties of this theory. It turned out to be sufficient just to somewhat modify the SM by introducing terms corresponding to neutrino masses and to the nonconservation of lepton flavors into its Lagrangian. This gives rise to the neutrino mixing matrix which is close in form to the CKM-matrix of quark mixing. The neutrino mixing matrix is known as the Pontecorvo–Maki–Nakagawa–Sakata (PMNS, see Refs [5–8]) matrix. However, while quark mixing leads to an enormous number of new effects in the SM quark sector, the neutrino mixing matrix may, generally speaking, exhibit a significantly more limited character. It may even be possible that neutrino oscillations will turn out to be the sole experimentally observable manifestation of the nonconservation of lepton flavors. If neutrinos are Majorana particles, then double neutrinoless β -decay with $|\Delta L| = 2$ may turn out to be the other observable effect. This issue is discussed in greater detail in the next section.

There exist two ways of studying regions of very high energies, where we expect manifestations of NP.

(1) The direct way based on experiments at supercolliders, in which we hope to observe new physical effects directly: the production of new heavy particles, quark substructure, additional dimensions of space, new types of interaction, etc. At present, such experiments are being carried out with the CDF and D0 facilities at the Fermilab collider Tevatron ($p\bar{p}$ -interactions at the energy $\sqrt{s} = 1.96$ TeV). But there are high hopes related to the new high-luminosity collider LHC at CERN (pp -interactions at $\sqrt{s} = 14$ TeV). This collider is to be commissioned in 2007.

(2) Indirect studies relying on the observation of new phenomena in rare decays in which certain effects are sensitive to the energy scale, not accessible even to supercolliders of the next generation.

At present, rapid developments are under way in studies on B-decays using the BaBar (Stanford, USA) and Belle (KEK, Japan) facilities — antisymmetric colliding beams of the e^+e^- storage rings. Also, to be expected in the future are studies at the collider B-factory LHCb (CERN, Switzerland). But, of special interest here are new experiments with K-mesons, where the high intensity of kaon beams together with their sufficiently long lifetime, will permit achieving maximum sensitivity to the partial widths of such anomalous decay processes.

A very important part of the program for the investigation of rare kaon decays comprises studies of the $K \rightarrow \pi\nu\bar{\nu}$ - and $K_L^0 \rightarrow \pi^0 l^+ l^-$ -decays. These studies have been discussed in detail in previous reviews by the author [9] and will not be considered here.

2. Lepton flavor violation in processes with charged leptons in the final state and kaon experiments

We will now look at the manifestations of lepton flavor violation in processes involving charged leptons (referred to as LFV-processes). The $\mu \rightarrow e\gamma$ -decay, for example, repre-

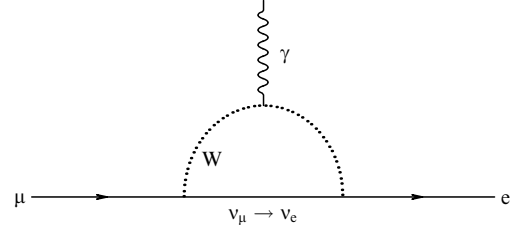


Figure 1. Diagram of the $\mu \rightarrow e\gamma$ -decay stemming from the neutrino mixing mechanism.

sents such an LFV-process. As follows from Fig. 1, at first sight it seems that this decay could occur via the diagram with neutrino oscillations. However, owing to the small neutrino masses, the neutrino mixing mechanism results in the $\mu \rightarrow e\gamma$ decay having a very small probability, since it will be suppressed by factors $(m_{\nu_i}/M_W)^4$ [10, 11]. The $\mu \rightarrow e\gamma$ decay probability is estimated as

$$\text{BR}(\mu \rightarrow e\gamma) = \frac{\Gamma(\mu \rightarrow e\gamma)}{\Gamma(\mu \rightarrow e\bar{\nu}_e\nu_\mu)} \simeq \frac{3}{32} \frac{\alpha}{\pi} \left| \sum_i U_{\mu i}^* U_{ei} \left(\frac{m_{\nu_i}}{M_W} \right)^2 \right|^2. \quad (13)$$

Here, the following notation is used:

$$\nu_\mu = \sum_i U_{\mu i} \nu_i, \quad \nu_e = \sum_i U_{ei} \nu_i, \quad (14)$$

where ν_i represent neutrino states with mass and lepton flavor eigenvalues, ν_μ , ν_e are neutrino states produced in muon and electron processes (they are not characterized by definite values of masses and lepton flavors). Then, for $m_{\nu_i} < 1$ eV, $\text{BR}(\mu \rightarrow e\gamma) \lesssim 10^{-48}$. A similar situation also occurs in the case of other LFV-processes with charged leptons.

All the same, within the general idea of the search for New Physics beyond the SM, searching for such forbidden LFV-decays involving charged leptons, viz. $\mu \rightarrow e\gamma$, $\mu \rightarrow 3e$, $K_L^0 \rightarrow e\bar{\mu}$, $K^+ \rightarrow \pi^+\mu^+e^-$, and others, is of extreme interest, and during the past several decades such studies have been carried out in many experiments with a continuously increasing accuracy. Actually, none of these processes has been observed yet. The upper limits established for them are presented in Table 1 [12–22] and in Fig. 2 [23] (in which the history of such searches is also demonstrated).

The significant interest in LFV-processes involving charged leptons is due to the fact that their observation would clearly go beyond the existing SM framework and would essentially require SM revision. The actual observation of lepton flavor violation in neutrino oscillations doubtless enhances the interest in such searches. As we shall see below, if LFV-decays do occur, then they are usually manifested at such small distances (for such high energy scales) that will remain inaccessible even to supercolliders of future generations. The investigation of rare anomalous decays apparently provides the only possibility of appreciating such a region of very high energies.

Lepton flavor violation in processes with charged leptons may occur in very different phenomena, such as:

- (a) purely leptonic decays $\mu \rightarrow e\gamma$, $\mu \rightarrow 3e$, etc.;
- (b) neutrinoless conversion of muons into electrons: $\mu^- + (Z, A) \rightarrow e^- + (Z, A)$. Here, various processes are possible — both purely leptonic and those with the participa-

Table 1. Upper limits on BR in LFV-processes [12–24].

| Process | Upper limit for BR (90% C.L.) | References | Prospects |
|--|-------------------------------|------------|---|
| $K_L^0 \rightarrow e^\mp \mu^\pm$ | 4.7×10^{-12} | [12] | |
| $K_L^0 \rightarrow \pi^0 e^\mp \mu^\pm$ | 3.3×10^{-10} | [13] | |
| $K_L^0 \rightarrow e^\mp e^\mp \mu^\pm \mu^\pm$ | 4.12×10^{-11} | [13] | |
| $K^+ \rightarrow \pi^+ \mu^+ e^-$ | 1.2×10^{-11} | [14] | CKM $\sim 10^{-12}$ (NA48/3) |
| $K^+ \rightarrow \pi^+ \mu^- e^+$ | 5.2×10^{-10} | [15] | |
| $K^+ \rightarrow \pi^- e^+ e^+$ | 6.4×10^{-10} | [15] | |
| $K^+ \rightarrow \pi^- e^+ \mu^+$ | 5.0×10^{-10} | [15] | |
| $K^+ \rightarrow \pi^- \mu^+ \mu^+$ | 3.0×10^{-9} | [15] | |
| $\Xi^- \rightarrow \pi^- \mu^+ \mu^+$ | 4.0×10^{-8} | [16] | PSI 10^{-14} [24] MECO 10^{-17} [23, 24] |
| $\mu \rightarrow e \gamma$ | 1.2×10^{-11} | [17] | |
| $\mu \rightarrow 3e$ | 1.0×10^{-12} | [18] | |
| $\Gamma(\mu^- + \text{Ti} \rightarrow e^- + \text{Ti})$ | 4.3×10^{-12} | [19] | |
| $\bar{\Gamma}(\mu^- + \text{Ti} \rightarrow \text{capture})$ | | | |
| $\tau \rightarrow e \gamma, \mu \gamma, 3l$ | $< 10^{-6} - 10^{-7}$ | [20–22] | |

tion of quarks of the first generation of fundamental particles: $d \rightarrow de\bar{\mu}$;

(c) hadron–lepton transitions of the type $s \rightarrow de\bar{\mu}$ with the participation of fundamental fermions of the first and second generations. Such are decays of strange particles: $K_L^0 \rightarrow \mu^\pm e^\mp$, $K_L^0 \rightarrow \pi \mu^\pm e^\mp$;

(d) processes involving violation of the total lepton number $L = L_e + L_\mu + L_\tau$: the neutrinoless double β -decay

$$(A, Z) \rightarrow 2e^- + (A, Z + 2),$$

and the decays $K^+ \rightarrow \pi^- l^+ l^+$.

All these processes may manifest totally different LFV-mechanisms: thus, for example, lepton–quark LFV-pro-

cesses may be due to the exchange of ‘horizontal’ X-bosons or to the exchange of leptoquarks (Fig. 3a, b).

At present, several new ambitious projects have been proposed that may increase the sensitivity of searches for muonic LFV-processes by several orders of magnitude [to achieve $\text{BR}(\mu \rightarrow e\gamma) \sim 10^{-14}$ and, in the future, at neutrino factories — $\text{BR}(\mu \rightarrow e\gamma)$ and $\text{BR}(\mu \rightarrow 3e) \sim 10^{-15} - 10^{-16}$]. The new technique of superconducting magnetic traps was proposed for studies of coherent $\mu - e$ conversion on nuclei in order to achieve ratios $\Gamma(\mu^- + (Z, A) \rightarrow e^- + (Z, A)) / \Gamma(\mu^- \rightarrow \text{capture}) \sim 10^{-17}$ (and, maybe, even 10^{-19}). The program of these new searches for muonic LFV-processes and relevant theoretical hypotheses are discussed in Refs [23, 24] and in the references cited therein. At the same time, certain pessimism has been voiced concerning the possibility of further enhancement of the accuracy in searches for LFV-processes in rare kaon decays.

It should be emphasized that decays of the type $s \rightarrow de\bar{\mu}$ exhibit a unique feature rendering them different from processes such as $d \rightarrow de\bar{\mu}$ (neutrinoless muon conversion into electrons) or from purely leptonic transitions with lepton flavor violation: $\mu \rightarrow e\gamma$, $\mu \rightarrow 3e$, etc.

It is precisely in kaon LFV-decays that quarks and leptons of various generations participate, so compensation for the change in generation in the quark sector becomes possible in them by a corresponding change in generation in the lepton sector. This trivial possibility has been discussed many times, but in the clearest manner it is formulated in Ref. [25] where the quantum numbers G were introduced in order to characterize the SM fundamental generations, and where classification of various processes was carried out in accordance with possible changes in this quantum number, $\Delta G = G_{\text{fin}} - G_{\text{in}}$ (see Table 2 and Fig. 3a).

If only transitions between fermions of the first two generations are considered then purely phenomenologically it is possible to introduce arbitrary quantum numbers differing from each other for these generations: for example, $G_1 = 2$ for the first generation, and $G_2 = 1$ for the second (in the case of antifermions $G_1 = -2$ and $G_2 = -1$). Then, as can be seen from Table 2, it is possible to separate all the processes considered into different classes corresponding to the value of the change ΔG in the respective transitions.

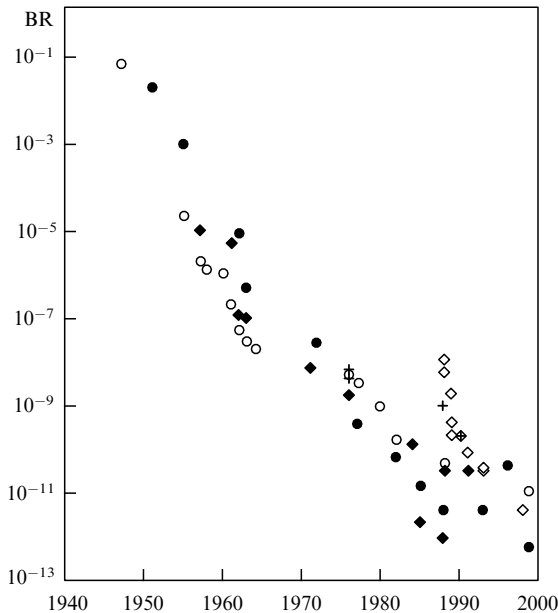


Figure 2. Time trace of the sensitivity of experiments on the search for lepton flavor violation in processes with muons and kaons [23]. Muon processes: \circ — ($\mu \rightarrow e\gamma$), \blacklozenge — ($\mu \rightarrow 3e$), and \bullet — ($\mu^- + A \rightarrow e^- + A$); kaon processes: \diamond — ($K_L^0 \rightarrow e\bar{\mu}$), and $+$ — ($K^+ \rightarrow \pi^+ e\bar{\mu}$). It can be seen from these data that the experimental sensitivity in searches for LFV-processes has undergone continuous enhancement (on the average, by two orders of magnitude every decade).

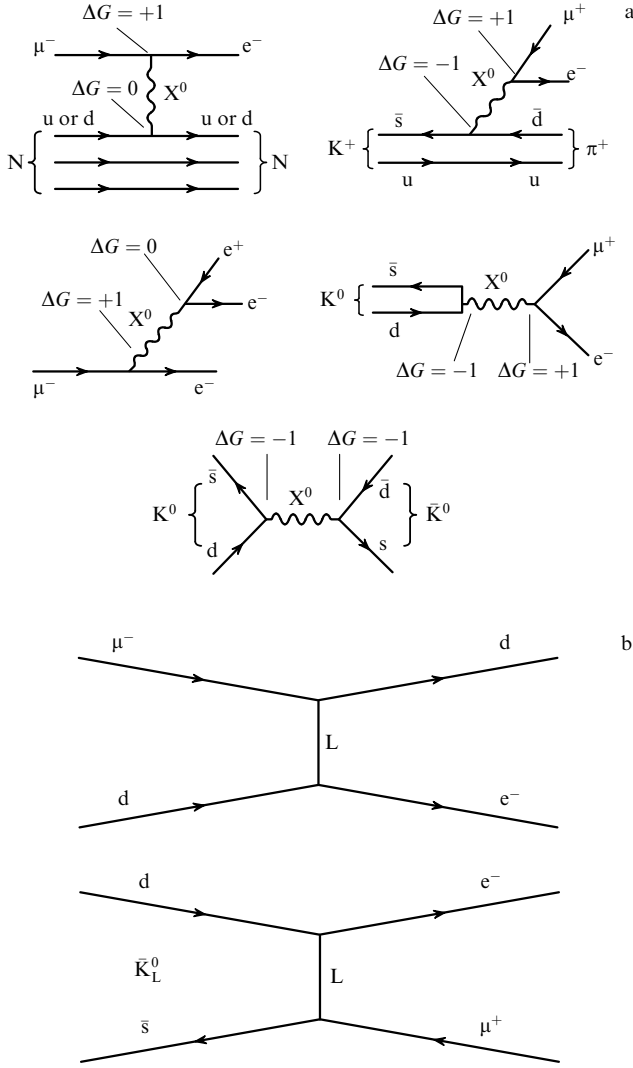


Figure 3. (a) Operation of selection rules for the quantum numbers G of SM fundamental fermion generations in the mechanism involving the exchange of 'horizontal' bosons X^0 . (b) The process of neutrinoless $\mu \rightarrow e$ -conversion $\mu^- + (A, Z) \rightarrow e^- + (A, Z)$ (top) and the $K_L^0 \rightarrow e\bar{\mu}$ -decay (bottom).

The physical concept of the quantum number G is not yet quite clear. Evidently, the peculiar properties of kaon LFV-decays and their unique capabilities will manifest themselves only if the selection rule for ΔG is sufficiently stringent. Then, certain kaon LFV-decays corresponding to $\Delta G = 0$ may exhibit higher probabilities than other processes for which, at best, $|\Delta G| = 1$.

Let us now illustrate the concept of generations of SM fundamental fermions with quantum numbers G that are conserved in the first approximation, taking advantage, as an example, of the dynamic model in a space with additional dimensions, developed in works [26]. We shall briefly highlight the main aspects of this model:

(A) The space with additional dimensions is characterized by the metric $M^4 \times S^2$, i.e., it corresponds to four-dimensional Minkowski space with an additional two-dimensional manifold compactified on a sphere of radius R . Fundamental fermions in this six-dimensional space form a unique generation which is subsequently reduced into three generations of SM fundamental fermions (1) that fill up different regions of the multidimensional space and are characterized by quantum numbers G_i of the generations, which in the first approximation are conserved. These quantum numbers correspond to certain angular momenta in the space of the sphere. In this case, the first generation of fundamental fermions is characterized by the value of $G_1 = 2$, the second by $G_2 = 1$, and the third by $G_3 = 0$ (the signs of G change for the respective antifermions).

(B) A distinctive feature of this model consists in decays involving lepton flavor violation, the probabilities of which are determined by the structure of space, i.e., the mass scale of compactification of the additional dimensions $1/R$ and by the Kaluza – Klein structures for gauge bosons.

(C) Owing to the relatively weak mixing between the SM fundamental generations, the probabilities of processes with $|\Delta G| \neq 0$ are strongly suppressed.

Thus, if the concept of fundamental generations with quantum numbers G conserved in the first approximation is actually valid and if the selection rule for $|\Delta G|$ imposes strong restrictions on the probabilities of the respective processes, then further searches for kaon LFV-decays acquire utmost importance.

Studies of kaon LFV-decays are complementary to searches for muonic LFV-processes and may exhibit very

Table 2. Selection rule for the quantum number G for the generation of SM fundamental fermions (see also Fig. 3a).

| | | |
|------------------------|------------------|--|
| First-order processes | $\Delta G = 0$ | $K^+ \rightarrow \pi^+ \mu^+ e^-$, $K_L^0 \rightarrow e^\mp \mu^\pm$, $K_L^0 \rightarrow \pi^0 e^\mp \mu^\pm$ |
| Second-order processes | $ \Delta G = 1$ | $\mu \rightarrow 3e$, $\mu \rightarrow e\gamma$, $\mu^- + N \rightarrow e^- + N$ |
| Third-order processes | $ \Delta G = 2$ | $K^0 \rightleftharpoons \bar{K}^0$ ($\Delta M = M(K_L^0) - M(K_S^0)$), $\mu^- e^+ \rightarrow \mu^+ e^-$, $K^+ \rightarrow \pi^+ \mu^- e^+$ |

Note. A few examples of the operation of the selection rule for ΔG :

(a) $K^+ \rightarrow \pi^+ \mu^+ e^-$: $(\bar{s}u) \rightarrow (u\bar{d})\mu^+ e^-$,

$$G_{in} = -1 + 2 = +1, \quad G_{fin} = 0 + (-1) + 2 = +1, \quad \Delta G = G_{fin} - G_{in} = 0;$$

(b) $K^0 \rightarrow e^- \mu^+$: $(\bar{s}d) \rightarrow e^- \mu^+$,

$$G_{in} = +1, \quad G_{fin} = +1, \quad \Delta G = 0;$$

$$K^0 \rightarrow e^+ \mu^-: \quad G_{in} = +1, \quad G_{fin} = -1, \quad \Delta G = -2;$$

$$\bar{K}^0 \rightarrow e^- \mu^+: \quad \Delta G = +2;$$

$$\bar{K}^0 \rightarrow e^+ \mu^-: \quad \Delta G = 0;$$

(c) $\mu^- + N \rightarrow e^- + N$: $G_{in} = +1 + G(N)$, $G_{fin} = +2 + G(N)$, $\Delta G = +1$;

(d) $K^0 \rightleftharpoons \bar{K}^0$: $G_{in} = +1$, $G_{fin} = -1$, $\Delta G = -2$.

if mainly decays with $\Delta G = 0$ occur, then

$$K_L^0 \simeq K_2^0 = \frac{1}{\sqrt{2}}(K^0 - \bar{K}^0) \rightarrow e^\mp \mu^\pm,$$

$$\hookrightarrow e^- \mu^+ \hookrightarrow e^+ \mu^-$$

but the matrix element of each of these decays contains the additional factor of $1/2$;

high, and even record, sensitivity in certain other models with approximately conserved quantum numbers of the fundamental fermion generations [27].

Naturally, models with approximate conservation of the quantum number of fundamental generations only exemplify one of the theories with possible lepton flavor violation. Lepton flavor violation in processes involving charged leptons may be of a very complex character and contributions to it may be due to many other mechanisms for which purely leptonic processes ($\mu \rightarrow e\gamma$, $\mu \rightarrow 3e$, $\tau \rightarrow 3\mu$, $\tau \rightarrow \mu + \gamma$, etc.) exhibit an even higher sensitivity than the kaon decays. In the case of mixed quark–lepton processes $s \rightarrow d\bar{u}e$ and $d \rightarrow \bar{u}e$, a detailed study of the relative capabilities provided by various mechanisms (with selection for the quantum number of generations, exchange of leptoquarks, etc.) would prove extremely interesting. And, finally, an important role may be played by processes with violation of the total lepton charge L , such as neutrinoless double β -decay $Z \rightarrow (Z+2) + 2e^-$, or such unusual processes as $K^+ \rightarrow \pi^- \mu^+ \mu^+$.

In any case, it must be stressed that the unique properties of kaon LFV-decays, related to the concept of partially conserved quantum numbers G of the generations of SM fundamental fermions and to the selection rules for $\Delta G = 0$, make it very important to perform new generation experiments on studying rare K-decays at accelerators in operation and under construction with average energies ranging 25–120 GeV in kaon beams of the highest intensities. It is necessary to create new experimental facilities providing maximum speed and maximum redundancy in determining the kinematics of events dealt with, so as to suppress the background and enhance the sensitivity of experiments by 2–4 orders of magnitude as compared with the data compiled in Table 1. These extremely difficult experiments must be considered an independent and complementary part of the general program of searches for lepton flavor violation in processes with charged leptons. All these issues were discussed in detail in Ref. [27].

3. Searches for new types of interactions in K-decays

3.1 General remarks

Searches for new types of weak interactions related, for instance, to the exchange of new intermediate bosons — scalar (S), pseudoscalar (P), tensor (T), right-handed vector W_R — to processes with leptoquarks and to other mechanisms are of utmost interest owing to the possible existence of a New Physics going beyond the framework of the Standard Model. In the SM, $(V-A)$ -interaction due to the exchange of intermediate vector bosons W^\pm is known to take place in the case of charged weak currents.

In this section, we shall consider leptonic and semileptonic decays of K-mesons:

$$K^+ \rightarrow l^+ \nu_l, \quad (15)$$

$$K^+ \rightarrow \pi^0 l^+ \nu_l. \quad (16)$$

In these processes, leptons are described by the spinors u_l , and antileptons by the spinors \bar{v}_l (the production of l^+ is described by the spinor v_l , and the production of $\bar{\nu}_l$ by the spinor \bar{u}_l).

The matrix elements of decays (15) and (16) have the form

$$M(K^+ \rightarrow l^+ \nu_l) = \frac{G_F}{\sqrt{2}} |V_{us}| \langle 0 | H_w | K^+ \rangle \langle \bar{u}_l 0_\alpha \nu_l \rangle \quad (17)$$

and

$$M(K^+ \rightarrow \pi^0 l^+ \nu_l) = \frac{G_F}{\sqrt{2}} |V_{us}| \langle \pi^0 | H_w | K^+ \rangle \langle \bar{u}_l 0_\alpha \nu_l \rangle. \quad (18)$$

Here, V_{us} is an element of the matrix V_{CKM} . We shall consider the most general type of Lorentz-covariant matrix elements accounting for all sorts of interactions.

In this case, leptons form Lorentz-covariant Dirac structures $\bar{u}_l 0_\alpha \nu_l$:

$$\left. \begin{aligned} S^l &= \bar{u}_l \nu_l && (\text{scalar}), \\ P^l &= \bar{u}_l \gamma_5 \nu_l && (\text{pseudoscalar}), \\ T^l &= \bar{u}_l \sigma_{\alpha\beta} \nu_l = \bar{u}_l \frac{i}{2} (\gamma_\alpha \gamma_\beta - \gamma_\beta \gamma_\alpha) \nu_l && (\text{tensor}), \\ V^l &= \bar{u}_l \gamma_\mu \nu_l && (\text{vector}), \\ A^l &= \bar{u}_l \gamma_5 \gamma_\mu \nu_l && (\text{axial}). \end{aligned} \right\} \quad (19)$$

We shall restrict ourselves to the approximation in which neutrinos are dealt with as two-component particles (the neutrino masses are negligible), only the left-handed components of which participate in weak interactions, i.e., the neutrinos are present in the matrix element as $(1/2)(1 - \gamma_5)u_\nu$ or as $\bar{u}_\nu(1/2)(1 + \gamma_5)$.

The matrix elements $\langle 0 | H_w | K^+ \rangle$ and $\langle \pi^0 | H_w | K^+ \rangle$ exhibit a structure determined by the possibilities of constructing them from the parameters of the problem. Thus, for example, one finds for $\langle 0 | H_w | K^+ \rangle$:

$$\left. \begin{aligned} \langle 0 | V | K^+ \rangle &= 0 \\ \langle 0 | S | K^+ \rangle &= 0 \end{aligned} \right\}, \quad \begin{aligned} &\text{since } K^+ \text{ is a pseudoscalar,} \\ &\text{it is not possible to construct a vector} \\ &\text{and a scalar from the parameters} \\ &\text{of the problem;} \end{aligned}$$

$$\left. \begin{aligned} \langle 0 | A | K^+ \rangle &\propto \varphi_K P_K^z \\ \langle 0 | P | K^+ \rangle &\propto \varphi_K M_K \\ \langle 0 | T | K^+ \rangle &\propto \varphi_K P_K^z P_K^\beta \end{aligned} \right\} \quad \begin{aligned} &\text{the only possible} \\ &\text{axial, pseudoscalar, and} \\ &\text{pseudotensor constructed from} \\ &\text{the parameters of the problem.} \end{aligned}$$

Here, φ_K is everywhere a pseudoscalar function of the K^+ -meson, normalized to $1/\sqrt{2M_K}$. Then, we obtain

$$\begin{aligned} M(K^+ \rightarrow l^+ \nu_l) &= |V_{us}| \left\{ \frac{G_F}{\sqrt{2}} \varphi_K P_K^z [\bar{u}_l (1 + \gamma_5) \gamma_\alpha \nu_l] + \right. \\ &\quad + \frac{G_P}{\sqrt{2}} \varphi_K M_K [\bar{u}_l (1 + \gamma_5) \nu_l] \\ &\quad \left. + \frac{G_T}{\sqrt{2}} \varphi_K P_K^z P_K^\beta [\bar{u}_l (1 + \gamma_5) \sigma_{\alpha\beta} \nu_l] \right\}. \end{aligned}$$

Here, G_P and G_T are coupling constants of anomalous pseudoscalar and tensor interactions.

Since $P_K^\alpha P_K^\beta$ is a symmetric tensor, and $\sigma_{\alpha\beta}$ is an antisymmetric tensor, then summation over α, β results in the tensor term becoming zero and not contributing to the matrix element of the decay $K^+ \rightarrow l^+ \nu_l$, i.e., we find ultimately that

$$\begin{aligned} M(K^+ \rightarrow l^+ \nu_l) &= \frac{G_F}{\sqrt{2}} |V_{us}| \varphi_K P_K^z [\bar{u}_l (1 + \gamma_5) \gamma_\alpha \nu_l] \\ &\quad + \frac{G_P}{\sqrt{2}} |V_{us}| \varphi_K M_K [\bar{u}_l (1 + \gamma_5) \nu_l]. \end{aligned} \quad (20)$$

For the matrix element to be written in a covariant form, the structures $\langle 0|H_w|K^+\rangle$ and $\langle \bar{u}_\nu v_\mu|H_w|0\rangle$ must be made consistent with each other, so as to make possible summation over such indices as α for the respective components $\langle 0|H_w|K^+\rangle^\alpha$, $\langle \bar{u}_\nu v_\mu|H_w|0\rangle_\alpha$, etc.

Thus, $M(K^+ \rightarrow l^+ \nu_l)$ in its general form may have axial (A) and pseudoscalar (P) components [and only the axial part in the SM with $(V-A)$ -interactions].

A similar analysis for $M(K^+ \rightarrow \pi^0 l^+ \nu_l)$ reveals that in the general case this matrix element may have vector (V), scalar (S), and tensor (T) components [and only the vector component in the SM with a weak $(V-A)$ -interaction].

We shall make one more comment in connection with the sensitivity of experiments on searching for new types of interactions, which could manifest themselves, for example, in the decays $K^+ \rightarrow l^+ \nu_l$ and $K^+ \rightarrow \pi^0 l^+ \nu_l$. The amplitude of each of these processes can be represented as

$$A = A_{\text{SM}} + A_{\text{NP}} = |A_{\text{SM}}| + |A_{\text{NP}}| \exp(i\varphi),$$

where A_{SM} is the amplitude of the process in the Standard Model, A_{NP} is the amplitude due to new interactions, and φ is their relative phase. Therefore, one has

$$\begin{aligned} |A|^2 &= |A_{\text{SM}}|^2 + |A_{\text{NP}}|^2 + 2 \operatorname{Re}(A_{\text{SM}} A_{\text{NP}}^*) \\ &= |A_{\text{SM}}|^2 + |A_{\text{NP}}|^2 + 2 \cos \varphi |A_{\text{SM}}| |A_{\text{NP}}| \\ &\simeq |A_{\text{SM}}|^2 \left(1 \pm \underbrace{\frac{|A_{\text{NP}}|}{|A_{\text{SM}}|}}_{\text{IT}} \right) \end{aligned} \quad (21)$$

(estimated under the assumption that $2|\cos \varphi| = \pm 1$). Thus, corrections due to new interactions are determined by the interference term IT, which is inversely proportional to the mass squared of the respective intermediate boson ($\text{IT} \sim M_{\text{boson}}^{-2}$). Experiments of this type turn out to be more sensitive to new interactions than, for example, processes with lepton flavor violation ($\mu^- + (A, Z) \rightarrow e^- + (A, Z)$, $K^0 \rightarrow e\bar{\mu}$, etc.), the probabilities of which equal $|A|^2 \simeq |A_{\text{NP}}|^2 \sim M_{\text{boson}}^{-4}$.

One must, however, bear in mind that in certain cases the interference term may contain an additional smallness. For instance, in the decay $K^+ \rightarrow \pi^0 l^+ \nu_l$, as we shall see below, owing to the matrix character of the vector and scalar (tensor) amplitudes and owing to summation over lepton spins in the final state, the interference term turns out to be proportional to the mass m_l of the charged lepton, and in the case of $K^+ \rightarrow \pi^0 e^+ \nu_e$ decays it becomes negligible. Then, new interactions will only manifest themselves in the component $|A_{\text{NP}}|^2$.

3.2 Lepton decays $K^+ \rightarrow l^+ \nu_l$

The matrix element of the decay $K^+(P_K) \rightarrow l^+(P_l) + \nu_l(P_\nu)$ takes the form

$$\begin{aligned} M &= \frac{G_F}{\sqrt{2}} |V_{us}| \langle l^+ \nu_l | H_w | 0 \rangle \langle 0 | H_w | K^+ \rangle = M_{\text{SM}} + M_{\text{NP}} \\ &= \frac{G_F}{\sqrt{2}} |V_{us}| \varphi_K P_K^\alpha [\bar{u}_\nu (1 + \gamma_5) \gamma_\alpha v_l] \\ &\quad + \frac{G_P}{\sqrt{2}} |V_{us}| \varphi_K M_K [\bar{u}_\nu (1 + \gamma_5) v_l]. \end{aligned} \quad (22)$$

Further transformation of formula (22) is carried out with the aid of the Dirac equation. The following notation is introduced for this equation:

$$\hat{P} = P^\alpha \gamma_\alpha. \quad (23)$$

The Dirac equation for the spinor u has the form

$$(\hat{P} - m)u = 0, \quad \bar{u}(\hat{P} - m) = 0, \quad (24)$$

and for the antispinor v we have the following form

$$(\hat{P} + m)v = 0, \quad \bar{v}(\hat{P} + m) = 0. \quad (25)$$

Introducing the notation $P_K^\alpha = q_\nu^\alpha + q_l^\alpha$, $\varphi_K = f_K / \sqrt{2M_K}$, where $f_K = (159.8 \pm 1.5) \text{ MeV}$ is the K -decay constant determined from experimental data (see [28]), we arrive at

$$\begin{aligned} M(K^+ \rightarrow l^+ \nu_l)_{\text{SM}} &= \frac{G_F}{\sqrt{2}} f_K \frac{|V_{us}|}{\sqrt{2M_K}} \\ &\quad \times [q_\nu^\alpha \bar{u}_\nu (1 + \gamma_5) \gamma_\alpha v_l + \bar{u}_\nu (1 + \gamma_5) q_l^\alpha \gamma_\alpha v_l] \\ &= \frac{G_F}{\sqrt{2}} f_K \frac{|V_{us}|}{\sqrt{2M_K}} [\bar{u}_\nu \hat{q}_\nu (1 - \gamma_5) v_l + \bar{u}_\nu (1 + \gamma_5) \hat{q}_l v_l] \\ &= \frac{G_F}{\sqrt{2}} f_K \frac{|V_{us}|}{\sqrt{2M_K}} [-m_l \bar{u}_\nu (1 + \gamma_5) v_l] \end{aligned} \quad (26)$$

($\bar{u}_\nu \hat{q}_\nu = 0$, $\hat{q}_l v_l = -m_l v_l$). The $K^+ \rightarrow l^+ \nu_l$ -decay width equals

$$\begin{aligned} \Gamma(K^+ \rightarrow l^+ \nu_l) &= (2\pi)^4 \int \frac{d^3 P_l}{2E_l} \frac{d^3 P_\nu}{2E_\nu} \frac{1}{(2\pi)^6} |M_{\text{SM}}|^2 \\ &\quad \times \delta^4(P_K - q_l - q_\nu). \end{aligned} \quad (27)$$

The conventional technique for calculating $M^* M$ (see Ref. [28]) gives

$$|M_{\text{SM}}|^2 = \frac{G_F^2}{2} |V_{us}|^2 f_K^2 \frac{m_l^2}{2M_K} 8q_l q_\nu.$$

Then, one obtains

$$\Gamma(K^+ \rightarrow l^+ \nu_l)_{\text{SM}} = \frac{G_F^2}{8\pi} f_K^2 |V_{us}|^2 M_K m_l^2 \left(1 - \frac{m_l^2}{M_K^2} \right)^2. \quad (28)$$

As can be seen from formula (28) and from Fig. 4a, the $K_l^+ \rightarrow l^+ + \nu_l$ -decay probability in the SM is strongly suppressed due to helicity conservation ($\Gamma \sim m_l^2$).

It is also possible to find the ratio of the decay probabilities:

$$\begin{aligned} R(K^+ \rightarrow l^+ \nu_l)_{\text{SM}} &= \frac{\text{BR}(K^+ \rightarrow e^+ \nu_e)}{\text{BR}(K^+ \rightarrow \mu^+ \nu_\mu)} \Big|_{\text{SM}} \\ &= \frac{m_e^2 (M_K^2 - m_e^2)^2}{m_\mu^2 (M_K^2 - m_\mu^2)^2} (1 + \delta_r) \\ &= 2.569 \times 10^{-5} (1 - 0.0378 \pm 0.0004) \\ &= (2.472 \pm 0.0010) \times 10^{-5}. \end{aligned} \quad (29)$$

Here, δ_r is the radiative correction calculated with a high precision [29]. Making use of the data for $\tau(K^+)$, $\text{BR}(K^+ \rightarrow \mu^+ \nu_\mu)$ (see Ref. [20]) and this value of

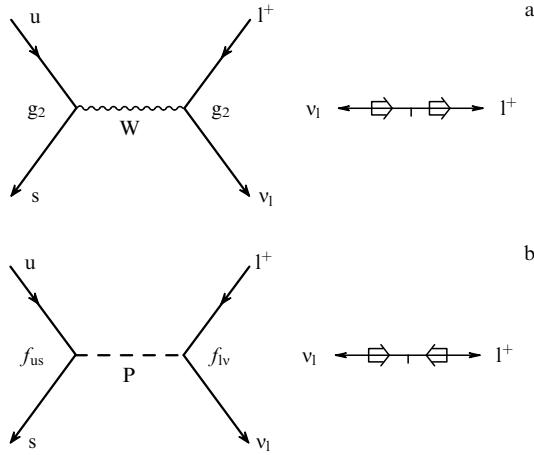


Figure 4. The decay $K^+ \rightarrow l^+ \nu_l$ in different models. (a) Diagram for the $K^+ \rightarrow l^+ \nu_l$ -decay in the SM [($V-A$)-interaction] involving an exchange of the vector W -boson. The Fermi interaction coupling constant is $G_F = g_2^2/4\sqrt{2}M_W^2$. The decay $K^+ \rightarrow l^+ \nu_l$ is suppressed by helicity conservation (the spin of the K^+ -meson is zero): amplitudes with helicity violation are proportional to the factor m_l . (b) Diagram for the $K^+ \rightarrow l^+ \nu_l$ -decay in the model with anomalous pseudoscalar weak interaction with the coupling constant $G_{UD}^{lv} = f_{lv}f_{UD}/4\sqrt{2}M_P^2$. For this interaction, the decay is no longer suppressed by helicity conservation. M_P is the mass of the pseudoscalar intermediate boson — the carrier of anomalous pseudoscalar interaction.

$R(K^+ \rightarrow l^+ \nu_l)_{SM}$, we arrive at the prediction of the Standard Model for the relative probability and width of the rare decay $K^+ \rightarrow e^+ \nu_e$:

$$BR(K^+ \rightarrow e^+ \nu_e)_{SM} = (1.570 \pm 0.005) \times 10^{-5}, \quad (30)$$

$$\Gamma(K^+ \rightarrow e^+ \nu_e)_{SM} = (0.834 \pm 0.003) \times 10^{-18} \text{ MeV}.$$

Note also that if $(\mu - e)$ -universality is violated, then formula (29) must be multiplied by the factor $(g_e^K/g_\mu^K)^2$ determining such violation, namely

$$R(K^+ \rightarrow l \nu_l) = R(K^+ \rightarrow l \nu_l)_{SM} \left(\frac{g_e^K}{g_\mu^K} \right)^2 \quad (31)$$

$[g_e^K$ and g_μ^K are the respective electroweak coupling constants for the kaon decays; in the case of $(\mu - e)$ -universality one has $g_e^K = g_\mu^K$].

On the other hand, if the pseudoscalar interaction did take place, then the decay $K^+ \rightarrow l^+ \nu_l$ would not be helicity-suppressed (Fig. 4b) and its probability would be determined by the expression

$$\Gamma(K^+ \rightarrow l^+ \nu_l)_{PS} = \frac{G_{PS}^2}{8\pi} f_K^2 M_K M^2 \left(1 - \frac{m_l^2}{M_K^2} \right)^2, \quad (32)$$

where M is a certain constant with the dimension of mass. Here, the constant G_{PS} of pseudoscalar interaction was determined by analogy with $G_F = g_2^2/4\sqrt{2}M_W^2$ and has the same dimensionality. The factor M^2 ensures the correct dimension in formula (32). Pseudoscalar interactions between quark and lepton currents are considered in greater detail in Ref. [30], where the respective constants are determined as $(G_{UD}^{lv})_{PS} = f_{lv}f_{UD}/4\sqrt{2}M_P^2$, while f_{lv} , f_{UD} are the coupling constants of interactions of leptons and quarks with intermediate pseudoscalar bosons of mass M_P

($U = u, c, t$ are the ‘up’ quarks; $D = d, s, b$ are the ‘down’ quarks). In Ref. [30], the mass factor M had the form $M = M_K^2/(m_u + m_s)$, where $m_u = 5 \text{ MeV}$, $m_s = 150 \text{ MeV}$ are the current masses of the quarks composing the K^+ -meson.

If pseudoscalar interaction did take place, then the probabilities of the $K^+ \rightarrow e^+ \nu_e$ - and $K^+ \rightarrow \mu^+ \nu_\mu$ -decays would be close to each other:

$$R(K^+ \rightarrow l^+ \nu_l)_{PS} \simeq \frac{(1 - m_e^2/M_K^2)^2}{(1 - m_\mu^2/M_K^2)^2} \simeq 1.1. \quad (33)$$

The small difference between them is explained by the decreased phase space in the case of the $K^+ \rightarrow \mu^+ \nu_\mu$ -decay.

Since the decay $K^+ \rightarrow e^+ \nu_e$ in the Standard Model is strongly suppressed by helicity conservation, it turns out to be especially sensitive even to a small admixture of pseudoscalar interaction. Now consider the amplitude of the decay $K^+ \rightarrow l^+ \nu_l$ to be due to $V-A$ contributions (Standard Model) and to anomalous PS-interaction:

$$A(K^+ \rightarrow l^+ \nu_l) = A(K^+ \rightarrow l^+ \nu_l)_{SM} + A(K^+ \rightarrow l^+ \nu_l)_{PS},$$

and, as discussed above, the inequality

$$A(K^+ \rightarrow \mu^+ \nu_\mu)_{SM} \gg A(K^+ \rightarrow e^+ \nu_e)_{SM}$$

is valid, while

$$A(K^+ \rightarrow \mu^+ \nu_\mu)_{PS} \simeq A(K^+ \rightarrow e^+ \nu_e)_{PS}.$$

Hence follows

$$R(K^+ \rightarrow l^+ \nu_l) = \frac{BR(K^+ \rightarrow e^+ \nu_e)}{BR(K^+ \rightarrow \mu^+ \nu_\mu)} \simeq R(K^+ \rightarrow l^+ \nu_l)_{SM} \left(1 \pm \frac{A_{PS}}{A_{SM}} \right). \quad (34)$$

Available experimental data give [20]

$$\begin{aligned} R(K^+ \rightarrow l^+ \nu_l)_{exp} &= \frac{(1.55 \pm 0.07) \times 10^{-5}}{0.6351 \pm 0.0018} \\ &= (2.441 \pm 0.110) \times 10^{-5} \\ &= R(K^+ \rightarrow l^+ \nu_l)_{SM} (0.987 \pm 0.045), \end{aligned} \quad (35)$$

which corresponds to

$$\Gamma(K^+ \rightarrow e^+ \nu_e)_{exp} = (0.824 \pm 0.037) \times 10^{-18} \text{ MeV}.$$

From formulas (34) and (35) it follows that the experimental limits on the contribution of pseudoscalar interaction to the decay $K^+ \rightarrow e^+ \nu_e$ amount to

$$|A(K^+ \rightarrow e^+ \nu_e)_{PS}| < 5.8 \times 10^{-2} |A(K^+ \rightarrow e^+ \nu_e)_{SM}|, \quad (36)$$

$$\begin{aligned} \Gamma(K^+ \rightarrow e^+ \nu_e)_{PS} &< 3.4 \times 10^{-3} \Gamma(K^+ \rightarrow e^+ \nu_e)_{SM} \\ &\simeq 3 \times 10^{-21} \text{ MeV}. \end{aligned}$$

In a number of works [see, for example, Ref. [30]] it was shown that

$$\begin{aligned} R(K^+ \rightarrow l^+ \nu_l) &= R(K^+ \rightarrow l^+ \nu_l)_{SM} \\ &\times \left[1 \pm \frac{|G_{us}^{ev}|_{PS}}{G_F V_{us}} \frac{M_K^2}{(m_s + m_u)m_e} \right]. \end{aligned} \quad (37)$$

Here, $|G_{us}^{ev}|_{PS}$ is the coupling constant of pseudoscalar interaction, connecting (us) and (ev) states (the contribution from pseudoscalar interaction to the $\pi^+ \rightarrow e^+ \nu_e$ -decay is determined by another coupling constant $|G_{ud}^{ev}|_{PS}$).

From formula (37) and the upper bound (36) it is possible to obtain experimental constraint on the constant

$$|G_{us}^{ev}|_{PS} < 3.6 \times 10^{-11} \text{ GeV}^{-2}.$$

In future studies in the IHEP separated kaon beam it will be possible to achieve a statistical measurement accuracy (taking into account the radiative correction) of $< 10^{-3}$. Systematic uncertainties may render this value somewhat less accurate, but it will be no worse than the existing measurement accuracy of the decay $\pi^+ \rightarrow e^+ \nu_e$, i.e., $< 3 \times 10^{-3}$. Thus, the sensitivity of searches for pseudoscalar interactions in the decay $K^+ \rightarrow e^+ \nu_e$ will amount to

$$\left. \begin{aligned} |A(K^+ \rightarrow e^+ \nu_e)_{PS}| &< (10^{-3} - 3 \times 10^{-3}) |A(K^+ \rightarrow e^+ \nu_e)_{SM}| \\ |A(K^+ \rightarrow e^+ \nu_e)_{PS}|^2 &< (10^{-6} - 10^{-5}) |A(K^+ \rightarrow e^+ \nu_e)_{SM}|^2 \end{aligned} \right\}, \quad (38)$$

or

$$\begin{aligned} \Gamma(K^+ \rightarrow e^+ \nu_e)_{PS} &< (10^{-6} - 10^{-5}) \Gamma(K^+ \rightarrow e^+ \nu_e)_{SM} \\ &\simeq (10^{-24} - 10^{-23}) \text{ MeV}. \end{aligned} \quad (39)$$

In accordance with formulas (36)–(39), this will correspond to the possible constraint for the pseudoscalar coupling constant [30]:

$$|G_{us}^{ev}|_{PS} < (0.6 - 2) \times 10^{-12} \text{ GeV}^{-2}. \quad (40)$$

The presently existing constraint for the other pseudoscalar constant, obtained from experimental studies of the $\pi^+ \rightarrow e^+ \nu_e$ -decay, amounts to $|G_{ud}^{ev}|_{PS} < 7 \times 10^{-12} \text{ GeV}^{-2}$.

Several circumstances make the decay $K^+ \rightarrow e^+ \nu_e$ especially sensitive and favorable when searching for pseudoscalar weak interactions:

(a) owing to helicity conservation this decay is strongly suppressed in the Standard Model with a weak ($V-A$)-interaction;

(b) the quantity

$$\begin{aligned} R(K^+ \rightarrow l^+ \nu_l)_{SM} &= \frac{\text{BR}(K^+ \rightarrow e^+ \nu_e)}{\text{BR}(K^+ \rightarrow \mu^+ \nu_\mu)} \Big|_{SM} \\ &= (2.472 \pm 0.001) \times 10^{-5} \end{aligned}$$

is predicted in the Standard Model with high precision. The radiative correction $\delta_R = -0.0378 \pm 0.0004$ [29] is also taken into account here;

(c) the quantity measured (the value of which is to be compared with theoretical predictions) in the two-particle decay $K^+ \rightarrow e^+ \nu_e$ is the decay probability. This simplifies searches for new weak interactions as compared, for example, with the decays $K^+ \rightarrow \pi^0 l^+ \nu_l$, where it is necessary to investigate the distribution of events over the Dalitz plot, taking into account the form factors $f_+(t)$ and $f_-(t)$;

(d) the process $K^+ \rightarrow e^+ \nu_e$ is much more sensitive to pseudoscalar interaction than, for example, the very rare decay $K_L^0 \rightarrow e^+ e^-$, which is also strongly suppressed in the Standard Model due to helicity conservation.

Since sensitive searches for new types of interactions require precision measurements of the ratio $R(K^+ \rightarrow l \nu_l)$,

the issue of systematic uncertainties in measurements of $K^+ \rightarrow e^+ \nu_e$ -decays is of utmost importance and, most of all, on examining background processes due, for example, to the decays $K^+ \rightarrow \pi^0 e^+ \nu_e$ and $K^+ \rightarrow e^+ \nu \gamma$ with lost photons.

Since the probability of the decay $K^+ \rightarrow \pi^0 e^+ \nu_e$ amounts to 5.1%, for measuring $R(K^+ \rightarrow l^+ \nu_l)$ with an accuracy of $\sim 10^{-3}$ it is necessary to suppress the background from the process $K^+ \rightarrow \pi^0 e^+ \nu_e$ with lost photons down to a level of $< 3 \times 10^{-7}$. Analysis of the operation of the guard system and of kinematic suppression of the background from the decay $K^+ \rightarrow \pi^0 e^+ \nu$ with two lost photons [by the missing mass $(P_K - P_e)^2$] revealed the potential of achieving in experiments with the OKA [Opyty (in Russian: experiments) with KAons] detector suppression of this background to the level of $< 2 \times 10^{-7}$ (i.e., $\sim 10^{-8}$ of the total decay probability of the K^+ -meson), which is quite sufficient for precision measurements of the probability ratio $R(K^+ \rightarrow l^+ \nu_l)$. The background from the process $K^+ \rightarrow l^+ \nu_l \gamma$ involving structural radiation (one lost photon) amounts to approximately the same value. The quantity $R(K^+ \rightarrow l^+ \nu_l)_{SM}$ in formula (34) actually represents the ratio

$$R(K^+ \rightarrow l^+ \nu_l(\gamma))_{SM} = \frac{\text{BR}(K^+ \rightarrow l^+ \nu_l(\gamma))_{SM}}{\text{BR}(K^+ \rightarrow \mu^+ \nu_\mu(\gamma))_{SM}},$$

where (γ) is soft bremsstrahlung, which is not registered in measurements. Since it is precisely the ratio $R(K^+ \rightarrow l^+ \nu_l(\gamma))$ that is determined in identical conditions for the decays $K^+ \rightarrow \mu^+ \nu_\mu$ and $K^+ \rightarrow e^+ \nu_e$, this radiation does not affect the measurement accuracy of possible deviations from predictions made using the Standard Model.

A more detailed discussion of the possibilities of measuring the decay $K^+ \rightarrow e^+ \nu_e$ in future experiments with the OKA facility is presented in Ref. [31].

3.3 Semileptonic decays $K^+ \rightarrow \pi^0 l^+ \nu_l$

The best data from studies of semileptonic decays of K-mesons have been obtained by the ISTRA+ Collaboration (see Fig. 5, where the layout of the experimental setup is presented, together with its main characteristics). As was already noted in Section 2.1, the matrix element of the semileptonic decay $K^+(P_K) \rightarrow \pi^0(P_\pi) + l^+(p_l) + \nu_l(p_\nu)$ has the form

$$M(K^+ \rightarrow \pi^0 l^+ \nu_l) = \frac{G_F}{\sqrt{2}} |V_{us}| \langle \bar{u}_\nu \nu_l | H_w | \pi \rangle \langle \pi | H_w | K^+ \rangle$$

(see Refs [32, 33]).

Here, the structure for $\langle \pi^0 | H_w | K^+ \rangle$ is determined by the possibilities of constructing them from the parameters of the problem. Thus, one finds

$$\left. \begin{aligned} \langle \pi^0 | A | K^+ \rangle &= 0, \\ \langle \pi^0 | P | K^+ \rangle &= 0, \end{aligned} \right\}$$

since in the case of the $|\text{pseudoscalar}\rangle \rightarrow |\text{pseudoscalar}\rangle$ transition it is not possible to construct an axial A and a pseudoscalar P from the parameters of the problem.

Further, it is believed that

$$\left. \begin{aligned} \langle \pi^0 | V | K^+ \rangle &\propto (P_K^\alpha \pm P_\pi^\alpha), \\ \langle \pi^0 | S | K^+ \rangle &\propto M_K, \\ \langle \pi^0 | T | K^+ \rangle &\propto \frac{i}{M_K} \sigma_{\alpha\beta} P_K^\alpha P_\pi^\beta, \end{aligned} \right\} \quad (41)$$

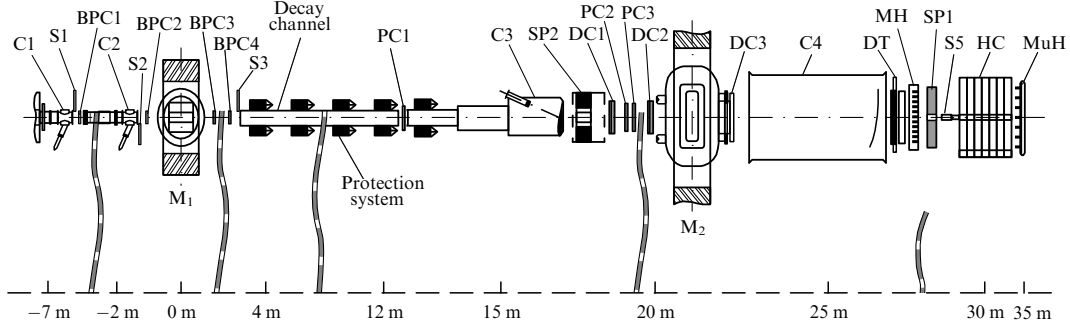


Figure 5. Layout of the ISTRA+ detector: S1–S5 — scintillation counters, C1–C4 — threshold Cherenkov counters, BPC, PC — proportional chambers, SP — spectrometers, DC — drift chambers, DT — drift tubes, MuH — muon hodoscope, HC — hadron calorimeter, MH — scintillation multitrack hodoscope, M1 and M2 — magnetic spectrometers, the trigger — $T = S1S2S3S4C0C1C2S5(\sum_{SP1} > mip)$ (the Cherenkov counter C0 and the scintillator S4 are not shown in the figure). The detector operated in a beam of negative particles with a momentum of 25 GeV/c and intensity of 3×10^6 particles per cycle. The content of K^- -mesons in the beam was $\simeq 3\%$.

i.e., contributions to the decays $K^+ \rightarrow \pi^0 l^+ \nu_l$ can be given by vector, scalar, or tensor weak interactions.

In the Standard Model with a weak ($V-A$)-interaction the hadron part of the matrix element takes the form

$$\begin{aligned} \langle \pi(P_\pi) | J_{\text{had}} | K(P_K) \rangle \\ = |V_{us}| \frac{1}{\sqrt{2}} [(P_K + P_\pi)^\alpha f_+(q^2) + (P_K - P_\pi)^\alpha f_-(q^2)] \\ = |V_{us}| \frac{1}{\sqrt{2}} f_+(q^2) [(P_K + P_\pi)^\alpha + (P_K - P_\pi)^\alpha \xi(q^2)]. \quad (42) \end{aligned}$$

Here, P_K^α , P_π^α , p_ν^α , p_l^α are the 4-momenta of the respective particles; $P^\alpha = P_K^\alpha + P_\pi^\alpha$, $q^\alpha = P_K^\alpha - P_\pi^\alpha = p_l^\alpha + p_\nu^\alpha$, and $t = q^2 = M_K^2 + M_\pi^2 - 2E_\pi M_K$ is the square of the momentum transferred to the leptons.

Making use of the notation of Refs [32, 33], one can write down the amplitude $A(K^+ \rightarrow \pi^0 l^+ \nu_l)_{SM}$ as

$$\begin{aligned} A_{SM} = -\frac{G_F}{2} |V_{us}| \left\{ \bar{u}_\nu (1 + \gamma_5) \left[(P_K^\alpha + P_\pi^\alpha) f_+(q^2) \right. \right. \\ \left. \left. + (P_K^\alpha - P_\pi^\alpha) f_-(q^2) \right] \gamma_\alpha \right\} v_l \\ = -\frac{G_F}{2} |V_{us}| f_+(q^2) \\ \times \left\{ \bar{u}_\nu (1 + \gamma_5) [P^\alpha \gamma_\alpha + (P_l^\alpha + P_\nu^\alpha) \xi(q^2)] v_l \right\}. \quad (43) \end{aligned}$$

The general Lorentz-invariant amplitude taking into account the possible contribution of scalar (S) and tensor (T) anomalous weak interactions has the form

$$\begin{aligned} A = \frac{G_F}{2} |V_{us}| \left\{ \bar{u}_\nu (1 + \gamma_5) \left[-(P_K^\alpha + P_\pi^\alpha) f_+(q^2) \gamma_\alpha \right. \right. \\ \left. \left. - (P_K^\alpha - P_\pi^\alpha) f_-(q^2) \gamma_\alpha + 2M_K f_S(q^2) \right. \right. \\ \left. \left. + i \frac{2f_T(q^2)}{M_K} P_K^\alpha P_\pi^\beta \sigma_{\alpha\beta} \right] v_l \right\} \\ = \frac{G_F}{2} |V_{us}| f_+(q^2) \left\{ \bar{u}_\nu (1 + \gamma_5) \left[-P^\alpha \gamma_\alpha - (p_l^\alpha + p_\nu^\alpha) \xi(q^2) \right. \right. \\ \left. \left. + 2M_K F_S + i \frac{2F_T}{M_K} P_K^\alpha P_\pi^\beta \sigma_{\alpha\beta} \right] v_l \right\}. \quad (44) \end{aligned}$$

Here, $f_+(q^2)$ and $f_-(q^2)$ are the vector form factors of the decay $K^+ \rightarrow \pi^0 l^+ \nu_l$, and $\xi(q^2) = f_-(q^2)/f_+(q^2)$. The follow-

ing notation was introduced for scalar and tensor form factors:

$$\frac{f_S(q^2)}{f_+(q^2)} \simeq \frac{f_S(0)}{f_+(0)} = F_S \quad \text{and} \quad \frac{f_T(q^2)}{f_+(q^2)} \simeq \frac{f_T(0)}{f_+(0)} = F_T,$$

i.e., for small scalar and tensor corrections we neglected their q^2 -dependence and, instead of the respective form factors, we introduced anomalous interaction constants F_S and F_T .

Further transformation of the amplitudes A_{SM} and A of the $K^+ \rightarrow \pi^0 l^+ \nu_l$ -decay is performed with the aid of the Dirac equation:

$$\begin{aligned} A_{SM} = -\frac{G_F}{2} |V_{us}| f_+(q^2) \left\{ \bar{u}_\nu (1 + \gamma_5) \right. \\ \left. \times [P^\alpha \gamma_\alpha + (p_l^\alpha + p_\nu^\alpha) \gamma_\alpha \xi(q^2)] v_l \right\} \\ = -\frac{G_F}{2} |V_{us}| f_+(q^2) \left\{ \bar{u}_\nu (1 + \gamma_5) P^\alpha \gamma_\alpha v_l \right. \\ \left. + \bar{u}_\nu p_\nu^\alpha \gamma_\alpha (1 - \gamma_5) \xi(q^2) v_l + \bar{u}_\nu (1 + \gamma_5) p_l^\alpha \gamma_\alpha \xi(q^2) v_l \right\} \\ = -\frac{G_F}{2} |V_{us}| f_+(q^2) \left\{ \bar{u}_\nu (1 + \gamma_5) [P^\alpha \gamma_\alpha - m_l \xi(q^2)] v_l \right\} \quad (45) \end{aligned}$$

(since $\bar{u}_\nu p_\nu^\alpha \gamma_\alpha = 0$ and $p_l^\alpha \gamma_\alpha v_l = -m_l v_l$).

In the general form, accounting for contributions from the scalar and tensor interactions, one obtains

$$\begin{aligned} A = \frac{G_F}{2} |V_{us}| f_+(q^2) \left\{ \bar{u}_\nu (1 + \gamma_5) \left[-P^\alpha \gamma_\alpha + m_l \xi(q^2) \right. \right. \\ \left. \left. + 2M_K F_S + i \frac{2F_T}{M_K} P_K^\alpha P_\pi^\beta \sigma_{\alpha\beta} \right] v_l \right\}. \quad (46) \end{aligned}$$

Instead of the form factor $f_-(t)$, one usually uses the so-called scalar form factor

$$f_0(t) = f_+(t) + \frac{t}{M_K^2 - M_\pi^2} f_-(t). \quad (47)$$

The vector and scalar form factors $f_+(t)$ and $f_0(t)$ correspond to the respective P-wave and S-wave components in the cross channel $\langle 0 | J_{\text{had}} | K \pi_{\text{in}} \rangle$.

In accordance with the ideas of Chiral Perturbative Theory (ChPT) and in the $O(p^6)$ approximation, a parametrization for the form factors is introduced that takes into account the term quadratic in t (to be more precise, in the dimensionless parameter q^2/M_π^2):

$$f_+(t) = f_+(0) \left[1 + \lambda_+ \left(\frac{q^2}{M_\pi^2} \right) + \lambda'_+ \left(\frac{q^4}{M_\pi^4} \right) \right] \quad (48)$$

and

$$f_0(t) = f_0(0) \left[1 + \lambda_0 \left(\frac{q^2}{M_\pi^2} \right) + \lambda'_0 \left(\frac{q^4}{M_\pi^4} \right) \right]. \quad (49)$$

Then, from formula (47) one can obtain

$$f_-(t) = f_+(0) \frac{M_K^2 - M_\pi^2}{M_\pi^2} \left[(\lambda_0 - \lambda_+) + \frac{q^2}{M_\pi^2} (\lambda'_0 - \lambda'_+) \right]. \quad (50)$$

The tensor and scalar interactions can be expressed via the vector and scalar interactions [33]:

$$V = f_+(q^2) \left(1 + \frac{m_l}{M_K} F_T \right) = f_+(q^2) V', \quad (51)$$

$$S = f_+(q^2) \left[F_S + \frac{m_l}{2M_K} \xi(q^2) + \left(1 + \frac{m_l^2}{2M_K^2} - \frac{2E_l + E_\pi}{M_K} \right) F_T \right] = f_+(q^2) S'. \quad (52)$$

Upon performing such a redefinition one can find the density distribution of events in the Dalitz plot for K_{l3} -decays:

$$\rho(E_\pi, E_l) \propto f_+(q^2) [A|V'|^2 + B \operatorname{Re}(V'^* S') + C|S'|^2]. \quad (53)$$

Here, the following notation was used:

$$A = M_K(2E_\nu E_l - M_K \Delta E_\pi) - m_l^2 \left(E_\nu - \frac{1}{4} \Delta E_\pi \right),$$

$$B = m_l M_K (2E_\nu - \Delta E_\pi),$$

$$C = M_K^2 \Delta E_\pi,$$

$$\Delta E_\pi = E_\pi^{\max} - E_\pi, \quad E_\pi^{\max} = \frac{M_K^2 - m_l^2 + M_\pi^2}{2M_K}.$$

Analysis of the distribution of K_{l3} -events in Dalitz plots for these decays permits determining the slopes of form factors (48) and (49) from the square of the momentum transfer λ_+ , λ_0 , etc., while also obtaining information on the possible strengths F_S and F_T of the anomalous scalar and tensor interactions. Analysis of the structure of the $\rho(E_\pi, E_l)$ -distribution (53) reveals that the interference term $B \operatorname{Re}(V'^* S')$ which contains the linear contributions F_S and F_T and exhibits, in principle, the highest sensitivity to these anomalous interactions going beyond the SM. However, as can be seen from formula (53), the interference term is proportional to the lepton mass m_l and in the case of the K_{e3} -decay it turns out to be negligible. Straightforward calculations show that such a dependence upon m_l is due to the chirality of the leptons produced in the K_{l3} -decay. Therefore, the effects due to new interactions are determined in the K_{e3} -decay by the quadratic term $C|S'|^2$ in formula (53). For $K_{\mu 3}$ -decays, the main contribution from F_S and F_T is due to the interference term $B(V'^* S')$. However, besides F_S and

F_T , the expression for S' also includes the vector term $\xi(q^2)m_l/M_K$. As follows from the form of the matrix element A [see Eqn (46)], it contains the combination

$$[m_l \xi(q^2) + 2M_K F_S] \simeq m_l \left[\xi(0) + \frac{2M_K}{m_l} F_S \right].$$

Therefore, independent data on $\xi(q^2) = f_-(q^2)/f_+(q^2) \simeq \xi(0)$ are necessary for obtaining information about the anomalous interaction. In Ref. [35], where the $K_{\mu 3}$ -decay was studied, information on $f_-(q^2)$ was derived from theoretical calculations within the framework of ChPT, according to which $\lambda_{0\text{theor}} = 0.017 \pm 0.004$, and from data on λ_+ obtained from the analysis of the K_{e3} -decay which was studied in the same experiment (see Ref. [34]). This made it possible [see formula (50)] to obtain the quantity

$$\begin{aligned} \xi(0) &= \frac{f_-(0)}{f_+(0)} = \left[\left(\frac{M_K}{M_\pi} \right)^2 - 1 \right] (\lambda_{0\text{theor}} - \lambda_+) \\ &= -0.132 \pm 0.049 \end{aligned}$$

and to set a limit on F_S . Here, the precision is determined by the uncertainty in $\lambda_{0\text{theor}}$ and results in an additional uncertainty in F_S , amounting to ± 0.0053 . The value of F_T can be determined by fitting the distribution of events $\rho(E_\pi, E_l)$ in the Dalitz plot without any additional theoretical assumptions.

Data on the K_{l3} -decay permit studying the dependence of $f_+(t)$ with the highest possible accuracy and reliably establishing that it contains a quadratic term. Analysis of the $K_{\mu 3}$ -decay provided information on the slope of the scalar form factor $f_0(t)$.

As was shown in Ref. [33], the density distribution of events in the Dalitz plot for K-decays can be represented in the rest frame of the lepton pair via other variables:

$$\rho(E_\pi, \vartheta) \propto \frac{\varepsilon^5 P_\pi}{E_K} \{ |M_K^2 F_S + \varepsilon P_\pi F_T \cos \vartheta|^2 + P_\pi^2 f_+^2 \sin^2 \vartheta \}. \quad (54)$$

Here, the notation was applied:

$$\begin{aligned} \varepsilon &= E_K - E_\pi = \sqrt{Q^2}, \quad P_\pi = \sqrt{E_\pi^2 - M_\pi^2}, \\ E_K &= \sqrt{P_\pi^2 + M_K^2}, \end{aligned}$$

ϑ is the angle between the momenta of π^0 and l^+ (both are in the dilepton rest frame, where $\mathbf{P}_K = -\mathbf{P}_\pi$). Then, in the case of K-decays, the angular distribution

$$\frac{dN}{d \cos \vartheta} \propto \sin^2 \vartheta$$

corresponds to vector interaction, the isotropic angular distribution corresponds to scalar interaction, while the distribution

$$\frac{dN}{d \cos \vartheta} \propto \cos^2 \vartheta$$

corresponds to tensor interaction.

Studies of the density distributions of 0.92×10^6 K_{e3} -events [34] and of 0.54×10^6 $K_{\mu 3}$ -events [35] in the Dalitz plot were analyzed in detail in Ref. [36]. The results of this analysis are summarized in Table 3. They significantly exceed in

Table 3. Main results of experiments performed by the ISTRA+ Collaboration [34, 35] on an investigation of K_{l3} -decays, and their comparison with subsequent KTeV measurements [37] and ChPT predictions in the $O(p^6)$ approximation.

| Experimental result | Decay $K^+ \rightarrow \pi^0 e^+ \nu_e$ [34] | Decay $K^+ \rightarrow \pi^0 \mu^+ \nu_\mu$ [35] | KTeV data [37] | ChPT predictions in $O(p^6)$ approximation |
|---------------------|---|---|----------------------|--|
| Number of events | 0.92×10^6 K_{l3} -decays | 0.54×10^6 $K_{\mu 3}$ -decays | — | — |
| λ_+ | $0.02774 \pm 0.00047 \pm 0.00032$ | $0.0277 \pm 0.0013 \pm 0.0009$ | 0.0281 ± 0.0005 | 0.0310 ± 0.0006 |
| λ'_+ | $0.00084 \pm 0.00027 \pm 0.00031$ | 0.001 ± 0.001 | 0.0016 ± 0.00035 | 0.00112 ± 0.0001 |
| λ_0 | — | $0.0183 \pm 0.0011 \pm 0.0006$ | 0.0131 ± 0.0013 | — |
| F_T | $-0.012 \pm 0.021 \pm 0.011$ $= -0.012 \pm 0.024$ or $ F_T < 0.043$ (90% C.L.) | $-0.0007 \pm 0.0071 \pm 0.002$ $= -0.0007 \pm 0.0074$ or $ F_T < 0.010$ (90% C.L.) | — | — |
| F_S | $-0.0037^{+0.0066}_{-0.0056} \pm 0.0041$ $= -0.0037 \pm 0.0078$ or $ F_S < 0.014$ (90% C.L.) | $0.0017 \pm 0.0014_{\text{stat}} \pm 0.0009_{\text{syst}}$ $\pm 0.0053_{\text{theor}} = 0.0017 \pm 0.0056$ or $ F_S < 0.0088$ (90% C.L.) | — | — |
| F_T (average) | -0.012 ± 0.024 or $ F_T < 0.043$ (90% C.L.) | -0.001 ± 0.007 or $ F_T < 0.010$ (90% C.L.) | — | — |
| F_S (average) | -0.003 ± 0.008 or $ F_S < 0.014$ (90% C.L.) | — | — | — |

Note. The main results of experiments performed by the ISTRA+ Collaboration [34, 35] on an investigation of K_{l3} -decays:

(1) the first precise data have been obtained that confirm the nonlinear dependence

$$f_+(t) = f_+(0) \left(1 + \lambda_+ \left(\frac{q^2}{M_\pi^2} \right) + \lambda'_+ \left(\frac{q^4}{M_\pi^4} \right) \right);$$

(2) the slope λ_0 of the form factor $f_0(t)$ has been measured for the first time;

(3) good agreement of the data for λ_+ in K_{l3} - and $K_{\mu 3}$ -decays confirms the $(\mu - e)$ -universality in these decays;

(4) the world's most stringent limits have been obtained on the possible contribution of anomalous scalar (F_S) and tensor (F_T) interactions. In deriving data on the scalar interaction F_S from the analysis of the $K_{\mu 3}$ -decay it turned out necessary to make use of theoretical predictions for

$\lambda_{0\text{theor}} = 0.017 \pm 0.004$ in chiral theory. Precisely this theoretical correction presently determines the accuracy for the limit to $|F_S|$ from the data for $K_{\mu 3}$ -decays. The corresponding accuracy will be enhanced with the developments of lattice QCD calculations in the unquenched approximation;

(5) the results for the form factors were subsequently confirmed by the data obtained by the KTeV Collaboration [37] with the accuracy similar to that of the ISTRA+ Collaboration.

accuracy data of other studies [37–39] in this field. Therefore, in addition to the results [34, 35] concerning the limits on the values of anomalous F_S - and F_T -interactions, we shall only present the averaged restrictions from Ref. [20] and not deal with the results of other studies.

In the work [37], carried out by the KTeV Collaboration, the main results obtained for the form factors $f_+(q^2)$ and $f_0(q^2)$ by the ISTRA+ Collaboration [34, 35] were confirmed.

In future experiments with the OKA detector in the separated beam of K^+ -mesons (see Appendix 9.1), a statistics of K_{l3} -decays may be collected that will exceed by 2–3 orders of magnitude the number of events collected by the experiments presented in Table 3. The new data will be used in further studies of form factors in these decays and for more sensitive searches for anomalous interactions.

Regretfully, at present we cannot cite the accuracy we will be able to achieve in measurements of the form factors f_+ , f_0 and of anomalous coupling constants of scalar and tensor interactions. These accuracies will depend on the actual decay systematics, and a comprehensive analysis of new large statistics will be required, together with the introduction of additional selection criteria and a number of other methods, for minimization of the systematic errors. We hope to achieve significant enhancement of the accuracy (at least by several times or even by an order of magnitude).

New refined data on the form factors f_+ and f_- are apparently important for comparison with the results of calculations in chiral perturbation theory [40] and in lattice studies of QCD. Both these fields are undergoing intensive development.

Obtaining as precise as possible data for the coupling constants of anomalous interactions in $K_{\mu 3}$ - and $K_{e 3}$ -decays is one of the top-priority goals of experiments with the OKA spectrometer. It is apparently important to carry out such searches independently for both decays, since the mechanisms of anomalous interactions may manifest themselves differently in these processes. Thus, Higgs-like interactions that depend on the lepton masses can be observed only in $K_{\mu 3}$ -decays. At the same time, scalar processes depending on new types of scalar intermediate bosons with $(\mu - e)$ -universal interactions, will contribute to both the $K_{e 3}$ - and $K_{\mu 3}$ -decays. Large statistics of $K_{e 3}$ -decays will permit us to impose sufficiently stringent limits on F_S or F_T , in spite of their being only due to the quadratic contribution of these constants [i.e., the component $C|S'|^2$ in formula (53)]. Such limits (even though less sensitive than those obtained from the data on $\text{Re}(V'^* S')$ in $K_{\mu 3}$ -decays) do not depend on theoretical assumptions concerning the form of $\xi(q^2)$ (see note to Table 3). Thus, a detailed analysis of both types of semileptonic K_{l3} -decays will allow us to perform independent sensitive searches for new types of interactions of various dynamic nature.

3.4 On certain mechanisms of anomalous interactions in K_{l3} - and K_{l2} -decays

3.4.1 Models involving charged Higgs bosons [41, 42]. As can be seen from the diagram presented in Fig. 6a, the exchange of charged Higgs bosons in models with two (2HDM) or several (3HDM) Higgs doublets allows one to reveal the connection between the constraints on F_S in $K_{\mu 3}$ -decays (see Table 3) and the parameters of the model.

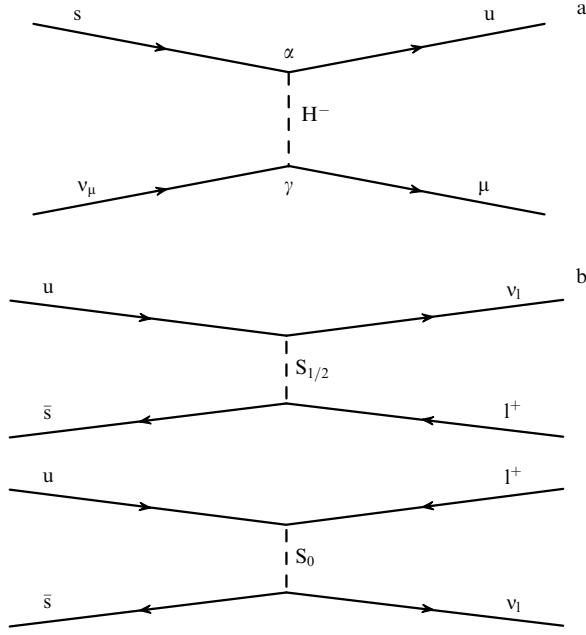


Figure 6. (a) Diagram for scalar semileptonic decay $K^- \rightarrow \pi^0 \mu^- \bar{\nu}_\mu$ via the exchange of the charged Higgs boson H^- . Here, α and γ are the interaction constants of H^- with quarks and leptons, respectively: $g_S = (2M_K/m_\mu)F_S$, and M_H is the mass of the charged Higgs boson. In this model $\text{Im } g_S = \text{Im } \alpha^* \gamma (M_K/M_H)^2$, and $\text{Re } g_S = \text{Re } \alpha^* \gamma (M_K/M_H)^2$. (b) Anomalous lepton decays $K^+ \rightarrow l^+ \nu_l$ of charged kaons in models with leptoquarks $S_{1/2}$ and S_0 . Similar diagrams with additional spectator quarks contribute to anomalous K_{l3} -decays.

For the quantity $g_S = (2m_K/m_\mu)F_S$ in formula (46) it is possible to obtain

$$\begin{aligned} \text{Im } g_S &= \text{Im } \alpha^* \gamma \left(\frac{M_K}{M_H} \right)^2, \\ \text{Re } g_S &= \text{Re } \alpha^* \gamma \left(\frac{M_K}{M_H} \right)^2. \end{aligned} \quad (55)$$

In the 3HDM model, M_H is the mass of the lightest charged Higgs boson (H^\pm), and α and γ are the complex interaction coupling constants of H^\pm with the down s , d quarks and with leptons. The following limit was set within 3HDM from the data of Table 3 ($F_S < 0.013$, 90% C.L.):

$$\begin{aligned} \text{Re } \alpha^* \gamma \left(\frac{M_K}{M_H} \right)^2 &= F_S \frac{2M_K}{m_\mu} \\ &= 0.036 \pm 0.047 \pm 0.047 < 0.12. \end{aligned} \quad (56)$$

The following was obtained within 2HDM:

$$\frac{M_K^2 - M_\pi^2}{M_H^2} \tan^2 \beta \simeq \frac{2M_K}{m_\mu} F_S, \quad (57)$$

where $\tan \beta = V_2/V_1$ is the ratio of the vacuum expectations for two Higgs doublets. From the data of Ref. [35] (see Table 3) one finds

$$\frac{\tan \beta}{M_H} \simeq \left[\frac{2F_S}{M_K m_\mu (1 - M_\pi^2/M_K^2)} \right]^{1/2} < 0.5 \text{ GeV}^{-1} \text{ (90\% C.L.)}. \quad (58)$$

Notice that a similar limit was obtained from LEP data on searches for $B \rightarrow \tau \nu_\tau + X$:

$$\frac{\tan \beta}{M_H} < 0.4 - 1.0 \text{ GeV}^{-1} \text{ (90\% C.L.)}.$$

3.4.2 Models with leptoquarks [43]. In Ref. [43], an analysis was presented of the constraints on the anomalous interactions F_S and F_T in the model with leptoquarks. Figure 6b presents the diagrams for processes $K^+ \rightarrow l^+ \nu_l$ involving the exchange of leptoquarks, such as

$$\begin{aligned} S_{1/2} &\text{ (doublet with } q = -2/3 \text{ and } q = -5/3), \\ S_0 &\text{ (singlet with } q = -1/3). \end{aligned}$$

The same diagrams contribute to the description of anomalous interactions in K_{l3} -decays.

Leptoquarks are characterized by the parameter $1/\Lambda_{LQ}^2 = Y_R Y_L^*/M_S^2$, where M_S is the mass of the leptoquark, while Y_R and Y_L are the respective constants of its interaction with right-handed and left-handed quarks (Fig. 6b). It was shown in Ref. [43] that the constants F_S and F_T of anomalous interactions can be expressed through the parameter Λ_{LQ} :

$$\begin{aligned} F_S &= \frac{\sqrt{2}}{16G_F|V_{us}|} \frac{M_K^2 - M_\pi^2}{(m_s - m_u)M_K} \frac{1}{\Lambda_{LQ}^2}, \\ F_T &= -\frac{\sqrt{2}}{32G_F|V_{us}|} \frac{M_K}{M_{K^*}} \frac{1}{\Lambda_{LQ}^2} \end{aligned} \quad (59)$$

(m_s, m_u are the masses of the respective quarks, and M_{K^*} is the mass of the K^* -meson playing the role of an intermediate state in the K_{l3} -decay).

From data for F_T and formula (59) the following restriction was obtained:

$$\Lambda_{LQ} = 0.48_{-0.17}^{+\infty} \text{ TeV} > 0.26 \text{ TeV} \text{ (90\% C.L.)}. \quad (60)$$

A stronger constraint can be obtained from the data on F_S and formula (59):

$$\begin{aligned} \Lambda_{LQ}^2 &= 0.298 \times 10^5 \text{ GeV}^2 \times F_S^{-1} > 2.23 \text{ TeV}^2 \text{ (90\% C.L.)}, \\ \Lambda_{LQ} &> 1.49 \text{ TeV} \text{ (90\% C.L.)}. \end{aligned} \quad (61)$$

It is also shown in Ref. [43] that the scalar interaction F_S in the leptoquark model violates $(\mu - e)$ -universality in $K^+ \rightarrow l^+ \nu_l$ -decays and leads to values of the electroweak constants $g_l^K = 1 - 2F_S M_K/m_l$ in Eqn (31). Therefore, the relationship for the ratio $(g_e^K/g_\mu^K)^2$ is given by

$$\begin{aligned} \left(\frac{g_e^K}{g_\mu^K} \right)^2 &= \frac{1 - 4F_S M_K/m_e}{1 - 4F_S M_K/m_\mu} = 1 - 4F_S M_K \left(\frac{1}{m_e} - \frac{1}{m_\mu} \right) \\ &= 1 - 3.87 \times 10^3 F_S. \end{aligned} \quad (62)$$

As was shown in Section 2.2, from available data for the decay $K^+ \rightarrow l^+ \nu_l$ it is possible to set a limit on the possible violation of $(\mu - e)$ -universality:

$$\begin{aligned} R(K^+ \rightarrow l^+ \nu_l)_{\text{exp}} &= R(K^+ \rightarrow l^+ \nu_l)_{\text{SM}} (0.987 \pm 0.045) \\ &= R(K^+ \rightarrow l^+ \nu_l)_{\text{SM}} \left(\frac{g_e^K}{g_\mu^K} \right)^2, \\ \left(\frac{g_e^K}{g_\mu^K} \right)^2 &= 0.987 \pm 0.045. \end{aligned} \quad (63)$$

From formulas (62) and (63) we have

$$F_S = \frac{0.013 \pm 0.045}{3.87 \times 10^3} < 1.8 \times 10^{-5} \text{ (90\% C.L.)}, \quad (64)$$

i.e., a significantly more stringent limit has been obtained for the anomalous scalar interaction F_S in the leptoquark model from data on $\text{BR}(K^+ \rightarrow e^+ \nu_e)/\text{BR}(K^+ \rightarrow \mu^+ \nu_\mu)$ than from direct data on K_{l3} -decays. The upper limit

$$A_{LQ} > 41 \text{ TeV} \quad (65)$$

corresponds to the F_S value (64).

Measurement of $R(K^+ \rightarrow l^+ \nu_l)$ with an accuracy of $\sim 3 \times 10^{-3} - 10^{-3}$ is planned in the OKA experiment. If no deviation from the SM and $(\mu - e)$ -universality is found, this will correspond to the limit $A_{LQ} > 150 - 250 \text{ TeV}$.

3.5 The decays $K^+ \rightarrow \pi^+ e^+ e^-$ and $K^+ \rightarrow \pi^+ \mu^+ \mu^-$

Studies of the decays of charged kaons, in which a pion and a lepton pair $l^+ l^-$ are produced, namely

$$K^+ \rightarrow \pi^+ e^+ e^-, \quad (66)$$

$$K^+ \rightarrow \pi^+ \mu^+ \mu^-, \quad (67)$$

open up new possibilities for validating ChPT predictions for weak interactions with a change in strangeness $\Delta S = 1$ and for searches for new types of interactions. To this end, it is necessary to perform thorough measurements of the branching fractions for decays (66), (67), to analyze the distributions of their events in the respective Dalitz plots in order to determine the decay form factors, and to compare the data obtained with calculations done within various ChPT approximations. As noted in a number of works [44, 45], investigation of the integral ratio

$$R\left(\frac{\mu^+ \mu^-}{e^+ e^-}\right) = \frac{\text{BR}(K^+ \rightarrow \pi^+ \mu^+ \mu^-)}{\text{BR}(K^+ \rightarrow \pi^+ e^+ e^-)}$$

for the probabilities of these two processes and of their differential distributions $\rho(\mu^+ \mu^-/e^+ e^-)$ over kinematic variables will permit excluding a number of theoretical uncertainties and obtaining more complete information on the physics

of these decays. As was shown, it is possible to estimate the contribution of second-order weak interactions to the respective decays from the ratios of differential probabilities $\rho(\mu^+ \mu^-/e^+ e^-)$ in the region of low π^+ -meson energies [46]. Anomalous weak interactions of the Higgs type with a coupling constant proportional to the lepton mass may also manifest themselves in this ratio.

The values of $R(\mu^+ \mu^-/e^+ e^-)$, predicted by various models, lie between 0.2 and 0.3. It is predicted within the framework of the ChPT chiral model that $R(\mu^+ \mu^-/e^+ e^-)_{\text{ChPT}} \gtrsim 0.23$ [47]. Measurement of $R(\mu^+ \mu^-/e^+ e^-)$ with an experimental accuracy $\delta R \simeq 2 - 3\%$ will permit testing predictions of the chiral model with an accuracy $\sim 10\%$.

The $K^+ \rightarrow \pi^+ l^+ l^-$ -decays data available to date are presented in Table 4. It must be noted that the results of measurements of the electron decays (66), presented in Refs [48–50], are in reasonable agreement with each other. There existed, however, a clear experimental contradiction between the results of Refs [51] and [52] for the muon decay $K^+ \rightarrow \pi^+ \mu^+ \mu^-$. The latest results of Ref. [53] confirm the data obtained earlier in Ref. [52] and remove this contradiction. Study of decay (67) seems to be very promising in experiments with the OKA detector, since it permits us to essentially increase available statistics (see Appendix 9.1).

We briefly summarize the experimental data for decays (66), (67), obtained as a result of the most complete studies performed in the BNL E865 experiment [50, 52]. This first of all concerns decay (66), for which a large amount of statistics (10,300 events) has been collected [50].

The main results of experiment E865 can be formulated as follows:

(1) The experimental data for the decay $K^+ \rightarrow \pi^+ e^+ e^-$ are in good agreement with the vector version of the interaction which involves single-photon exchange and exhibits the form

$$\frac{\alpha G_F}{4\pi} f_v(z) P^\alpha \bar{u}_e \gamma_\alpha v_c$$

(here, the 4-momenta $P^\alpha = P_K^\alpha + P_\pi^\alpha$, $q^\beta = P_K^\beta - P_\pi^\beta$, and $z = q^2/M_K^2 = m_{e^+e^-}^2/M_K^2$). The possible contribution of scalar and tensor interactions is very small.

Table 4. Experimental data from studies of decays $K^+ \rightarrow \pi^+ l^+ l^-$ [48–53] and expected statistics in the OKA experiment.

| Experiment | $N \text{ events } \{\text{BR}\}$ | | $R(\mu^+ \mu^-/e^+ e^-)$ | λ (for parametrization of the form factor as $F(z) = 1 + \lambda z$) |
|---|---|---|--------------------------|---|
| | $K^+ \rightarrow \pi^+ e^+ e^-$ | $K^+ \rightarrow \pi^+ \mu^+ \mu^-$ | | |
| BNL E777 [49] | ~ 500 $\{(2.75 \pm 0.26) \times 10^{-7}\}$ | — | — | 1.31 ± 0.48 |
| BNL E851 [48] | ~ 800 $\{(2.81 \pm 0.20) \times 10^{-7}\}$ | — | — | — |
| BNL E787 [51] | — | 196 ± 17 $\{(5.0 \pm 1.0) \times 10^{-8}\}$ | — | — |
| BNL E865 [50, 52] | ~ 10300 [50] $\{(2.94 \pm 0.15) \times 10^{-7}\}$ | ~ 430 [52] $\{(9.22 \pm 0.77) \times 10^{-8}\}$ | 0.314 ± 0.031 | 2.14 ± 0.20 $K^+ \rightarrow \pi^+ e^+ e^-$ [50] $2.45^{+1.30}_{-0.95}$ $K^+ \rightarrow \pi^+ \mu^+ \mu^-$ [52] |
| Hyper CP Fermilab [53] | — | ~ 100 $\{(9.8 \pm 1.1) \times 10^{-8}\}$ | — | — |
| Expected statistics in the OKA experiment | $\sim 10^4$ | $\sim 5 \times 10^3$ | — | — |

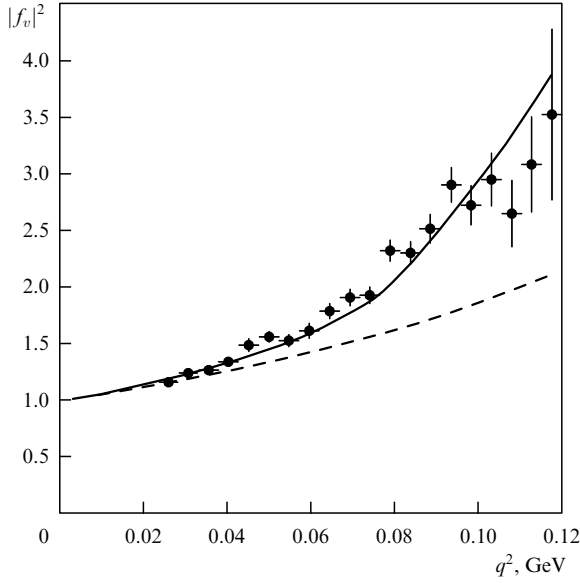


Figure 7. Results of measurement of the form factor $|f_v(q^2)|^2$ in the decay $K^+ \rightarrow \pi^+ e^+ e^-$ [51] (see also Ref. [54]). Here, instead of the variable $z = q^2/M_K^2$ (see text), the variable $q^2 = M_{e^+e^-}^2$ was used in the form factor. The contribution of the loop ChPT diagram is not accounted for in the dashed curve, while the solid curve does take into account this loop contribution.

(2) The form factor $f_v(z)$ in decay (66) can be represented within the ChPT framework as

$$f_v(z) = a_+ + b_+ z + W^{\pi\pi}(z),$$

where a_+ and b_+ are the parameters of the model, and $W^{\pi\pi}(z)$ is the contribution from the pion loop connected to the e^+e^- -system via a single-photon exchange. In the $O(p^4)$ ChPT approximation, one has $b_+ \simeq 0$. However, the experimental data for the slope of the form factor exhibit a stronger dependence upon z than predicted in the $O(p^4)$ approximation: $a_+ = -0.587 \pm 0.010$, and $b_+ = -0.655 \pm 0.044$. Although the linear-in- z approximation of the form factor is consistent with experimental data for $z \lesssim 0.3$, a nonlinearity is clearly observed for large values of z , which is related to the contribution of the loop ChPT diagram (Fig. 7). In Ref. [54], the data for $f_v(z)$ are well described taking into account the total contribution of the pion and kaon form factors in the vector dominance model and the loop pion diagram. Accounting for the form factor, determination was performed of the branching fraction for the decay (66):

$$\begin{aligned} \text{BR}(K^+ \rightarrow \pi^+ e^+ e^-) \\ = (2.94 \pm 0.05_{\text{(stat)}} \pm 0.13_{\text{(syst)}} \pm 0.05_{\text{(model)}}) \times 10^{-7}. \end{aligned}$$

(3) In the experiments [50, 52], determination was performed of the ratio

$$R\left(\frac{\mu^+ \mu^-}{e^+ e^-}\right)_{\text{exp}} = 0.314 \pm 0.031. \quad (68)$$

The previous value of this quantity, determined from the data of Ref. [51], amounted to

$$R\left(\frac{\mu^+ \mu^-}{e^+ e^-}\right)_{\text{exp}} = 0.167 \pm 0.036.$$

The new result [53] is in good agreement with that in formula (68) and amounts to

$$R\left(\frac{\mu^+ \mu^-}{e^+ e^-}\right) = 0.333 \pm 0.041.$$

In experiments with the OKA detector we expect to register $\sim 10^4$ events of the type (66), and $\sim 5 \times 10^3$ events of the type (67), to measure their branching fractions, to investigate the differential distributions $\rho(\mu^+ \mu^-/e^+ e^-)$ for such decays over kinematical variables, and to compare these results with the predictions of the chiral model. Thus, the main goal of the planned measurements is a precision comparative analysis of data for decays (66) and (67).

We shall now proceed with analyzing the possibilities of searching for new anomalous interactions in the decays $K^+ \rightarrow \pi^+ l^+ l^-$. In Ref. [50], the matrix element of the decay $K^+(P_K) \rightarrow \pi^+(P_\pi) l^+(p_{l^+}) l^-(p_{l^-})$ was represented in the form

$$M = \frac{\alpha G_F}{4\pi} f_V P^\alpha \bar{l} \gamma_\alpha l + G_F M_K f_S \bar{l} l + G_F f_T \frac{P^\alpha q^\beta}{M_K} \bar{l} \sigma_{\alpha\beta} l. \quad (69)$$

Here, $f_{V,S,T}$ are the dimensionless form factors of the vector, scalar, and tensor interactions, $P^\alpha = P_K^\alpha + P_\pi^\alpha$, and $q^\beta = P_K^\beta - P_\pi^\beta$. Detailed analysis of formula (69) was carried out in the study of the decay $K^+ \rightarrow \pi^+ e^+ e^-$ [50], with large collected statistics (see Table 4). The vector term arising in the single-photon exchange plays a dominant role in this matrix element. The possible contribution of the scalar and tensor interactions does not exceed 2% of the total width $\Gamma(K^+ \rightarrow \pi^+ e^+ e^-)$. The following restrictions have been obtained for the coupling constants of anomalous scalar and tensor interactions:

$$|f_S| < 6.6 \times 10^{-5}, \quad |f_T| < 3.7 \times 10^{-4} \text{ (90\% C.L.)}. \quad (70)$$

It is more correct to single out the $|V_{us}|$ factors in these constants and to write them down as $|f_S| = |V_{us}| |f'_S|$, $|f_T| = |V_{us}| |f'_T|$. Then, one finds

$$|f'_S| < 3 \times 10^{-4}, \quad |f'_T| < 1.7 \times 10^{-3} \text{ (90\% C.L.)}. \quad (71)$$

It should be emphasized that anomalous scalar and tensor currents in Eqn (70) differ from the anomalous currents in K_{l3} -decays, which represent tree neutral currents with quark flavor violation (FCNC). Thus, constraints (70), (71) are independent constraints with respect to the limits on F_S and F_T , presented in Table 3. Naturally, a situation may occur when no independent tree FCNC-currents exist and the neutral scalar and tensor contributions in formula (70) are due to loop diagrams of higher orders in the F_S or F_T interactions (Fig. 8). However, the limits for these anomalous interactions, presented in Table 3, result in very small effective coupling constants for such anomalous FCNC-currents of higher orders. Rough estimates of the processes from the diagram in Fig. 8 show that in this case one has

$$\begin{aligned} \text{BR}(K^+ \rightarrow \pi^+ l^+ l^-)_{\text{scal}} &\sim \text{BR}(K^+ \rightarrow \pi^0 e^+ \nu_e) \underbrace{[G_F^2 M^4]}_{\text{loop}} \\ &= \text{BR}(K^+ \rightarrow \pi^0 e^+ \nu_e)_{\text{scal}} N \\ &\lesssim \text{BR}(K^+ \rightarrow \pi^0 e^+ \nu_e)_{\text{SM}} F_S^2 N \\ &\sim 5 \times 10^{-2} (1.3 \times 10^{-2})^2 N \sim 10^{-5} N. \end{aligned} \quad (72)$$

Here, N occurs through the loop process and for a mass of the scalar boson $\gtrsim 250 \text{ GeV} - 1 \text{ TeV}$ it lies within the range of

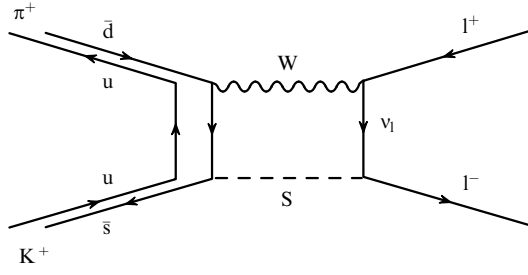


Figure 8. Diagram with neutral scalar interaction of a higher order in the $K^+ \rightarrow \pi^+ l^+ l^-$ -decay, which is due to the scalar intermediate boson S responsible for anomalous scalar interaction in the $K^+ \rightarrow \pi^+ l^+ \nu_l$ -decay.

$10^{-4} - 5 \times 10^{-5}$ (for diagrams taking into account only virtual u -quarks). Accounting for possible compensation by the contributions of heavy quarks (a mechanism of the GIM type), the factor N decreases greatly and can be estimated as $N \sim 10^{-4} (m_c/M_W)^4 \sim 5 \times 10^{-12}$ (such estimates are dealt with in greater detail in Ref. [55]). But even for a factor $N \sim 10^{-4}$ one obtains $\text{BR}(K^+ \rightarrow \pi^+ l^+ l^-)_{\text{scal}} < 10^{-9}$ (most likely, even $\ll 10^{-9}$). Such a value of the effective scalar FCNC-interaction of higher order lies essentially lower than the restrictions that can be obtained in studies of $K^+ \rightarrow \pi^+ l^+ l^-$ -decays. Therefore, such decays are only promising for searches for anomalous tree scalar and tensor FCNC-currents. The possible influence of such tree currents on rare CP-conserving decays, such as $K^+ \rightarrow \pi^+ \nu \bar{\nu}$ or $K_S^0 \rightarrow \pi^0 l^+ l^-$, depends on the mechanisms of anomalous interactions and must be dealt with separately.

Thus, searches for new anomalous interactions in the decays $K^+ \rightarrow l^+ \nu_l$, $K^+ \rightarrow \pi^0 l^+ \nu_l$, and $K^+ \rightarrow \pi^+ l^+ l^-$ turn out to be independent and complementary. Implementing such searches with the maximum possible sensitivity is an important task of the OKA experiment.

The prospects for searching for anomalous interactions in the decay $K^+ \rightarrow \pi^+ l^+ l^-$ by the forward-backward asymmetry in the angular distribution of leptons were considered in Ref. [56]. In the rest frame of the $l^+ l^-$ -pair, the distribution of ϑ , the angle between K^+ and l^- (Fig. 9),

takes the form

$$\begin{aligned} \frac{d^2\Gamma}{dq^2 d\cos\vartheta} = C(q^2) & \left\{ |f_V|^2 \frac{\alpha^2}{16\pi^2} \lambda(q^2) (1 - \beta_l^2 \cos^2\vartheta) \right. \\ & + |f_S|^2 q^2 \beta_l^2 M_K^2 + |f_T|^2 \frac{q^2 \lambda(q^2)}{M_K^2} \left(\cos^2\vartheta + \frac{4m_l^2}{q^2} \sin^2\vartheta \right) \\ & + \text{Re}(f_V^* f_S) \frac{\alpha m_l M_K}{\pi} \beta_l \lambda^{1/2}(q^2) \cos\vartheta \\ & \left. - \text{Im}(f_S f_T^*) 2q^2 \beta_l \lambda^{1/2}(q^2) \cos\vartheta - \text{Im}(f_V f_T^*) \frac{\alpha \lambda(q^2)}{\pi} \frac{m_l}{M_K} \right\}, \end{aligned} \quad (73)$$

$$\begin{aligned} \frac{d\Gamma}{dq^2} = C(q^2) & \left\{ |f_V|^2 \frac{\alpha^2}{4\pi^2} \lambda(q^2) \frac{1}{3} \left(1 + \frac{2m_l^2}{q^2} \right) \right. \\ & + 2|f_S|^2 q^2 \beta_l^2 M_K^2 + |f_T|^2 \frac{2q^2 \lambda(q^2)}{3M_K^2} \left(1 + \frac{8m_l^2}{q^2} \right) \\ & \left. - \text{Im}(f_V f_T^*) \frac{2\alpha \lambda(q^2)}{\pi} \frac{m_l}{M_K} \right\}. \end{aligned} \quad (74)$$

Here, the following notation was used:

$$\begin{aligned} C(q^2) &= \frac{G_F^2}{2^8 \pi^3 M_K^3} \beta_l \lambda^{1/2}(q^2), \\ \lambda(q^2) &= M_K^4 + M_\pi^4 + q^4 - 2M_\pi^2 q^2 - 2M_K^2 q^2 - 2M_\pi^2 M_K^2, \\ \beta_l &= \left(1 - \frac{4m_l^2}{q^2} \right)^{1/2}, \quad q^2 = M^2(l^+ l^-), \\ 4m_l^2 &\leq q^2 \leq (M_K - M_\pi)^2. \end{aligned}$$

The angular distribution is simplified for the $K^+ \rightarrow \pi^+ e^+ e^-$ -decay, since the contribution of terms containing the electron mass is negligible:

$$\begin{aligned} \frac{d^2\Gamma(K^+ \rightarrow \pi^+ e^+ e^-)}{dq^2 d\cos\vartheta} &= C(q^2) \left\{ |f_V|^2 \frac{\alpha^2 \lambda(q^2)}{16\pi^2} \underbrace{(1 - \cos^2\vartheta)}_{\sin^2\vartheta} \right. \\ &+ |f_S|^2 q^2 M_K + |f_T|^2 \frac{q^2 \lambda(q^2)}{M_K^2} \cos^2\vartheta \\ &\left. - \text{Im}(f_S f_T^*) 2q^2 \lambda(q^2)^{1/2} \cos\vartheta \right\}. \end{aligned} \quad (75)$$

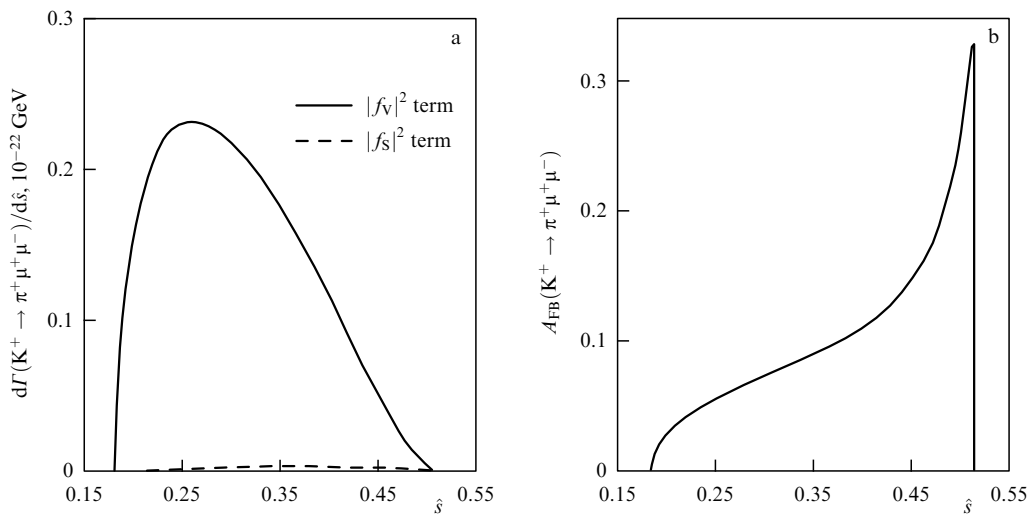


Figure 9. Characteristics of the $K^+ \rightarrow \pi^+ \mu^+ \mu^-$ -decay: (a) differential distribution $d\Gamma(K^+ \rightarrow \pi^+ \mu^+ \mu^-)/d\hat{s}$ versus the variable $\hat{s} = M(\mu^+ \mu^-)^2/M_K^2$; (b) forward-backward asymmetry $A_{\text{FB}}(\hat{s})$ in the distribution of the outgoing angle ϑ between K^+ and μ^- (in the rest frame of the $\mu^+ \mu^-$ -pair) for the scalar interaction coupling constant $f_S = 6.6 \times 10^{-5}$ (for $f_T = 0$) [56].

Hence it follows that

$$\begin{aligned} \frac{d\Gamma}{d\cos\vartheta} &\propto |f_V|^2 \sin^2\vartheta \text{ for vector interaction,} \\ \frac{d\Gamma}{d\cos\vartheta} &\propto |f_S|^2 \text{ (isotropy) } (f_T = 0) \text{ for scalar interaction,} \\ \frac{d\Gamma}{d\cos\vartheta} &\propto |f_T|^2 \cos^2\vartheta (f_S = 0) \text{ for tensor interaction.} \end{aligned}$$

As stated above, the analysis of data for the $K^+ \rightarrow \pi^+ l^+ l^-$ -decay in Ref. [50] permitted obtaining restrictions for anomalous interactions:

$$|f_S| < 6.6 \times 10^{-5} \quad (|f'_S| < 3.0 \times 10^{-4}),$$

and

$$|f_T| < 3.7 \times 10^{-4} \quad (|f'_T| < 1.7 \times 10^{-3})$$

at the 90% C.L. [see formulas (71), (72)]. The forward–backward asymmetry in Eqn (73) is given by

$$\begin{aligned} A_{FB}(q^2) &= \left[\int_0^1 d\cos\vartheta \frac{d^2\Gamma}{dq^2 d\cos\vartheta} - \int_{-1}^0 d\cos\vartheta \frac{d^2\Gamma}{dq^2 d\cos\vartheta} \right] \\ &\times \left[\int_0^1 d\cos\vartheta \frac{d^2\Gamma}{dq^2 d\cos\vartheta} + \int_{-1}^0 d\cos\vartheta \frac{d^2\Gamma}{dq^2 d\cos\vartheta} \right]^{-1} \\ &= C(q^2) \left[\operatorname{Re}(f_V^* f_S) \frac{\alpha m_l M_K}{\pi} - \operatorname{Im}(f_S f_T^*) 2q^2 \right] \left(\frac{d\Gamma}{dq^2} \right)^{-1} \\ &\simeq C(q^2) \operatorname{Re}(f_V^* f_S) \frac{\alpha m_l M_K}{\pi} \left(\frac{d\Gamma}{dq^2} \right)^{-1}. \end{aligned} \quad (76)$$

Consequently, one arrives at:

(a) $A_{FB}(K^+ \rightarrow \pi^+ \mu^+ \mu^-) \gg A_{FB}(K^+ \rightarrow \pi^+ e^+ e^-)$;

(b) the asymmetry A_{FB} is determined by the contribution of the scalar interaction f_S and differs from zero only beyond the SM.

Figure 9b presents the distribution of the asymmetry $A_{FB}(K^+ \rightarrow \pi^+ \mu^+ \mu^-)$ versus $\hat{s} = q^2/M_K^2$ for $f_S = 6.6 \times 10^{-5}$. It must be noted that there exists no information on f_S for the decay $K^+ \rightarrow \pi^+ \mu^+ \mu^-$. This interaction may, in principle, essentially exceed the scalar interaction in the $K^+ \rightarrow \pi^+ e^+ e^-$ -decay. Phenomenologically, the value of $A_{FB}(K^+ \rightarrow \pi^+ \mu^+ \mu^-)$ may even be $\gtrsim 0.1$, and then it will be reliably measured making use of the statistics of $\sim 5 \times 10^3$ events of $K^+ \rightarrow \pi^+ \mu^+ \mu^-$ -decay expected to be collected in the OKA experiment. However, in the supersymmetric MSSM model, the asymmetry A_{FB} turns out to be quite small ($A_{FB} \sim 10^{-3}$ [56]).

3.6 Other data on anomalous scalar and tensor interactions

To conclude this section we note that certain data on the possible existence of tensor interaction were obtained in studies of radiative decays $\pi^- \rightarrow e^- \bar{\nu}_e \gamma$ in experiments with the ISTRA facility [57] and in the more precise PIBETA experiment [58], where the possible tensor interaction coupling constant $f_T^0 = (-1.8 \pm 0.3) \times 10^{-3}$ was determined from an analysis of high statistics ($\gtrsim 40,000$ decays $\pi^+ \rightarrow e^+ \nu_e \gamma$ of stopping π^+ -mesons). To compare these data with the restrictions obtained in studying K_{l3} -decays ($F_T = f_T(0)/f_+(0) < 0.01$ 90% C.L., see Table 3), it is necessary to

take advantage of the relationships

$$\left. \begin{aligned} 3.8 f_T^0 &= \frac{f_T(0)}{f_+(0)} = F_T \text{ [59]} \\ \text{or} \quad 2.8 f_T^0 &= \frac{f_T(0)}{f_+(0)} = F_T \text{ [60]} \end{aligned} \right\}, \text{ i.e., } f_T^0 \simeq \frac{3.3 f_T(0)}{f_+(0)}.$$

Thus, the limit on $|f_T^0|$ obtained in the K_{l3} -decays is $< 3 \times 10^{-3}$ (90% C.L.), which is quite close to $f_T^0 = (-1.8 \pm 0.3) \times 10^{-3}$. Consequently, further improvement of the accuracy of searches for anomalous interactions in K_{l3} -decays would permit investigation of possible deviation (or its absence) from the data on radiative decays $\pi^+ \rightarrow e^+ \nu_e \gamma$. Notice that theoretical interpretation of the results of the PIBETA experiments is not unambiguous [33, 61, 62]. Therefore, improvement in the precision of searches for anomalous tensor interactions both in further studies of K_{l3} -decays and in new experimental exploration of radiative decays $\pi^+ \rightarrow e^+ \nu_e \gamma$ seems to be very interesting and promising.

We also note that in experimental studies of super-allowed $0^+ \rightarrow 0^+$ β -decays [63] limits were obtained on the possible existence of scalar interaction with $C_S/C_V < 0.0013$ (90% C.L.) [apparently, here $C_S/C_V = F_S = f_S(0)/f_+(0)$].

Discussion of theoretical models with new interactions can also be found in Refs [33, 41–43, 59, 63–66].

4. Direct nonconservation of CP-invariance in charged kaon decays

4.1 Searches for CP-violation effects in the decays

$K^\pm \rightarrow \pi^\pm \pi^+ \pi^-$ and $K^\pm \rightarrow \pi^\pm \pi^0 \pi^0$

As already discussed above, searches for CP-violating effects in the decays of charged K^\pm -mesons are of very significant interest, most importantly, from the point of view of new possible mechanisms of CP-violation going beyond the SM framework. CP-violation could manifest itself in the charge asymmetry of various characteristics of charge conjugate $K^\pm \rightarrow f(\bar{f})$ -decay channels, for example, in decays $K^\pm \rightarrow \pi^\pm \pi^+ \pi^-$, $\pi^\pm \pi^0 \pi^0$, $\pi^\pm \pi^0 \gamma$ and in other decay channels of charged kaons.

We shall first deal with the issue of CP-violation in decays of this type in a general case (see, for example, Refs [67, 68]). Let us consider charge-conjugate decays $K^+ \rightarrow f$ and $K^- \rightarrow \bar{f}$, which are described by the amplitudes

$$\operatorname{out}\langle f | \hat{H} | K^+ \rangle_{\text{in}} = A_f, \quad \operatorname{out}\langle \bar{f} | \hat{H} | K^- \rangle_{\text{in}} = A_{\bar{f}}.$$

Also, let each amplitude A_f represent a sum of two independent amplitudes

$$\left. \begin{aligned} A_f &= a \exp(i\delta_a) + b \exp(i\delta_b), \\ A_{\bar{f}} &= a^* \exp(i\delta_a) + b^* \exp(i\delta_b) \end{aligned} \right\}. \quad (77)$$

Here, the phase factors $\exp(i\delta_a)$ and $\exp(i\delta_b)$ characterize scattering processes in the final state $\operatorname{out}\langle f | H_{\text{st}} | f \rangle_{\text{in}}$. Thus, in passage from particles to antiparticles ($K \rightarrow \bar{K}$), the weak decay amplitudes a and b transform into the complex conjugate amplitudes a^* and b^* , while the strong scattering phases do not change. The amplitudes a and b of the weak decays can be represented as $a = |a| \exp(i\varphi_a)$ and $b = |b| \exp(i\varphi_b)$.

Table 5. The prospects for searches for direct CP-violation in the $K^\pm \rightarrow 3\pi$ -decays.

| Experiment | Process studied; expected statistics | Measurement accuracy $\delta g/g$ | Status of experiment | Theoretical predictions | |
|-----------------------------|---|--|----------------------|--|--|
| | | | | SM | Other models |
| OKA [71] (IHEP) | $K^\pm \rightarrow \pi^\pm \pi^+ \pi^-$; $N(\tau) \simeq 6 \times 10^9$ $K^\pm \rightarrow \pi^\pm \pi^0 \pi^0$; $N(\tau') \simeq 5 \times 10^8$ | $\lesssim 1.0 \times 10^{-4}$ $\lesssim 1.3 \times 10^{-4}$ | Preparation | $10^{-5} - 2 \times 10^{-6}$ [67, 68] [76] | Up to (several units) $\times 10^{-4}$ [77] |
| INF-IHEP [70] (IHEP) | $K^\pm \rightarrow \pi^\pm \pi^0 \pi^0$ | $\lesssim 10^{-3}$ | Data handling | | |
| NA48/2 [72] (CERN) | $K^\pm \rightarrow \pi^\pm \pi^+ \pi^-$; $N(\tau) \simeq 3 - 4 \times 10^9$ $K^\pm \rightarrow \pi^\pm \pi^0 \pi^0$; $N(\tau') \simeq 2 \times 10^8$ | $\lesssim 10^{-4}$ $\lesssim 10^{-4}$ | Data handling | | |
| Hyper CP [73] (Fermilab) | $K^\pm \rightarrow \pi^\pm \pi^+ \pi^-$; $N(\tau^+) = 1.1 \times 10^8$ $N(\tau^-) = 0.5 \times 10^8$ | $\lesssim 7 \times 10^{-4}$ | Data handling | | |
| KLOE [74] (DAΦNE) | $K^\pm \rightarrow \pi^\pm \pi^+ \pi^-$; $N(\tau) \sim 5 \times 10^8$ $K^\pm \rightarrow \pi^\pm \pi^0 \pi^0$; $N(\tau') \sim 1.5 \times 10^8$ | $\lesssim 3 \times 10^{-4}$ | Preparation | | |

Note. Since the experiment NA48/2 (CERN) [72] started earlier than it was possible with the OKA detector, the decision was made that it is reasonable to consider performing experimental studies of charge asymmetry with the OKA detector only if NA48/2 would observe unexpected results.

The charge asymmetry of the decays $K^+ \rightarrow f^+$ and $K^- \rightarrow f^-$ can be shown to be characterized by the quantity

$$\Delta = \frac{|A_f|^2 - |\bar{A}_f|^2}{|A_f|^2 + |\bar{A}_f|^2} = \frac{2 \operatorname{Im}(a^* b) \sin(\delta_a - \delta_b)}{|a|^2 + |b|^2 + 2 \operatorname{Re}(a^* b) \cos(\delta_a - \delta_b)}$$

$$= \frac{2|a||b| \sin(\varphi_b - \varphi_a) \sin(\delta_a - \delta_b)}{|a|^2 + |b|^2 + 2|a||b| \cos(\varphi_a - \varphi_b) \cos(\delta_a - \delta_b)}. \quad (78)$$

The charge asymmetry in the decays $K^+ \rightarrow f$ and $K^- \rightarrow \bar{f}$, which depends on processes of direct CP-violation, will be manifested only when there are at least two different amplitudes a and b in the final state with different ‘weak phases’ φ_a and φ_b , respectively, and strong scattering phases δ_a and δ_b in the final state ($\varphi_a \neq \varphi_b$, $\delta_a \neq \delta_b$).

This assertion is, naturally, of a general character and concerns any decays $P \rightarrow f$ and $\bar{P} \rightarrow \bar{f}$. The quantity $|A_f|^2$ may characterize the decay width or the differential distribution of final states in the Dalitz plot.

Let us consider, for instance, the decays $K^\pm(P_K) \rightarrow \pi^\pm(q_1)\pi^\pm(q_2)\pi^\mp(q_3)$ and $K^\pm(P_K) \rightarrow \pi^0(q_1)\pi^0(q_2)\pi^\pm(q_3)$. We denote the 4-momentum of the nonsymmetric pion by q_3 (π^\mp for $K^\pm \rightarrow \pi^\pm \pi^\pm \pi^\mp$ or π^\pm for $K^\pm \rightarrow \pi^0 \pi^0 \pi^\pm$).

The distribution of $K^+ \rightarrow 3\pi$ -events in the Dalitz plot is described as

$$|A(K \rightarrow 3\pi)|^2 \propto 1 + gX + hX^2 + jY + kY^2. \quad (79)$$

Here, the notation was introduced as follows:

$$X = \frac{S_3 - S_0}{M_\pi^2}, \quad Y = \frac{S_1 - S_2}{M_\pi^2},$$

$$S_i = (P_K - q_i)^2 = (M_K - M_{\pi_i})^2 - 2M_K T_i, \quad i = 1; 2; 3$$

($i = 3$ for the nonsymmetric pion) and $S_0 = (1/3) \sum S_i$; T_i is the respective kinetic energy (see, for example, Ref. [20]).

The most sensitive measurements of CP-violation in $K^\pm \rightarrow 3\pi$ -decays concern the slope g in the distribution over the Dalitz plot in the variable X :

$$A_g = \frac{g(K^+) - g(K^-)}{g(K^+) + g(K^-)} = \frac{\delta g(K^+)}{2g}. \quad (80)$$

The measurement accuracy of the distribution slope g is related to the accuracy in determining the total $K^\pm \rightarrow 3\pi$ -decay width $[\Gamma(K^+ \rightarrow 3\pi)]$ by the relationship

$$\frac{\delta g}{2g} = R \frac{\delta \Gamma}{2\Gamma} = R \frac{\sqrt{1 + (1/K)}}{2\sqrt{n(K^+)}}. \quad (81)$$

For the $K^\pm \rightarrow \pi^\pm \pi^+ \pi^-$ -decay (τ -decay) one has $R_\tau = 7.56$ [69], and for the $K^\pm \rightarrow \pi^\pm \pi^0 \pi^0$ -decay (τ' -decay) $R_{\tau'} = 3.0$ [70] (the parameter R depends on the slope g of the spectrum). Here, $n(K^+)$ and $n(K^-)$ are the respective numbers of registered events of $K^+ \rightarrow 3\pi$ - and $K^- \rightarrow 3\pi$ -decays, while $K = n(K^-)/n(K^+)$. The optimum relationship between $n(K^-)$ and $n(K^+)$ (i.e., the optimum measurement accuracy for a given time) depends on the ratio of the K^- and K^+ beam intensities, $r = I(K^-)/I(K^+)$, and is given by the expression $K = \sqrt{r}$.

Table 5 collates the statistics and planned accuracy of CP-asymmetry measurements in the $K^\pm \rightarrow 3\pi$ - and $K^+ \rightarrow \pi^+ \pi^0 \gamma$ -decays in experiments using the OKA detector in the IHEP separated kaon beam, and in other experiments [71–74]. It is compared with theoretical expectations for asymmetry within the SM and beyond it.

As is seen from this table, the limit on the accuracy of the measurement of the difference between the slope parameters for the decays $K^\pm \rightarrow 3\pi$ amounts to $\delta \Gamma/2\Gamma = 1.4 \times 10^{-5}$ and $\delta g/2g \simeq 1.0 \times 10^{-4}$. In spite of the introduction of the factor R , the quantity $\delta g/2g$ turns out to be more sensitive to CP-violation in $K \rightarrow 3\pi$ -decays than $\delta \Gamma/2\Gamma$, since the effect of CP-violation is significantly weakened when the total widths are measured (which corresponds to integration over the entire Dalitz plot). The issue of systematic uncertainties in the measurement of asymmetry parameters is very important and complicated and requires careful experimental investigation. It may be noted that if the quantity $\delta \Gamma/2\Gamma$ is measured simultaneously for the decay $K^\pm \rightarrow \pi^\pm \pi^0$, where the expected statistical accuracy is no worse than in measurements for $K^\pm \rightarrow 3\pi$ -decays, this will permit (to a certain extent) controlling the possible systematic uncertainties in the measurement of charge asymmetry for kaon decays. The point is that expected asymmetry of the decay $K^\pm \rightarrow \pi^\pm \pi^0$ is very small ($\delta \Gamma/2\Gamma < 10^{-9}$ [75]). This is also evident for

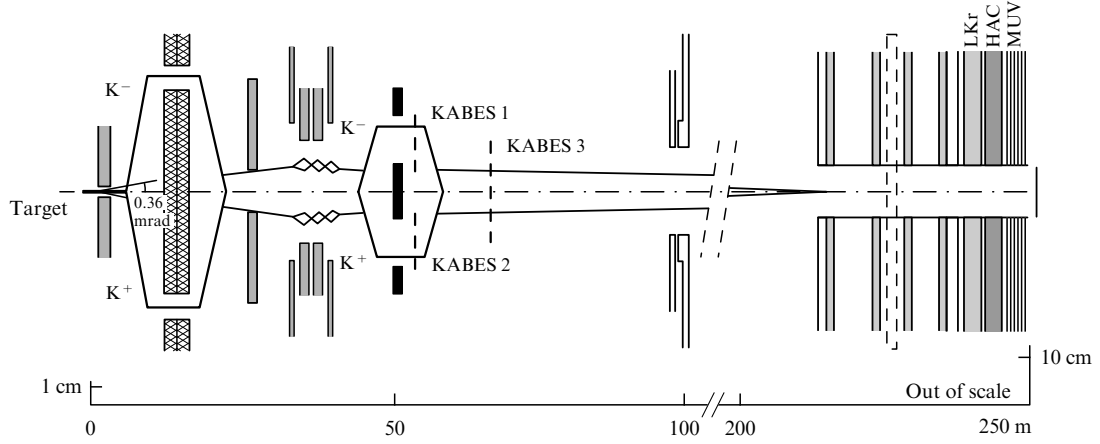


Figure 10. Layout of the setup for merging K^+ - and K^- -beams and the NA48/2 experiment. Nonseparated K^+ - and K^- -beams are produced in the interaction of the primary SPS proton beam with the beryllium target. Two beams of secondary particles with momentum 60 GeV/c are formed symmetrically (they are split in the vertical plane), are ‘tagged’ in relevant beams, pass through a beam spectrometer with the KABES track detectors that are capable of operating in beams of very high intensity, then are merged into a single beam with K^+ - and K^- -components in front of the decay volume of the setup. The ratio $n(K^+)/n(K^-)$ in the merged beam is 1.8. The length of the decay volume is ~ 114 m. Merging of the K^+ - and K^- -beams is performed with an accuracy of ~ 1 mm. The NA48/2 detector used for registering the decays $K^\pm \rightarrow \pi^\pm \pi^+ \pi^-$ and $K^\pm \rightarrow \pi^\mp \pi^0 \pi^0$ includes the magnetic spectrometer with drift chambers, the electromagnetic liquid-krypton calorimeter LKr, the hadron calorimeter HAC, and the muon detector MUV.

general reasons. Because of the CPT-invariance, the total decay widths of K^+ - and K^- -mesons should be identical. Therefore, in the case of the $K^\pm \rightarrow \pi^\pm \pi^0$ -decays, exhibiting large branching fractions [$\text{BR}(K^\pm \rightarrow \pi^\pm \pi^0) = 0.2$], the charge asymmetry should decrease (compared to the case of relatively rare decays). This holds true to an even greater extent for the main decay $K^\pm \rightarrow \mu^\pm \nu_\mu (\bar{\nu}_\mu)$, which can also be used for implementing monitoring.

Let us briefly dwell upon theoretical predictions for effects of direct CP-violation in $K^\pm \rightarrow 3\pi$ -decays. Predictions by the Standard Model for charge asymmetry $\delta g/2g$ in decays are presented in Table 5 and are much lower than the reach of modern experiments (see Refs [67, 68]). Among these works, however, a special place is occupied by Ref. [76], in which a possible strong enhancement of charge asymmetry is predicted due to the contribution from higher-order approximations of chiral perturbation theory. The value of this enhancement $F > 10^2$ results in an increase in the charge asymmetry in the slopes of the distributions in the Dalitz plot for $K \rightarrow 3\pi$ -decays up to $\delta g/2g \sim (3-6) \times 10^{-4}$. But in other works (see Refs [67, 68]) it was shown that, although asymmetry enhancement due to higher-order ChPT approximations is, in principle, possible, it should not be so significant ($F < 10$) and cannot lead to $\delta g/2g > 10^{-5}$.

After establishing the large value of $\text{Re}(\epsilon'/\epsilon)$, particular attention was paid to the mechanisms of direct CP-violation beyond the Standard Model. The charge asymmetry effects in $K \rightarrow 3\pi$ -decays were considered in the case of spontaneous CP-violation in the model with several Higgs doublets [77]. It turned out that the possible charge asymmetry in the distribution slopes g may greatly exceed the predictions of the Standard Model and reach the level $O(10^{-4})$, when there exist several independent sources of CP-violation.

In view of this situation it became clear that, in spite of the pessimistic predictions by the Standard Model, thorough measurements of the charge asymmetry in $K^\pm \rightarrow 3\pi$ -decays with as high an experimental accuracy as possible ($\sim 10^{-4}$) are required. This is also related to the possible manifestation of new CP-violation mechanisms and to the

difficulties of ChPT calculations, especially of higher orders.

The most thorough and sensitive experimental investigation of CP-asymmetry in $K \rightarrow 3\pi$ -decays was performed at CERN by the NA48/2 Collaboration. The general layout of the NA48/2 experimental setup, including the systems of merged K^+ - and K^- -beams, is shown in Fig. 10. A distinctive feature of this experiment consists in the simultaneous formation of the K^+ - and K^- -meson beams by the proton beam in two channels (K^+ and K^-) and their subsequent merging before the decay volume of the setup into a sole mixed beam of ‘tagged’ K^+ - and K^- -mesons. The measurement of CP-asymmetry in this beam allows us to significantly reduce systematics related to a possible ‘drift’ of the equipment in time and to create identical background conditions for the measurements of kaons with different charges.

The preliminary results of CP-asymmetry measurements in the NA48/2 experiment have already been published [78]. The asymmetry amounts to

$$\delta g = (-0.2 \pm 1.0_{(\text{stat})} \pm 0.9_{(\text{trig})} \pm 0.9_{(\text{syst})}) \times 10^{-4}$$

or

$$\begin{aligned} A_g = \frac{\delta g}{2g} &= (0.5 \pm 2.4_{(\text{stat})} \pm 2.1_{(\text{trig})} \pm 2.1_{(\text{syst})}) \times 10^{-4} \\ &= (0.5 \pm 3.8) \times 10^{-4}. \end{aligned} \quad (82)$$

This result exceeds other measurements of A_g [79] in accuracy by more than an order of magnitude. The measurement accuracy is also expected to be significantly enhanced in the final analysis:

(a) total statistics will be increased by more than a factor of 2;

(b) systematics will be essentially reduced (first and foremost, systematics related to the trigger);

(c) data on the $K^\pm \rightarrow \pi^\pm \pi^0 \pi^0$ -decay will be used.

All the above would allow improving the accuracy to 1×10^{-4} .

4.2 Searches for T-odd correlations in the decays

$K^+ \rightarrow \pi^0 \mu^+ \nu_\mu$ and $K^+ \rightarrow \mu^+ \nu_\mu \gamma$ involving measurement of the transverse muon polarization $P_{\mu\perp}$

Searches for T-odd transverse polarization in the decays $K^+ \rightarrow \pi^0 \mu^+ \nu_\mu$ ($K_{\mu 3}^+$) and $K^+ \rightarrow \mu^+ \nu_\mu \gamma$ ($K_{\mu 2\gamma}^+$) allow us to carry out searches for T-odd effects (or, under the assumption of CPT-invariance, for the CP-violating effects) beyond the SM framework (the expected effect is very small in the SM). The T-odd character of the transverse polarization of muons in the decays considered becomes evident if one takes into account that this polarization, being normal to the decay plane, is determined by the three-dimensional correlation:

$$\langle \sigma_\mu \rangle_\perp = \frac{\boldsymbol{\sigma}_\mu \cdot (\mathbf{p}_\pi \times \mathbf{p}_\mu)}{|\boldsymbol{\sigma}_\mu| \cdot |\mathbf{p}_\pi \times \mathbf{p}_\mu|}, \quad (83)$$

which changes sign under time reversal (here, $\boldsymbol{\sigma}_\mu$ and \mathbf{p}_μ are the muon spin and momentum, respectively, and \mathbf{p}_π is the pion momentum for the $K_{\mu 3}^+$ -decay). The three-particle correlation for the decay $K^+ \rightarrow \mu^+ \nu_\mu \gamma$ takes the form

$$\langle \sigma_\mu \rangle_\perp = \frac{\boldsymbol{\sigma}_\mu \cdot (\mathbf{p}_\gamma \times \mathbf{p}_\mu)}{|\mathbf{p}_\pi \times \mathbf{p}_\mu|}. \quad (84)$$

The transverse polarization of muons in $K_{\mu 3}$ -decays can be represented in the SM as

$$P_{\mu\perp}(K_{\mu 3}) = \langle \sigma_\mu \rangle_\perp \simeq 0.2 \operatorname{Im} \xi = 0.2 \operatorname{Im} \frac{f_-(q^2)}{f_+(q^2)},$$

where 0.2 is a kinematic factor related to the averaging of data for the $K_{\mu 3}$ -decay over the Dalitz plot for this process. In the SM, T-violation effects are very small and a certain transverse muon polarization may be related to the final-state interaction (FSI) of particles and is in no way related to T(CP)-violation. Straightforward calculations demonstrate that in the case of $K_{\mu 3}^+$ -decays this effect is also very small: $P_{\mu\perp}(K_{\mu 3})^{\text{SM}} \simeq P_{\mu\perp}(K_{\mu 3})^{\text{FSI}} \sim 4 \times 10^{-6}$ (see Refs [80, 81]).

Notice that for $K_{\mu 3}^0$ -decays the FSI background amounts to $\sim 10^{-3}$, i.e., the $K_{\mu 3}^+$ -decay is much more appropriate for searches for subtle nonstandard T-odd effects. Such effects may be related to manifestations of anomalous scalar or tensor interactions in $K_{\mu 3}^+$ -decays.

Let us consider the possible role, due to the exchange of the charged Higgs boson [86], of scalar interactions in the matrix element of this decay. In this case, instead of $m_\mu \xi(q^2)$, the matrix element A (46) contains the quantity

$$m_\mu \left(\xi(q^2) + \frac{2M_K}{m_\mu} F_S \right) \simeq m_\mu (\xi + g_S),$$

where

$$g_S = \frac{2M_K}{m_\mu} F_S.$$

Then, one finds

$$\begin{aligned} P_{\mu\perp}(K_{\mu 3}) &= \langle \sigma_\mu \rangle_\perp \simeq 0.2 \operatorname{Im} g_S \\ &= 0.2 \frac{2M_K}{m_\mu} \operatorname{Im} F_S \simeq 1.9 \operatorname{Im} F_S. \end{aligned} \quad (85)$$

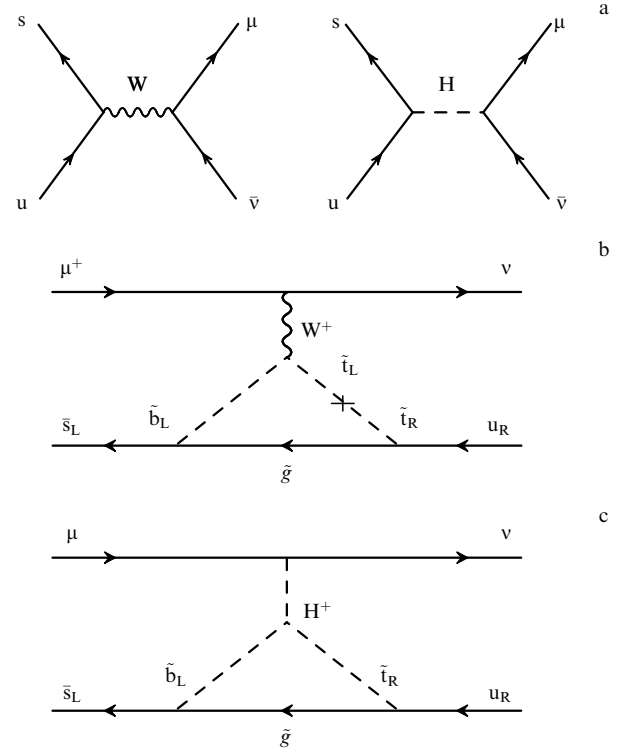


Figure 11. Mechanisms for nonstandard violation of T-invariance in $K_{\mu 3}^+$ - and $K_{\mu 2\gamma}^+$ -decays (see Ref. [89]): (a) diagrams for the $K_{\mu 3}^+$ -decay in the model with three doublets of Higgs bosons. Interference between the diagrams with exchange of the W-boson and exchange of the Higgs H-boson leads to the relation $P_{\mu\perp}(K_{\mu 3}^+) \sim 2P_{\mu\perp}(K_{\mu 2\gamma}^+)$ [86]; (b) SUSY model with quark mixing and exchange of the W^+ -boson: in this model $P_{\mu\perp}(K_{\mu 3}^+) \sim 0.2P_{\mu\perp}(K_{\mu 2\gamma}^+) \neq 0$ [84], and (c) SUSY model with exchange of the Higgs H^+ -boson: in this mechanism $P_{\mu\perp}(K_{\mu 3}^+) \sim 2P_{\mu\perp}(K_{\mu 2\gamma}^+)$ [84].

As noted above, T-odd correlations may also be observed in the radiative decay $K^+ \rightarrow \mu^+ \nu_\mu \gamma$ ($K_{\mu 2\gamma}^+$) [see formula (84)]. Nonstandard T-odd effects in this decay may also be due to new anomalous interactions beyond the SM. However, the effects of interaction between particles in the final state are stronger in the case of the $K_{\mu 2\gamma}^+$ -decay: $P_{\mu\perp}(K_{\mu 2\gamma}^+)^{\text{FSI}} = \langle \sigma_\mu \rangle_\perp^{\text{FSI}} < 10^{-3}$ [83]. Therefore, this background must be taken into account in very sensitive measurements of the transverse muon polarization in the $K_{\mu 2\gamma}^+$ -decay.

In Refs [84–86], various nonstandard mechanisms of T-invariance violation were considered, which may lead to the values of the transverse muon polarization up to 10^{-3} , both in $K_{\mu 3}^+$ - and $K_{\mu 2\gamma}^+$ -decays. Some of these mechanisms are illustrated by the diagrams in Fig. 11. Different mechanisms may lead to different relationships between $P_{\mu\perp}(K_{\mu 3}^+)$ and $P_{\mu\perp}(K_{\mu 2\gamma}^+)$. Therefore, it is likely that the more sensitive measurement of transverse muon polarization in both decays (of $K_{\mu 3}^+$ and of $K_{\mu 2\gamma}^+$), if found, will provide additional information on the nature of nonstandard T-violation.

At present, experiments are under way at KEK (E246 Collaboration [87, 88]) in search of T-odd transverse muon polarization in decays $K^+ \rightarrow \pi^0 \mu^+ \nu_\mu$ (83) and $K^+ \rightarrow \mu^+ \nu_\mu \gamma$ (84). The following preliminary results have been obtained in these experiments:

$$\begin{aligned} P_{\mu\perp}(K_{\mu 3}^+) &= (-1.12 \pm 2.17_{\text{(stat)}} \pm 0.90_{\text{(syst)}}) \times 10^{-3}, \\ \operatorname{Im} g_S &= (-0.28 \pm 0.69_{\text{(stat)}} \pm 0.30_{\text{(syst)}}) \times 10^{-3}. \end{aligned} \quad (86)$$

It is expected that a sensitivity will be achieved in $P_{\mu\perp}(K_{\mu 3}^+) \sim 1.5 \times 10^{-3}$ ($\text{Im } g_5 \sim 0.6 \times 10^{-2}$) after completing the data processing. In the case of the $K_{\mu 2\gamma}^+$ -decay, the expected sensitivity will amount to $P_{\mu\perp}(K_{\mu 2\gamma}^+) \sim 0.01$. An improved experiment on searches for transverse muon polarization in $K_{\mu 3}^+$ - and $K_{\mu 2\gamma}^+$ -decays has been proposed for the J-PARC accelerator [89, 90]. The sensitivity of this new experiment is expected to reach the level of $P_{\mu\perp} \sim 10^{-4}$ for both decays.

4.3 Searches for T-odd correlations

in the decay $K^+ \rightarrow \pi^0 \mu^+ \nu_\mu \gamma$

Another kaonic process, in which searches for T-odd triple correlations are possible, is represented by the decay

$$K^+ \rightarrow \pi^0 l^+ \nu_l \gamma, \quad (87)$$

in which it is possible to observe correlations between the momenta of three particles in the final state:

$$\varepsilon = T_{\pi l \gamma} \equiv \frac{\mathbf{p}_\gamma \cdot (\mathbf{p}_\mu \times \mathbf{p}_\pi)}{|\mathbf{p}_\gamma| \cdot |\mathbf{p}_\mu \times \mathbf{p}_\pi|}, \quad (88)$$

or, given another normalization, measuring the quantity

$$\varepsilon = T'_{\pi l \gamma} \equiv \frac{\mathbf{p}_\gamma \cdot (\mathbf{p}_\mu \times \mathbf{p}_\pi)}{M_K^3}. \quad (89)$$

The quantity $T'_{\pi l \gamma}$ may turn out to be more useful in such studies, since it contains information on the momenta of the particles in the final state.

The manifestation of nonstandard T-odd mechanisms in processes of the type (87) can only be expected in the decay

$$K^+ \rightarrow \pi^0 \mu^+ \nu_\mu \gamma \quad (90)$$

(see Fig. 12a), since only in such processes can there exist a significant interaction between muons and Higgs bosons, resulting in nonstandard effects. Moreover, it is necessary to single out processes involving prompt photon emission (Fig. 12a). In bremsstrahlung processes, it is difficult to expect NP manifestations, since T-asymmetry in these processes can only be due to interactions in the final state. The expected value of such asymmetry is given by [91]

$$A(\varepsilon)^{\text{FSI}} = \frac{N(\varepsilon > 0) - N(\varepsilon < 0)}{N(\varepsilon > 0) + N(\varepsilon < 0)} \sim 1.1 \times 10^{-4}.$$

These data may be very useful for calibration. Similar arguments concern the decay $K^+ \rightarrow \pi^0 e^+ \nu_e \gamma$, also for which only an FSI effect exists with the expected value of $T_{\pi l \gamma}^{\text{FSI}} = -0.59 \times 10^{-4}$. The conditions for identifying the decay (90) involving prompt photon emission are usually formulated as the requirements that $E_\gamma^* > 30$ MeV, and $\vartheta_{\mu\gamma} > 30^\circ$ in the rest frame of K^+ . This condition, however, requires additional investigation.

The charge conjugate decay $K^- \rightarrow \pi^0 \mu^- \bar{\nu}_\mu \gamma$ was first observed in the ISTRA+ experiment [92]. Here, all the events registered were separated into two kinematical regions:

(a) $5 < E_\gamma^* < 30$ MeV. The invariant mass spectrum for the $\pi^0 \mu^- \bar{\nu}_\mu \gamma$ system is shown in Fig. 12b. The $K_{\mu 3\gamma}^-$ -decay is clearly identified in this kinematic region. The value obtained

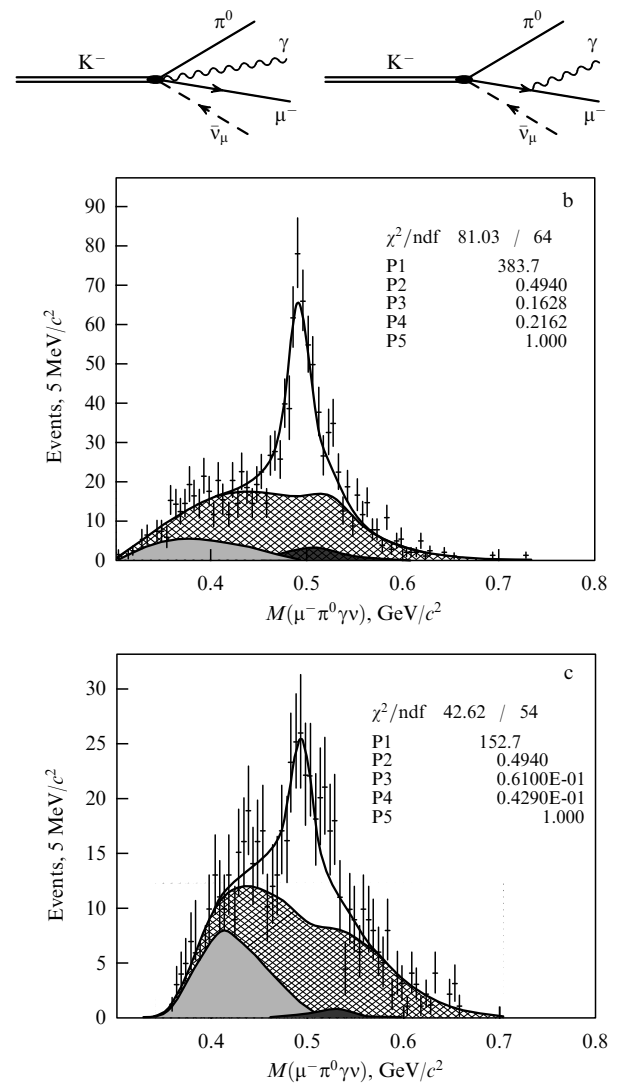


Figure 12. First data on the decay $K^- \rightarrow \pi^0 \mu^- \bar{\nu}_\mu \gamma$ ($K_{\mu 3\gamma}^-$) [92]: (a) diagrams for prompt γ emission and for bremsstrahlung; (b) invariant mass spectrum for the $\pi^0 \mu^- \bar{\nu}_\mu \gamma$ system in the region of $5 < E_\gamma^* < 30$ MeV. The peak from the $K_{\mu 3\gamma}^-$ -decay is clearly singled out in this region, and (c) invariant mass spectrum for the $\pi^0 \mu^- \bar{\nu}_\mu \gamma$ system in the region of $30 < E_\gamma^* < 60$ MeV. The decay ($K_{\mu 3\gamma}^-$) is also observed in this region, even though the background increases here. The parameters P1–P3 in the figures b, c correspond to the integral, to the average, and to the width (σ) of the Gaussian describing the K-meson invariant mass; the parameters P4, P5 describe the background. The χ^2 value obtained from the fit is also presented. The hatched region corresponds to the contribution of the background; the shaded (dark) region to the left (right) shows the contribution due to the $K_{\pi 3}^-$ ($K_{\mu 3}^-$)-process.

for the branching fraction is

$$\begin{aligned} & \frac{\text{BR}(K_{\mu 3\gamma}^-; 5 < E_\gamma^* < 30 \text{ MeV})}{\text{BR}(K_{\mu 3})} \\ &= (0.270 \pm 0.029_{(\text{stat})} \pm 0.026_{(\text{syst})}) \times 10^{-2}, \end{aligned}$$

which is in good agreement with the theoretical prediction of 0.21×10^{-2} . The angular distribution over $\vartheta_{\mu\gamma}$ has been analyzed, and the asymmetry of this distribution has been determined: $A(\cos \vartheta_{\mu\gamma}) = 0.093 \pm 0.141$ (the theoretically predicted value amounts to 0.354);

(b) the invariant mass spectrum for the $\pi^0\mu^-\bar{\nu}_\mu\gamma$ system in the kinematical region of $30 < E_\gamma^* < 60$ MeV is shown in Fig. 12c. The peak of the $K_{\mu 3\gamma}^-$ -decay is also clearly seen here, in spite of the background increasing. The value determined for the branching fraction is

$$\frac{\text{BR}(K_{\mu 3\gamma}^-; 30 < E_\gamma^* < 60 \text{ MeV})}{\text{BR}(K_{\mu 3}^-)} = (0.0448 \pm 0.0068 \pm 0.0099) \times 10^{-2}$$

(the theoretically predicted value of this ratio amounts to 0.0467×10^{-2});

(c) the T-odd asymmetry $T_{\pi\gamma} = -0.03 \pm 0.13$ was determined over the entire region where the decay $K^- \rightarrow \pi^0\mu^-\bar{\nu}_\mu\gamma$ was observed. The theoretical value for possible nonstandard T-asymmetry (beyond the SM framework) amounts to 2.6×10^{-4} [93].

The background observed in the $K_{\mu 3\gamma}^-$ -channel (Figs 12b and 12c) was analyzed and it was shown to be dominated by the $K_{\mu 3}^-$ -decays involving an additional fake photon, by events with a fake ‘ π^0 -peak’, and by $K_{\pi 3}^-$ -decays (with one of the pions decaying in flight, $\pi \rightarrow \mu\nu$, and with a fake photon).

For further investigation of the $K^+ \rightarrow \pi^0\mu^+\nu_\mu\gamma$ -decay with the OKA detector it is necessary to formulate more accurately the criteria for identifying decays with prompt photon emission, to carefully study the background conditions expected for the new detector with a good guard system, and to elaborate the criteria for maximum suppression of all background sources, and then, upon collecting the maximum possible amount of statistics of $K_{\mu 3\gamma}^+$ -events with prompt photon emission, to estimate the possible asymmetry $T'_{\pi\mu\gamma}$ of the nonstandard T-odd process.

Coincidentally with decay (90), the decay $K^- \rightarrow \pi^0e^-\bar{\nu}_e\gamma$ was also studied with the ISTRA+ detector. The number of registered events of this decay was 1382, and the following branching fractions were determined:

$$R_1 = \frac{\text{BR}(K^- \rightarrow \pi^0e^-\bar{\nu}_e\gamma; E_\gamma^* > 10 \text{ MeV})}{\text{BR}(K^- \rightarrow \pi^0e^-\bar{\nu}_e)} = (1.53 \pm 0.03) \times 10^{-2},$$

$$R_2 = \frac{\text{BR}(K^- \rightarrow \pi^0e^-\bar{\nu}_e\gamma; E_\gamma^* > 30 \text{ MeV}; \vartheta_{e\gamma} > 20^\circ)}{\text{BR}(K^- \rightarrow \pi^0e^-\bar{\nu}_e)} = (0.62 \pm 0.03) \times 10^{-2}.$$

The results of the measurements are in good agreement with theoretical predictions.

To conclude this section, it must be noted that the sensitivity of experiments with the OKA detector is insufficient to search for the effect of nonstandard CP-asymmetry $T'_{\pi\mu\gamma}$, predicted in the model with Higgs processes: $T'_{\pi\mu\gamma} \simeq 3 \times 10^{-4}$, let alone to reach the natural limit due to interaction in the final state with $T_{\pi\gamma}^{\text{FSI}} = 0.6 - 1.0 \times 10^{-4}$. In our opinion, however, it is necessary in experiments with the OKA detector to go through all the complicated details related to background suppression, to identify the region of prompt photon emission, and so forth, and to obtain the best possible results in our conditions. First of all, this may open the road for future experiments with enhanced statistics. Earlier, we had planned to carry out such experiments with the CKM detector, in parallel with the main program for studying the decay $K^+ \rightarrow \pi^+\nu\bar{\nu}$. Since the closure of CKM, our hopes are now connected with the possibility of creating a

new CERN–IHEP–Fermilab Collaboration for performing a similar experiment at CERN.

Second, investigation of possible effects with $T'_{\pi\mu\gamma}$ is applicable to a broad class of models with NP. In such models, the manifestation of nonstandard effects of CP-violation are also possible in $K^+ \rightarrow \pi^0e^+\nu_e\gamma$ -processes, where the statistics is larger than in the case of $K^+ \rightarrow \pi^0\mu^+\nu_\mu\gamma$ -decays.

5. Searches for new light particles produced in K-meson decays

5.1 Decays of the type $K^+ \rightarrow \pi^+ + X$ and the limits on their branching fractions from the BNL E787 experiment

Decays of the type $K^+ \rightarrow \pi^+ + X$, where X represents an invisible, relatively light particle, have been discussed in various models for a long time. The decays $K^+ \rightarrow \pi^+ + X$ can be experimentally identified by studying the momentum spectrum of the observed π^+ -meson (i.e., by singling out a monochromatic line in this spectrum). It is also possible that in the $K^+ \rightarrow \pi^+ + X$ -decay a pair of invisible particles is escaped. Such processes could even fake the decay $K^+ \rightarrow \pi^+\nu\bar{\nu}$. Thus, in models involving additional dimensions the $K \rightarrow \pi + G$ -decays were considered in which gravitons (G) were emitted in a space with additional dimensions, leading to a loss of energy and momentum in the space. However, estimation of such a process results in values of $\text{BR} < 10^{-12} - 10^{-13}$, i.e., it is practically unobservable [94]. Most likely, the probability of decays with escaping pair of very light supersymmetric particles (photinos, goldstinos) is very small [95].

From the BNL E787 experiment, in which the $K^+ \rightarrow \pi^+\nu\bar{\nu}$ -decay was discovered and which is characterized by a very effective guard system, limits have been set on the probability $\text{BR}(K^+ \rightarrow \pi^+ + X)$ as a function of the mass $M(X^0)$ (Fig. 13). Here, X^0 is a hypothetical invisible stable weakly interacting particle. For the particle X^0 with a very

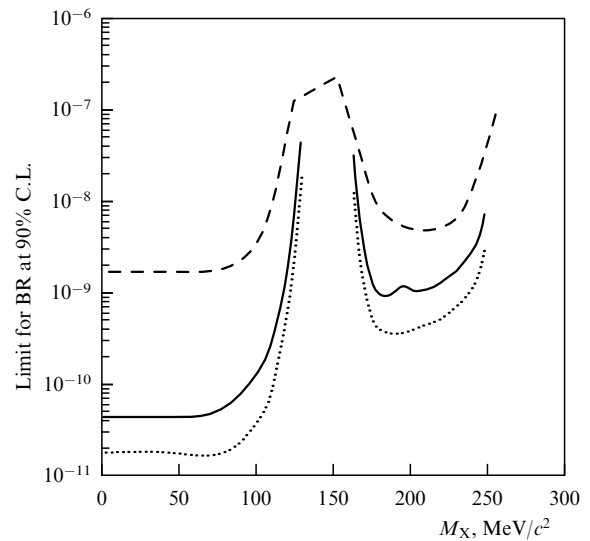


Figure 13. Limits on the branching fraction $\text{BR}(K^+ \rightarrow \pi^+ X)$, obtained in the experiment E787 [96]. The solid line corresponds to the result of Ref. [96], and the dashed line — to the previous E787 result [98]. The dotted line shows the measurement sensitivity corresponding to a single observed event.

small mass [96], the branching fraction is

$$\text{BR}(K^+ \rightarrow \pi^+ + X) < 5.9 \times 10^{-11} \text{ (90\% C.L.)}. \quad (91)$$

Such particles were discussed, for instance, in the model involving familons [97, 98], in which $K^+ \rightarrow \pi^+ f$, and f is a neutral weakly interacting invisible particle. In the case of effective familon interaction, limit (91) results in the following lower limit obtained for the familon interaction coupling constant:

$$G_{\text{fam}} \lesssim \frac{1}{7.6 \times 10^{11} \text{ GeV}}.$$

5.2 Searches for light pseudoscalar sgoldstinos in K-decays with the ISTRA+ detector

In models with spontaneous supersymmetry breaking, there exist pseudoscalar (P) and scalar (S) sgoldstinos as superpartners of the goldstino (fermion). In some versions of the theory (see Ref. [99]) one or both of these weakly interacting bosons turn out to be quite light and can be observed in K-decays. If the sgoldstino conserves parity in interactions with quarks (as, for example, in right-left symmetric MSSM expansion) and the P-sgoldstino is lighter than the S-sgoldstino, then for $M_S > (M_K - M_\pi)$ and $M_P < (M_K - 2M_\pi)$ the P-sgoldstino may be observed in $K \rightarrow \pi\pi P$ -decays, while the S-sgoldstino is absolutely unobservable in K-decays. If $M_S < (M_K - M_\pi)$, then strong constraints on the $K \rightarrow \pi S$ -decay probabilities can be obtained from the data presented in Fig. 13.

The phenomenology of models with light sgoldstinos was elaborated in detail in Ref. [100]. The following Lagrangian describing the interaction between pseudoscalar P-sgoldstinos and quarks at low energies was introduced under the assumption that the interaction of sgoldstinos with quarks and gluons changes quark flavors, but conserves parity:

$$L = -P(h_{ij}^D \bar{d}_i \gamma^5 d_j + h_{ij}^U \bar{u}_i \gamma^5 u_j), \quad (92)$$

where $d_i = (d; s; b)$, and $u_i = (u; c; t)$.

The coupling constants h_{ij} in formula (92) have the form

$$h_{ij}^D = \frac{(\tilde{m}_{D,ij}^{\text{LR}})^2}{\sqrt{2}F} \quad \text{and} \quad h_{ij}^U = \frac{(\tilde{m}_{U,ij}^{\text{LR}})^2}{\sqrt{2}F} \quad (93)$$

(they are proportional to the soft right-left symmetry-violating terms in the mass matrix for squarks). The energy scale of supersymmetry breaking is denoted by \sqrt{F} . In the case of sgoldstino-quark interaction changing quark flavor, the limit on the coupling constants can be obtained from data on the $K_L^0 - K_S^0$ mass difference and on the CP-violation parameter ε_K in the system of neutral kaons:

$$|h_{12}^D| < 7 \times 10^{-8}, \quad |\text{Re } h_{12}^D \text{Im } h_{12}^D| < 1.5 \times 10^{-17} \quad (94)$$

(these limits are given at the 90% C.L.).

There exist two mutually complementary ways of searching for pseudoscalar P-sgoldstinos in rare kaon decays — looking for them in the decays of both charged and neutral kaons. On the one hand, the sensitivity of these searches depends on the values and phases of the coupling constants

(93). As was shown in Ref. [100], if $\text{Im } h_{12}^D \sim \text{Re } h_{12}^D$, then limits (94) lead to the limit on the decay branching fraction: $\text{BR}(K_L^0 \rightarrow \pi^0 \pi^0 P) < 10^{-3}$ (90% C.L.). Now, if $\text{Im } h_{12}^D \sim 0$, then it is just impossible to obtain a limit on the branching fraction, while if $\text{Re } h_{12}^D \sim 0$, then the decay $K_L^0 \rightarrow \pi^0 \pi^0 P$ is suppressed by the factor ε_K^2 and its probability will be confined as follows: $\text{BR}(K_L \rightarrow \pi^0 \pi^0 P) < 10^{-6}$.

On the other hand, the decays of charged K-mesons involving the emission of P-sgoldstinos are suppressed by ~ 3 orders of magnitude compared to the decays of K_L^0 -mesons, owing to isospin nonconservation. The limits from data on ε_K and $\Delta M = M(K_L^0) - M(K_S^0)$ lead to the decay probability

$$\text{BR}(K^\pm \rightarrow \pi^\pm \pi^0 P) < 1.5 \times 10^{-6} - 4 \times 10^{-4},$$

where the weaker limit corresponds to a purely imaginary or a purely real value of h_{12}^D . Thus, the general picture of the decays of charged and neutral kaons involving the emission of P-sgoldstinos is characterized by the ratio

$$R = \frac{\text{BR}(K_L^0 \rightarrow \pi^0 \pi^0 P)}{\text{BR}(K^\pm \rightarrow \pi^\pm \pi^0 P)},$$

which in different scenarios for the coupling constants may vary between $\sim 10^{-2}$ and $\sim 10^3$. Therefore, independent searches for P-sgoldstinos in the decays of neutral and charged kaons are very interesting and their results will be complementary.

In experiments with the ISTRA+ detector searches were conducted for the production of P-sgoldstinos in $K^- \rightarrow \pi^- \pi^0 P$ -decays [101] (Fig. 14a). No P-sgoldstino decays were observed in these studies, and quite tight limits were imposed on their branching fractions, presented in Fig. 14b. To obtain these limits, the entire kinematic region of possible P-sgoldstino masses, produced in K-decays, was divided into bins 10 MeV wide, and searches for the decay $K^- \rightarrow \pi^- \pi^0 P$ were performed independently in each bin. The event selection suppressed background processes due to the decays $K^- \rightarrow \pi^- \pi^0$, $K^- \rightarrow \pi^- \pi^0 \pi^0$, and $K^- \rightarrow \pi^0 l^- \bar{\nu}_l$. As can be seen from Fig. 14b, upper limits in the experiment were obtained on $\text{BR}(K^- \rightarrow \pi^- \pi^0 P)$ (with 90% confidence) in the region of invariant masses covering $0 < M_P < 200$ MeV at a level of $\sim 9 \times 10^{-6}$ (with the exception of the region near M_{π^0} , where the limit is weakened to the level of 3.5×10^{-5}). The ISTRA+ results are compared in Figs 14b and 14c with the limits on the same decay obtained in the E787 experiment [102], and also with certain indirect estimates made from data on the coupling constant h_{12}^D . Thus, it is seen from Fig. 14c that the straightforward ISTRA+ measurements provide significantly higher sensitivity than estimates from $\Delta M = M(K_L^0) - M(K_S^0)$. However, such an improvement does not happen in all scenarios involving the coupling constants.

We hope that in future experiments with the OKA detector, which has a very good guard system, it will be possible to enhance significantly the sensitivity of searches for $K^+ \rightarrow \pi^+ \pi^0 P$ -processes. At the same time, as already noted above, it is very interesting to search for production of P-sgoldstinos in the $K_L^0 \rightarrow \pi^0 \pi^0 P$ -decays in neutral kaon beams. Based on our proposal, such searches have been included in the program of studies with the KOPIO detector [103]. Such independent studies with the detector with a very good guard system will permit us to investigate the decay

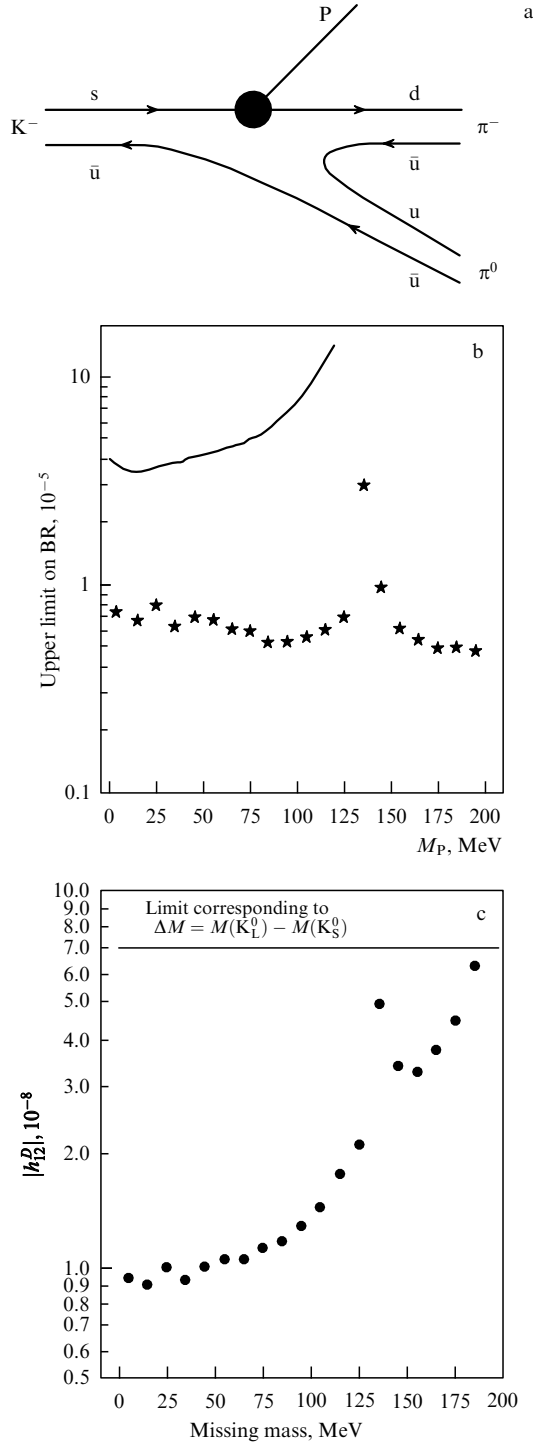


Figure 14. Searches for the P-sgoldstino: (a) diagram of the decay $K^- \rightarrow P\pi^-\pi^0$ involving emission of the P-sgoldstino; (b) upper limits on $\text{BR}(K^- \rightarrow P\pi^-\pi^0)$ versus the P-sgoldstino mass. The asterisks mark the results of the ISTRA+ experiment [101], the solid line represents the result of measurements with the E787 detector [102], and (c) limits on $|h_{12}^D|$, obtained in Ref. [101] and compared to the predictions for $|h_{12}^D|$, based on the mass difference $\Delta M = M(K_L^0) - M(K_S^0)$.

$K_L^0 \rightarrow \pi^0\pi^0P$ with a sensitivity to the branching fraction not worse than $10^{-9} - 10^{-10}$. Therefore, it will become possible to essentially improve the information on the supersymmetry breaking parameter \sqrt{F} . At present, in the case of maximum CP-violation in the squark sector ($\text{Im } \delta_{12}^D \sim \text{Re } \delta_{12}^D$

and $\delta_{12}^D \sim 2 \times 10^{-9}$), the estimates were obtained for $\sqrt{F} > 30$ TeV [100].¹

In conclusion, we shall present some comments related to the possible $P \rightarrow 2\gamma; e^+e^-$ -decays. The two-photon decay will dominate practically throughout the whole region of allowed parameters. The sgoldstino lifetime depends on the quantity

$$g_\gamma = \frac{1}{2\sqrt{2}} \frac{M_{\gamma\gamma}}{F}$$

($M_{\gamma\gamma} = M_1 \cos^2 \theta_W + M_2 \sin^2 \theta_W$ determines the sgoldstino-photon coupling constant; here, M_i are the masses of gauge field superpartners). If this lifetime is sufficiently long, then the sgoldstino will escape the experimental setup ('invisible' sgoldstinos). As shown in Ref. [100], for $M_{\gamma\gamma} \sim 100$ GeV and $\sqrt{F} \gtrsim 1$ TeV, sgoldstinos with the mass $M_P < 10$ MeV will leave the detector. In the case of $\sqrt{F} \gtrsim 10$ TeV, the sgoldstinos will be invisible up to $M_P \sim 200$ MeV. In experiments at ISTRA+ searches were conducted for 'invisible' sgoldstinos. Apparently, the sensitivity of future experiments at KOPIO will also be the best for 'invisible' sgoldstinos, although searches for $P \rightarrow 2\gamma$ -decays inside the detector will also become possible.

6. Searches for the decay $K^+ \rightarrow \pi^+ + \gamma$

The decay

$$K^+ \rightarrow \pi^+ + \gamma, \quad (95)$$

representing a $0^+ \rightarrow 0^-$ -transition, is forbidden in ordinary theory by

- (a) the conservation of angular momentum,
- (b) gauge invariance of electromagnetic interactions.

Therefore, searches for decay (95) open up possibilities of searching for new physics phenomena in certain exotic theories, in which there may occur violation of Lorentz invariance [104], nonlocal effects related to superstrings [105], the introduction of a certain new vector field [106], or noncommutative models in which the photon no longer behaves like a $U(1)$ gauge boson [107]. In noncommutative theory, certain estimates are even derived for the probability of the anomalous decay $K^+ \rightarrow \pi^+ + \gamma$:

$$\text{BR}(K^+ \rightarrow \pi^+ + \gamma) \simeq 1.0 \times 10^{-5} \frac{(1 \text{ GeV})^4}{\Lambda_{\text{NC}}^4}, \quad (96)$$

where Λ_{NC} represents the energy scale for manifestation of the noncommutativity effects. In the case of $\Lambda_{\text{NC}} \simeq 0.10; 0.25; 0.50$, and 1.0 TeV, the probability $\text{BR}(K^+ \rightarrow \pi^+ + \gamma) \simeq 1.0 \times 10^{-13}; 2.6 \times 10^{-15}; 1.6 \times 10^{-16}$, and 1.0×10^{-17} , respectively.

Different estimates have been obtained for Λ_{NC} :

$\Lambda_{\text{NC}} > 68$ GeV (from neutrino data);

$\Lambda_{\text{NC}} > 118$ GeV (from the upper limit for the branching fraction $\text{BR}(Z \rightarrow \gamma\gamma) < 5.2 \times 10^{-5}$).

According to formula (96), the corresponding branching fraction of decay (95) is given by

$$\text{BR}(K^+ \rightarrow \pi^+ + \gamma) < 5 \times 10^{-13} - 5 \times 10^{-14}.$$

¹ As we have learned from discussions at the KAON-2005 Workshop, Evanston, USA, June 2005, searches for neutral kaon decays involving the emission of P-sgoldstinos will be conducted in the near future during the analysis of data from the KTeV and KEK 391A experiments (V F Obraztsov, private communication).

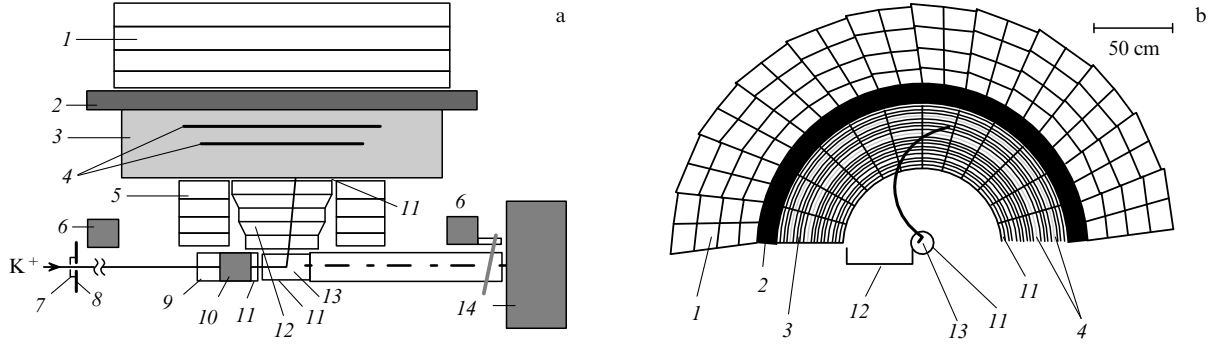


Figure 15. BNL E949 experimental setup: (a) lateral view, and (b) downstream view. This detector is an updated version of the BNL E787 detector and differs from it by an improved guard and trigger systems, as well as the data acquisition system. Shown in the figure are the upper halves of the detector: K^+ is the separated kaon beam; 1 — barrel guard system composed of multisection calorimeters and scintillation counters interspersed with lead; 2, 6 — additional detectors of the guard system; 3 — scintillation counters of the range stack; 4 — drift tubes; 5 — endcap guard system of CsI spectrometers; 7 — Cherenkov counter for identification of K^+ -mesons; 8 — upstream veto; 9 — BeO degrader of beam kaons; 10 — active kaon moderator; 11 — scintillation counters; 12 — drift chamber of the magnetic spectrometer; 13 — active target of scintillating-fiber counters, and 14 — downstream veto. The guard system practically exhibited a 4π -geometry and effectively suppressed the background due to photons and charged particles. Measurement of the momentum and track range of the π^+ -meson in the magnetic spectrometer and the range stack and registering of the decay chain $\pi^+ \rightarrow \mu^+ \rightarrow e^+$ permitted identifying π^+ -mesons in the working range.

In Ref. [107] it is stressed that relationship (96) was obtained in a static limit and that accounting for dynamic effects may lead to an essential increase in

$$BR(K^+ \rightarrow \pi^+ + \gamma).$$

No estimates for this branching fraction have been made in other models [104–106]. Since no reliable theoretical estimates of $BR(K^+ \rightarrow \pi^+ + \gamma)$ exist, the task of experiments consists in searching for decay (95) with the maximum possible sensitivity (considering $\sim 10^{-12}$ a tentative value of the possible branching fraction).

The sensitivity of experimental searches for decay (95) has been improving continually starting from 1969. The limit obtained in the most recent experiment with the E787 detector [108] is $BR(K^+ \rightarrow \pi^+ + \gamma) < 3.6 \times 10^{-7}$ (90% C.L.). It turned out possible to enhance significantly the sensitivity of searches for decay (95) with the upgraded E949 detector, at which studies of the decay $K^+ \rightarrow \pi^+ \nu \bar{\nu}$ and of other rare kaon decays were continued. For the most part, this is due to modernization of the data acquisition system and of the trigger system of the modified detector. It has now turned out possible to make use of the unprescaled trigger for searches for decay (95) without preliminary prescaling.

The BNL experimental E949 setup is presented in Fig. 15. Events corresponding to decay (95) were identified as two-prong decays of stopping kaons with the π^+ -meson exhibiting a momentum of 227 MeV/c, and the photon escaping in the opposite direction with an energy $E_\gamma = 227$ MeV. Here, no signals were to be present in the calorimeters 1, 2 (i.e., suppression of the background by a good guard system was required). Events of decay (95) were not found, and a new upper limit was established [109]:

$$BR(K^+ \rightarrow \pi^+ + \gamma) < 2.3 \times 10^{-9} \text{ (90\% C.L.)}. \quad (97)$$

New experiments with enhanced sensitivity to the corresponding searches for decay (95) are extremely desirable.

7. Experiments with ‘tagged’ π^0 -mesons produced in K-decays

Besides straightforward studies of rare K-decays, of significant interest are investigations of a number of subtle properties of π^0 -mesons, which can be singled out much more cleanly in the decays of K-mesons than in hadron interactions resulting in the production of π^0 -mesons. This is the so-called method of ‘tagged’ π^0 -mesons. We shall illustrate its peculiarities and possibilities, taking advantage of the two following examples.

7.1 Studies of the $\pi^0 \rightarrow e^+e^-$ -decays in the KTeV experiment using $K_L^0 \rightarrow 3\pi^0$ -decays

The first accurate data on the $\pi^0 \rightarrow e^+e^-$ -decay, which were based on high statistics and permitted verifying that the decay width exceeded the unitary lower limit, were obtained in Ref. [110] with the KTeV detector in studies of the $K_L^0 \rightarrow 3\pi^0$ -decays. The layout of the experimental KTeV setup is shown in Fig. 16a.

For identifying $\pi^0 \rightarrow e^+e^-$ -events, K_L^0 -decay events were selected with e^+, e^- and four γ -showers. The spectrum of invariant masses $M(e^+e^-)$, taken in these experiments, is presented in Fig. 16b, from which it is seen that the peak corresponding to the $\pi^0 \rightarrow e^+e^-$ -decay is very well singled out. After subtraction of the background, 253.6 ± 16.6 events remained in the peak. The branching fraction

$$BR\left(\pi^0 \rightarrow e^+e^-, \left(\frac{M(e^+e^-)}{M_{\pi^0}}\right)^2 > 0.95\right) = (6.09 \pm 0.40 \pm 0.24) \times 10^{-8}$$

was determined (taking into account radiative corrections). Extrapolation of this result to the branching fraction in the lowest-order approximation without radiation in the final state yielded the quantity

$$\frac{\Gamma_{e^+e^-}(\text{lowest order})}{\Gamma_{\text{tot}}} = (7.04 \pm 0.46 \pm 0.28) \times 10^{-8}$$

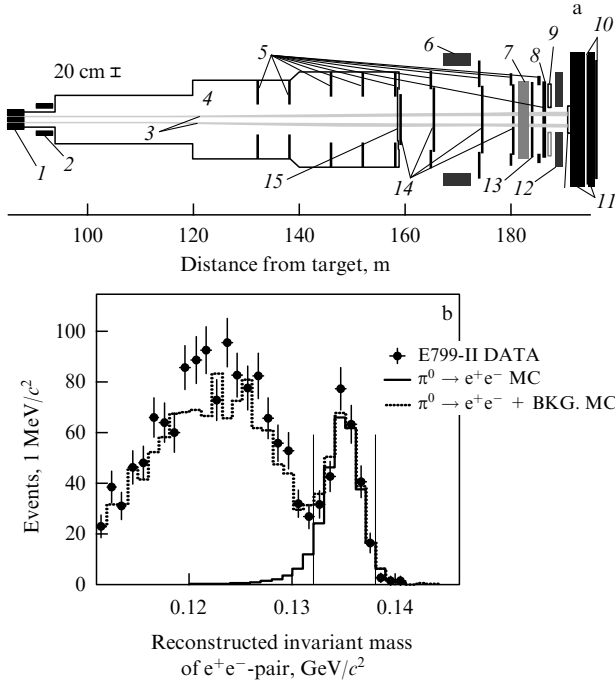


Figure 16. (a) Layout of the KTeV experimental setup: 1 — collimator; 2 — deflecting magnet; 3 — two beams of K_L -mesons; 4 — decay volume; 5 — guard system counters; 6 — magnet of the spectrometer; 7 — counters of transition radiation for registering electrons; 8 — electromagnetic calorimeter with CsI counters; 9 — guard systems eliminating hadron background; 10 — hodoscopic magnetic detector; 11 — muon filter; 12 — downstream anticoincidence counter; 13 — muon hodoscopes; 14 — drift chambers, and 15 — output window of high-vacuum region. (b) $M(e^+e^-)$ spectrum in decays $K_L^0 \rightarrow 3\pi^0 \rightarrow e^+e^- +$ (four photon showers). Also shown are the results of the MC simulations of the background and signal of the decay $\pi^0 \rightarrow e^+e^-$. The vertical dotted lines indicate the signal region $0.132 < M(e^+e^-) < 0.138$ GeV.

(this quantity is more convenient for comparison with theoretical models). It exceeds the unitary lower limit by more than four standard deviations.

All the remaining data for the $\pi^0 \rightarrow e^+e^-$ -decay, obtained either in hadron processes with charge exchange or in kaon experiments with low statistics (see Ref. [20]), are characterized by a large dispersion of branching fraction values and large uncertainties.

In the KTeV experiment, the decay $\pi^0 \rightarrow e^+e^- \gamma$, which served to determine the π^0 -meson form factor and to carry out normalization, was also investigated. To this end, K_L^0 -decay events with e^+, e^- and five γ -showers were selected. The data on the slope of the form factor are consistent with the predictions of the vector dominance model. General discussion of the form factors of neutral mesons in the decays $M \rightarrow l^+l^- \gamma$ and $M \rightarrow M' l^+l^-$ can be found in Ref. [111].

7.2 The upper limit on $BR(\pi^0 \rightarrow \nu\bar{\nu})$ from the BNL E949 experiment from an analysis of ‘tagged’ pions in the decay $K^+ \rightarrow \pi^+\pi^0$

We shall first of all consider all possible theoretical estimates for the probability $BR(\pi^0 \rightarrow \nu\bar{\nu})$. This decay is forbidden by conservation of the angular momentum for massless neutrinos with left helicity and antineutrinos with right helicity. When neutrino oscillations were discovered, it became evident that the neutrino masses differ from zero. Then, the

decay $\pi^0 \rightarrow \nu\bar{\nu}$ can occur, in principle, but strong chiral suppression of its probability will take place. If a neutrino is related to the Z^0 -bosons by standard weak interaction, then it follows that [112]

$$BR(\pi^0 \rightarrow \nu\bar{\nu}) = 6.3 \times 10^{-8} \left(\frac{m_\nu}{M_{\pi^0}} \right)^2 \sqrt{1 - 4 \left(\frac{m_\nu}{M_{\pi^0}} \right)^2} \quad (\text{for each type of neutrino}). \quad (98)$$

From the very weak experimental constraint on $m(\nu_\tau) < 18.2$ MeV [20] and from Eqn (98) we have

$$BR(\pi^0 \rightarrow \nu\bar{\nu}) < 1.1 \times 10^{-9}. \quad (99)$$

Cosmological estimate yields $m_\nu < 0.23$ eV [20] and the limit on the decay probability into all three types of ν becomes very small:

$$BR(\pi^0 \rightarrow \nu\bar{\nu}) < 2.9 \times 10^{-18} \times 6.3 \times 10^{-8} = 1.8 \times 10^{-25}. \quad (100)$$

The very strong chiral suppression of the $\pi^0 \rightarrow \nu\bar{\nu}$ -decays in the SM with small neutrino masses opens up certain new possibilities for this decay due to anomalous interactions beyond the SM, which remove the chiral suppression. Such is anomalous pseudoscalar interaction. In Ref. [113], the influence of the pseudoscalar (and of the tensor and scalar) interactions on the $BR(\pi^0 \rightarrow \nu\bar{\nu})$ was studied. Here, the upper limits on these anomalous interaction constants were obtained assuming these interactions to be responsible for the neutrino masses. The $\pi\nu\bar{\nu}$ -interaction Lagrangian with the anomalous pseudoscalar term has the form

$$\mathcal{L}_{\pi\nu\bar{\nu}} = -\frac{G_F}{\sqrt{2}} \frac{F_\pi M_\pi^2}{m_u + m_d} (a_{PS,II'}^{uu} - a_{PS,II'}^{dd}) \pi^0 \bar{\nu}_1 \gamma_5 \nu_{1'}. \quad (101)$$

Here, $F_\pi = 92.4$ MeV is the π -decay constant; $m_u = m_d = (m_u + m_d)/2 = 4$ MeV [20], and the previously obtained upper limit $< 10^{-3}$ is applied for the interaction constants $a_{PS,II'}^{qq}$. Under these assumptions of the existence of nonstandard pseudoscalar interaction, the following upper limit was obtained on the branching fraction for $m_\nu < 0.23$ eV (from cosmological data):

$$BR(\pi^0 \rightarrow \nu\bar{\nu}) = 10^{-4} (a_{PS,II'}^{uu} - a_{PS,II'}^{dd})^2 < 10^{-10}. \quad (102)$$

The previously available experimental limits on the $\pi^0 \rightarrow \nu\bar{\nu}$ -decay probability corresponded to

$$BR(\pi^0 \rightarrow \nu\bar{\nu}) < 8.3 \times 10^{-7} \text{ (90\% C.L.) (BNL E787 [114])}, \quad (103)$$

$$BR(\pi^0 \rightarrow \nu_\mu \bar{\nu}_\mu) < 1.6 \times 10^{-6} \text{ (90\% C.L.) (beam-dump experiment LSND [115])}. \quad (104)$$

At present, a new improved result is available from BNL E949 [112]:

$$BR(\pi^0 \rightarrow \nu\bar{\nu}) < 2.7 \times 10^{-7} \text{ (90\% C.L.)}. \quad (105)$$

In this experiment, ‘tagging’ of the π^0 -meson in the decay $K^+ \rightarrow \pi^+\pi^0$ of stopping kaons was done when the π^+ -meson of momentum 205 MeV/c was registered. For

identification of the decay $\pi^0 \rightarrow \nu\bar{\nu}$, the decay $K^+ \rightarrow \pi^+\pi^0$ was required not to be accompanied by any other signals in the detector.

In spite of the very efficient guard system of the E949 detector, the limit achieved on the decay probability (105) was determined by the background from the lost photons in the $\pi^0 \rightarrow \gamma\gamma$ -decay. The number of background events was about 10^2 , which reduced the sensitivity of experimental searches for the $\pi^0 \rightarrow \nu\bar{\nu}$ -decay by two orders of magnitude. The reason for the residual inefficiency of the guard system was explained by fluctuations in the development of photon showers at an energy of ~ 20 MeV and by photo-nuclear reactions producing neutrons (i.e., undetected particles in the guard system).

In this connection, it is apparently interesting for future experiments with the KOPIO detector to search for $\pi^0 \rightarrow \nu\bar{\nu}$ -decays of the ‘tagged’ π^0 -mesons produced in $K_L^0 \rightarrow 3\pi^0$ -decays. The guard system of the KOPIO detector should be more efficient than the E949 one. Therefore, one can hope for a reduction of the background from lost photons and for significant enhancement of the sensitivity of searches for the $\pi^0 \rightarrow \nu\bar{\nu}$ -decay.²

7.3 Searches for decays $\pi^0 \rightarrow \mu^\pm e^\mp$ in the case of ‘tagged’ π^0 -mesons

In experiments with the BNL E865 detector, in which searches were conducted for the $K^+ \rightarrow \pi^+\mu^+e^-$ -decays with lepton flavor violation [116], an upper limit was also obtained on the decay $\pi^0 \rightarrow \mu^+e^-$ in the process $K^+ \rightarrow \pi^+\pi^0$:

$$\text{BR}(\pi^0 \rightarrow \mu^+e^-) < 3.8 \times 10^{-10} \text{ (90\% C.L.)}. \quad (106)$$

At the same time, in experiments at KTeV in studies of ‘tagged’ π^0 -mesons in decays $K_L^0 \rightarrow 3\pi$ the following upper limit was found [117]:

$$\text{BR}(\pi^0 \rightarrow \mu^\pm e^\mp) < 7.85 \times 10^{-10} \text{ (90\% C.L.)}. \quad (107)$$

This process is very well identified and therefore an increase in the body of statistics may lead to an enhancement of the sensitivity in searches for the $\pi^0 \rightarrow \mu^\pm e^\mp$ -decays.

8. Conclusion

Searches for anomalous processes in rare decays represent a necessary composite part of the program of searches for effects of the New Physics beyond the Standard Model. Although the present review is of a general character, its topic is closely related to future experiments at the IHEP superconducting separated kaon channel, to be conducted with the new OKA detector, and we hope they will be initiated by the end of 2006. In this connection, data concerning the separated kaon channel and the OKA detector are briefly summarized in Appendix 9.1.

The material of this review was reported at several sessions of the Chicago Flavor Seminar (January 17, 2003 and February 27, 2004), at Workshops of the CKM Collaboration and at a BNL seminar (March 13, 2003). I am grateful to the participants in these seminars for helpful comments. I express my gratitude to S S Bulanov, D V Vavilov, V V Kiselev, T Komatsubara, P Cooper, M V Libanov, K Mizouchi, E Ya Nugaev, V F Obraztsov, L B Okun’,

S V Troitskii, and R Tschirhart for numerous stimulating discussions and for help in my work.

During preparation of the article for publication it became known that the CKM and KOPIO projects were terminated. Nevertheless, reference to these experiments has remained in the text for historical reasons. It may turn out that similar experiments will be performed at CERN.

9. Appendices

9.1 The IHEP superconducting separated channel of K^+ -mesons and the OKA detector

The IHEP channel of separated K -mesons will operate according to the Panofsky scheme with two high-frequency separators. To separate particles in the kaon channel, use is made of the Karlsruhe–CERN high-frequency superconducting separators [118], which have been used in 1978–1980 at CERN in the separated beams for the Ω -spectrometer [119]. In accordance to a special agreement, these separators were handed over to IHEP. They underwent several full-scale tests with the cryogenic system constructed at IHEP. At present, they are being assembled as part of the channel for separated particles, the layout of which is shown in Fig. 17.

The expected parameters of the IHEP kaon channel are presented in Table 6. In Fig. 18, the possible K^+ -beam intensity versus the admissible beam contamination ($\pi^+ + p$)/ K^+ is shown.

Table 6. Properties of the IHEP channel of separated K -mesons.

| Beam parameters | Value |
|--|---|
| Target | 50-cm Be |
| Energy of primary protons | 65–70 GeV |
| Proton beam intensity | 10^{13} p cycle ⁻¹ |
| Number of cycles per hour | 4×10^2 |
| K^+ -beam momentum | 12 (or 18) GeV/ c |
| $\delta p/p$ | $\pm 4\%$ |
| Horizontal acceptance of the channel | ± 10 mrad |
| Vertical acceptance of the channel | ± 19 mrad |
| Length of the channel | ~ 200 m |
| Intensity of the K^+ -beam within the decay volume | 5×10^6 K^+ cycle ⁻¹ |
| Dumping time | 1.8 s |
| Beam contamination ($\pi^+ + p$)/ K^+ | $< 25\%$ |
| Muon halo | $< 100\%$ |
| Parameters of separators | |
| Frequency | 2865 MHz |
| Wavelength | 10.46 cm |
| Effective length of the deflector | 2.74 m |
| Number of sections in the deflector | 104 |
| Average field | 1.2 MV m ⁻¹ |
| Working temperature | 1.8 K |
| Distance l between separators | 76.3 m |

The OKA detector (Fig. 19), at which studies on the channel of separated kaons will be carried out, includes the principal elements of the SPHINX, GAMS, and ISTRAP+ experimental facilities and will be supplemented with new equipment, electronics, and a fast data acquisition system (DAQ). The OKA detector is composed of the following main elements:

(1) The K^+ -beam magnetic spectrometer: proportional chambers with ± 1 mm pitch; Cherenkov counters (threshold and RICH); six trigger scintillation hodoscopes; measurement of K^+ -meson momentum with accuracy $\delta p/p \simeq 1\%$.

² When this review was being prepared for publication, it became known that the KOPIO experiment was cancelled.

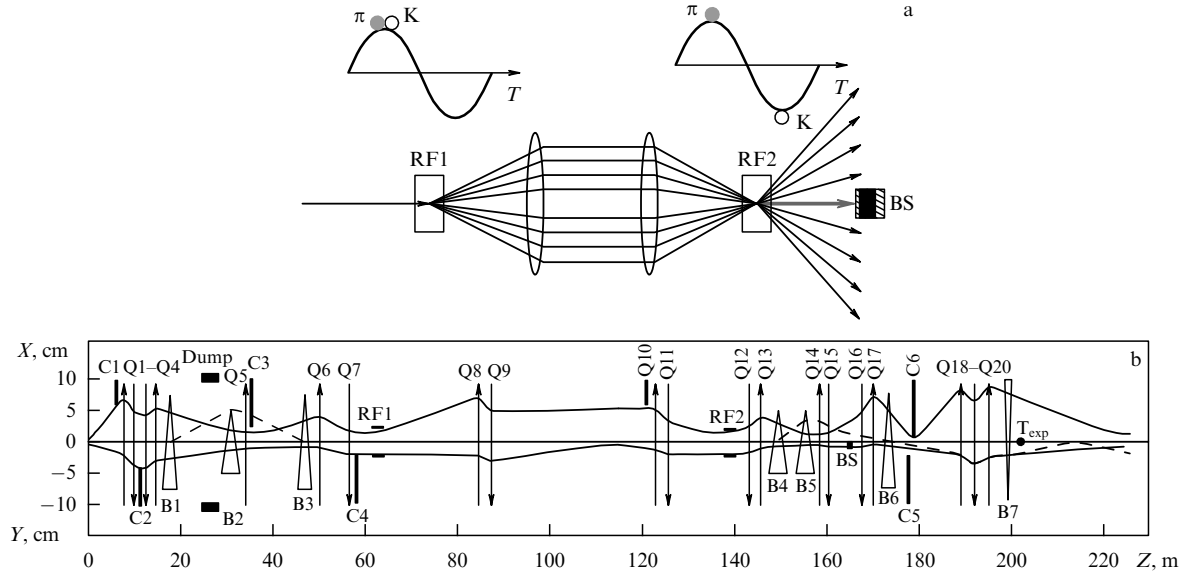


Figure 17. (a) Operation principle of high-frequency separators using the Panofsky scheme: after the second separator, the K^+ -mesons pass through a collimator, while π^+ and p are absorbed in a special absorber: RF1, RF2 — high-frequency separators; BS — beam absorber. (b) Layout of magneto-optical channel for IHEP separated K^+ -beam: C1–C6 — collimators; Q1–Q20 — quadrupole magnets; B1–B7 — dipole magnets; Dump — beam absorber; RF1, RF2 — high-frequency separators; BS — absorber, and T_{exp} — experimental target.

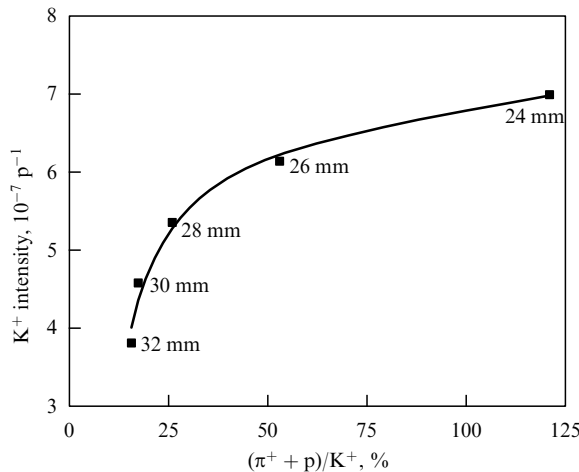


Figure 18. Dependence of the possible K^+ -meson intensity per single beam proton in separated beam versus contamination $(\pi^+ + p)/K^+$: the data points correspond to the absorber widths for which MC simulation was performed; solid curve is the result of fit.

(2) Decay volume with the guard system of length $l = 10.5$ m; 670 in number lead–scintillator sandwich $[20 \times (5 \text{ mm Sc} + 1.5 \text{ mm Pb})]$ guard counters with fiber light-collection.

(3) Magnetic spectrometer for decay particles: magnet with the field integral $\int B ds \sim 1 \text{ T m}$; aperture 200×90 cm: proportional chambers, drift tubes, hodoscopes.

(4) Cherenkov detector of secondary electrons (in the measurement section).

(5) Electromagnetic calorimeters GAMS-2000 + GAMS-EHS (~ 4000 counters of lead glass, and 100 PWO-crystals).

(6) Muon identifier: four sections of an iron/scintillator hadron calorimeter; the second part of the facility is a muon range detector of aperture 3×3 m with 20 planes of drift tubes of $\varnothing 3$ cm.

(7) Trigger system:

T_1 (K^+ -meson (Sc + C-counters)) $\rightarrow 5 \times 10^6$ triggers;

T_2 (K^+ -decay and hodoscopic logic) $\rightarrow 5 \times 10^5$ triggers;

T_3 (suppression of the process $K^+ \rightarrow \mu^+ \nu_\mu$ (threshold in EM calorimeter $\sim 1 \text{ MIP}$)) $\rightarrow 2 \times 10^5$ triggers;

T_4 (PC farm for suppression of $K^+ \rightarrow \pi^+ \pi^0$) $\rightarrow 1 \times 10^5$ triggers.

(8) DAQ $\sim 2 \times 10^5 \text{ cycle}^{-1} = 25 \text{ Mb s}^{-1}$ (5000 ADC with conversion time of 10 μs); 1000 TDC [0.8 ns (CERN HPTDC)]; 10^4 PC (10 ns shift registers).

Tables 7 and 8 collate approximate estimates for the possibilities of the experiment. The data in Table 8 correspond to an effective number of 3.1×10^{11} K^+ -decays along the decay base. These data should be considered preliminary and tentative. On the one hand, no optimization (for example, for the decay $K^+ \rightarrow \pi^+ e^+ e^-$) of the setup was performed in calculations. On the other hand, in the case of nonstandard processes it is necessary to take into account an additional loss factor related to the trigger conditions, to selection procedures for suppression of background processes, etc. The issue of different triggers is still being explored. It may turn out that for the decays involving electrons, trigger will require the use of a Cherenkov detector for identifying the

Table 7. Possibilities of the OKA experiment.

| Parameter | Value |
|---|---|
| Decay length | 10.5 m |
| Probability of kaon decay | $\sim 11\%$ |
| Measurement time | $3.5 \times 10^3 \text{ h}$ |
| Number of cycles | 1.4×10^6 |
| Number of kaon decays | $\sim 7.8 \times 10^{11}$ |
| Experimental efficiency | 0.05–0.30 |
| Sensitivity of the experiment | $2.6 \times 10^{-11} - 4 \times 10^{-12}$ |
| Loss factor due to the dead time, interruptions, etc. | 2.5 |
| Real number of K^+ -decays | 3.1×10^{11} |
| Real sensitivity | $6.5 \times 10^{-11} - 1.0 \times 10^{-11}$ |

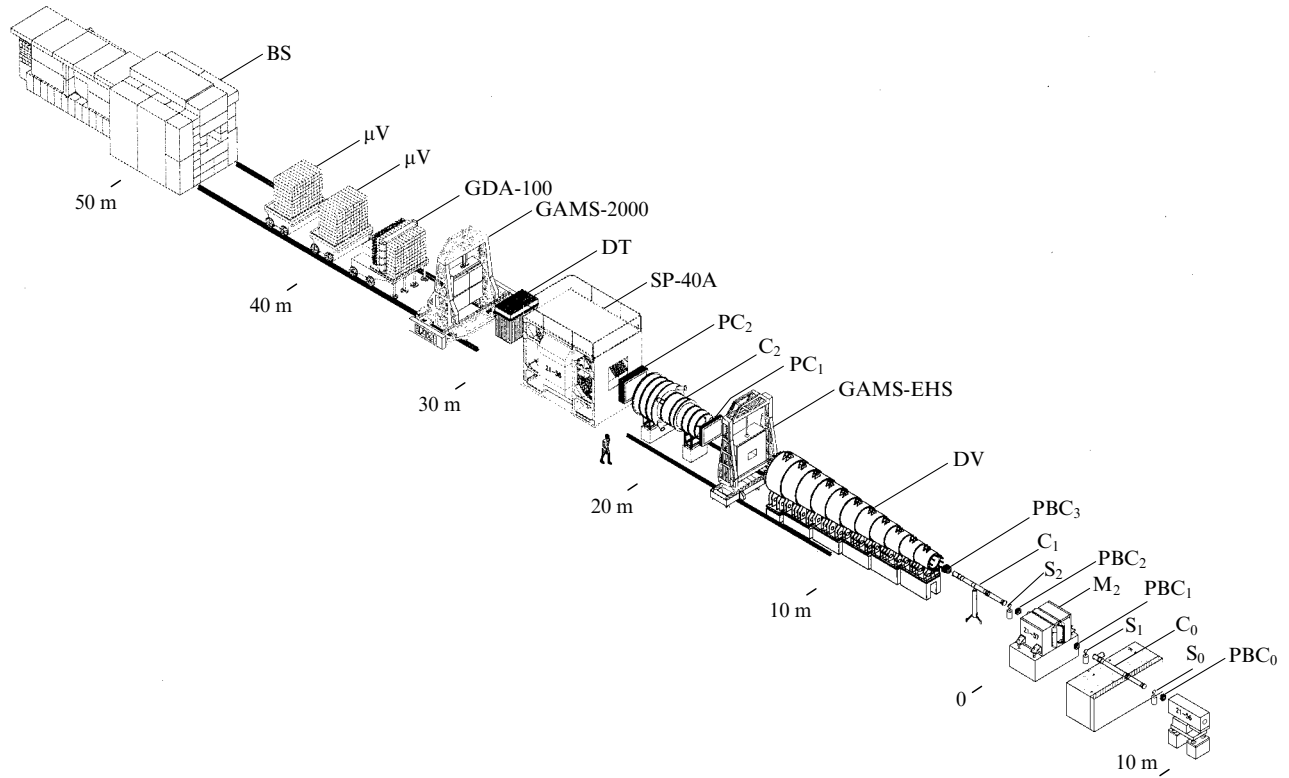


Figure 19. Layout of OKA experimental setup (see text): PBC₀–PBC₃ — beam proportional counters; S₀–S₂ — scintillation hodoscopes; C₀–C₂ — Cherenkov counters; M₂ — magnet; DV — decay volume; GAMS-EHS and GAMS-2000 — Cherenkov electromagnetic calorimeters; PC₁ and PC₂ — proportional chambers; SP-40A — magnet of the spectrometer; DT — drift tubes; GDA-100 — hadron calorimeter; μV — muon veto, and BS — beam shield.

Table 8. Expected statistics of kaon decays in experiments with the OKA detector (preliminary estimates).

| Decay | BR | Acceptance | Statistics | PDG |
|--|-----------------------|------------|----------------------|---------------------|
| $K^+ \rightarrow e^+ \nu_e$ | 1.55×10^{-5} | 0.45 | 2.2×10^6 | $\sim 10^3$ |
| $K^+ \rightarrow \pi^0 e^+ \nu_e$ | 5.1×10^{-2} | 0.18 | 2.8×10^9 | $\sim 10^6$ (*) |
| $K^+ \rightarrow \pi^0 \mu^+ \nu_\mu$ | 3.2×10^{-2} | 0.27 | 2.7×10^9 | $\sim 10^6$ (*) |
| $K^+ \rightarrow e^+ \nu_e \gamma$ | 3.8×10^{-5} | 0.30 | 3.5×10^6 | $\sim 10^2$ |
| $K^+ \rightarrow \mu^+ \nu_\mu \gamma$ | 5.5×10^{-3} | 0.40 | 6.8×10^8 | 2×10^3 |
| $K^+ \rightarrow \pi^0 e^+ \nu_e \gamma$ | 2.6×10^{-4} | 0.12 | 9.7×10^6 | ~ 6000 (*) |
| $K^+ \rightarrow \pi^0 \mu^+ \nu_\mu \gamma$ | 2×10^{-5} | 0.18 | 1.1×10^6 | ~ 550 (*) |
| $K^+ \rightarrow \pi^+ \pi^+ \pi^-$ | 5.6×10^{-2} | 0.62 | 1.1×10^{10} | 4×10^9 (*) |
| $K^+ \rightarrow \pi^+ \pi^0 \pi^0$ | 1.7×10^{-2} | 0.17 | 0.9×10^9 | 2×10^8 (*) |
| $K^+ \rightarrow \pi^+ \pi^- e^+ \nu_e$ | 3.9×10^{-5} | 0.26 | 3.1×10^6 | 4×10^5 |
| $K^+ \rightarrow \pi^0 \pi^0 e^+ \nu_e$ | 2.1×10^{-5} | 0.08 | 5.3×10^5 | 35 |
| $K^+ \rightarrow \pi^+ \pi^- \mu^+ \nu_\mu$ | 1.4×10^{-5} | 0.62 | 2.7×10^6 | 7 |
| $K^+ \rightarrow \pi^0 \pi^0 \mu^+ \nu_\mu$ | 0.7×10^{-5} | 0.16 | 3.4×10^5 | — |
| $K^+ \rightarrow \pi^+ \pi^0 \gamma$ | 2.8×10^{-4} | 0.21 | 1.8×10^7 | 10^4 |
| $K^+ \rightarrow \pi^+ \gamma \gamma$ | 1.1×10^{-6} | 0.30 | 1.0×10^5 | 31 |
| $K^+ \rightarrow \pi^+ e^+ e^-$ | 2.7×10^{-7} | 0.10 | 0.84×10^4 | $\sim 10^4$ |
| $K^+ \rightarrow \pi^+ \mu^+ \mu^-$ | 5.0×10^{-8} | 0.35 | 0.54×10^4 | 4×10^2 |

Note. In column PDG, the data given for certain channels (*) were obtained in a series of recent works.

electrons. It still remains unclear which processes from Table 8 can be studied simultaneously, and for which of them special beam runs will be required.

The main lines of studies with the OKA detector can be summarized as follows:

(1) Searches for new types of interactions beyond the Standard Model — new scalar (S), pseudoscalar (P), and tensor (T) anomalous weak interactions and other deviations from $(V - A)$ theory in leptonic and semileptonic processes. Special attention will be paid to very sensitive searches for

pseudoscalar interactions in the measurements of branching fractions $\text{BR}(K^+ \rightarrow e^+ \nu_e(\gamma)) / \text{BR}(K^+ \rightarrow \mu^+ \nu_\mu(\gamma))$.

(2) Investigation of the decays $K^+ \rightarrow \pi^0 \mu^+ \nu_\mu \gamma$ and $K^+ \rightarrow \pi^0 e^+ \nu_e \gamma$ and searches for direct CP-violation in the decays of charged kaons in CP-odd triple correlations $\mathbf{p}_\gamma(\mathbf{p}_{\pi^0} \times \mathbf{p}_{\mu^+}) / M_K^3$.

(3) Further searches for new light particles produced in K-decays (P-sgoldstinos).

(4) Studies of hadron interactions at low energies and tests of predictions due to hadron models [chiral perturba-

tive theory (ChPT), lattice QCD, dispersion sum rules, etc.]. Here, precision studies of form factors in K_{l3} - and $K_{\pi^+l^+\pi^-}$ -decays will be continued and new data for $K^+ \rightarrow \pi^+\pi^0\gamma$, $K^+ \rightarrow \pi^+\gamma\gamma$, and other decay processes will also be obtained.

(5) Investigation of the radiative decay $\pi^+ \rightarrow e^+\nu_e\gamma$ (searches for possible anomalous tensor interaction).

(6) Studies in hadron spectroscopy and searches for new hadrons, exploration of rare radiative hadron decays and of Coulomb processes in the $K^\pm N$ - and $\pi^\pm N$ -interactions.

This program was discussed in Refs [55, 71, 120]. The first run with the OKA detector will start in November 2006.

9.2 Recent works

During preparation of this article for publication some new works appeared that are related to the $K \rightarrow \pi\nu\bar{\nu}$ -decays. To complete the overall picture, these new data are reflected in this Appendix.

(1) In Ref. [121], more accurate perturbative QCD calculations have been performed taking into account the NNLO-approximation (Next-Next-to-Leading Order) for estimation of the influence of c-quarks (see Section 3.2). The input parameters employed in the calculations of Ref. [121] differ somewhat from the data of Table 3 and those of Section 3.2. We here present the values of these parameters and the main results obtained in Ref. [121]:

$$\begin{aligned} m_c(m_c) &= 1.30 \pm 0.05 \text{ GeV}, \\ \alpha_s(M_Z) &= 0.1187 \pm 0.0020 \text{ (the strong coupling constant)}, \\ \text{Im } \lambda_t &= (1.407_{-0.098}^{+0.096}) \times 10^{-4}, \\ \text{Re } \lambda_t &= (-3.13_{-0.017}^{+0.020}) \times 10^{-4}, \\ \text{Re } \lambda_c &= (-0.22006_{-0.00091}^{+0.00093}). \end{aligned} \quad (\text{A.1})$$

Additionally, the branching fractions used for normalization of the $K \rightarrow \pi\nu\bar{\nu}$ -decays are considered equal to the old value

$$\text{BR}(K^+ \rightarrow \pi^0 e^+ \nu_e) = (4.93 \pm 0.07) \times 10^{-2},$$

which is, most likely, somewhat too low. In Section 3.2, the new value for this branching fraction was used:

$$\text{BR}(K^+ \rightarrow \pi^0 e^+ \nu_e) = (5.14 \pm 0.06) \times 10^{-2}.$$

The calculations of Ref. [121] resulted in the following new values:

$$\begin{aligned} m_t(m_t) &= 163.0 \pm 2.8 \text{ GeV}, \\ X(x_t) &= 1.464 \pm 0.041. \end{aligned} \quad (\text{A.2})$$

The parameter $P_c(\nu\bar{\nu})$ accounting for the influence of c-quarks in the decay $K^+ \rightarrow \pi^+\nu\bar{\nu}$ has been determined:

(a) the corrected value of $P_c(\nu\bar{\nu})$ in the NLO-approximation (Next-to-Leading Order):

$$\begin{aligned} P_c(\nu\bar{\nu}) &= 0.367 \pm 0.037_{\text{theory}} \pm 0.033_{m_c} \pm 0.009_{\alpha_s} \\ &= (0.37 \pm 0.06) \left(\frac{0.2248}{\lambda} \right)^4, \end{aligned} \quad (\text{A.3})$$

(b) the new value of $P_c(\nu\bar{\nu})$ in the NNLO-approximation:

$$\begin{aligned} P_c(\nu\bar{\nu}) &= 0.371 \pm 0.009_{\text{theory}} \pm 0.031_{m_c} \pm 0.009_{\alpha_s} \\ &= (0.37 \pm 0.04) \left(\frac{0.2248}{\lambda} \right)^4. \end{aligned} \quad (\text{A.4})$$

Taking advantage of the relation for $\text{BR}(K^+ \rightarrow \pi^+\nu\bar{\nu})_{\text{SM}}$, namely

$$\begin{aligned} \text{BR}(K^+ \rightarrow \pi^+\nu\bar{\nu})_{\text{SM}} &= K_+ \left[\frac{X(x_t)}{\lambda} \right]^2 \\ &\times \left\{ \left[\text{Re } \lambda_c \frac{(P_c(\nu\bar{\nu}) + \delta P)\lambda^4}{X(x_t)} + \text{Re } \lambda_t \right]^2 + (\text{Im } \lambda_t)^2 \right\}, \end{aligned} \quad (\text{A.5})$$

(accounting for the correction δP for the large distance effects [56]) from Ref. [121] it is possible to find that

$$\begin{aligned} \text{BR}(K^+ \rightarrow \pi^+\nu\bar{\nu})_{\text{SM}} &= (7.93 \pm 0.77_{P_c} \pm 0.84_{\text{other}}) \times 10^{-11} \\ &= (7.9 \pm 1.3) \times 10^{-11} \text{ (NLO)}, \end{aligned} \quad (\text{A.6})$$

$$\begin{aligned} \text{BR}(K^+ \rightarrow \pi^+\nu\bar{\nu})_{\text{SM}} &= (7.96 \pm 0.49_{P_c} \pm 0.84_{\text{other}}) \times 10^{-11} \\ &= (8.0 \pm 1.1) \times 10^{-11} \text{ (NNLO)}. \end{aligned}$$

If $\text{BR}(K^+ \rightarrow \pi^0 e^+ \nu_e) = (5.14 \pm 0.06) \times 10^{-2}$ is used for normalization, then from formula (A.6) it is possible to obtain

$$\begin{aligned} \text{BR}(K^+ \rightarrow \pi^+\nu\bar{\nu})_{\text{SM}} &= (0.82 \pm 0.14) \times 10^{-10} \text{ (NLO)}, \\ \text{BR}(K^+ \rightarrow \pi^+\nu\bar{\nu})_{\text{SM}} &= (0.83 \pm 0.11) \times 10^{-10} \text{ (NNLO)}. \end{aligned} \quad (\text{A.7})$$

These data are to be compared with the results of Ref. [121].

Thus, the precision of NNLO theoretical calculations for $P_c(\nu\bar{\nu})$ and $\text{BR}(K^+ \rightarrow \pi^+\nu\bar{\nu})_{\text{SM}}$ is several times higher than the precision of the NLO-approximation. At present, the uncertainty in these quantities are determined by the uncertainties in m_c and in the parameters of the CKM-matrix of quark mixing.

(2) In the experiment KLOE [122], new data have been obtained on the lifetime $\tau(K_L^0) = (50.84 \pm 0.23) \text{ ns}$, as well as the values

$$f_+^{K^0} |V_{us}| = \begin{cases} 0.21638 \pm 0.00067 \text{ (from } K_{e3}), \\ 0.21732 \pm 0.00087 \text{ (from } K_{\mu 3}), \\ 0.21673 \pm 0.00053 \text{ (averaged value)}. \end{cases} \quad (\text{A.8})$$

Hence, and from the data on $f_+^{K^0} = 0.961 \pm 0.008$, the matrix element of the CKM-matrix has been determined:

$$|V_{us}| = 0.2257 \pm 0.0022. \quad (\text{A.9})$$

References

1. Fukuda S et al. (Super-Kamiokande Collab.) *Phys. Rev. Lett.* **86** 5651 (2001); Ahmad Q R et al. (SNO Collab.) *Phys. Rev. Lett.* **87** 071301 (2001); **89** 011302 (2002); Davis R (Jr.) (Homestake Collab.) *Rev. Mod. Phys.* **75** 985 (2003)
2. Fukuda Y et al. (Super-Kamiokande Collab.) *Phys. Rev. Lett.* **81** 1562 (1998); **82** 2644 (1999); Fukuda S et al. (Super-Kamiokande Collab.) *Phys. Rev. Lett.* **85** 3999 (2000)
3. Eguchi K et al. (KamLAND Collab.) *Phys. Rev. Lett.* **90** 021802 (2003)
4. Ahn M H et al. (K2K Collab.) *Phys. Rev. Lett.* **90** 041801 (2003); hep-ex/0212007

5. Pontecorvo B M *Zh. Eksp. Teor. Fiz.* **33** 549 (1957); **34** 247 (1958) [*Sov. Phys. JETP* **6** 429 (1957); **7** 172 (1958)]
6. Alberico W M, Bilenky S M, Maieron C *AIP Conf. Proc.* **721** 350 (2004); hep-ph/0311053
7. Pontecorvo B M *Zh. Eksp. Teor. Fiz.* **53** 1717 (1967) [*Sov. Phys. JETP* **26** 984 (1968)]
8. Maki Z, Nakagawa M, Sakata S *Prog. Theor. Phys.* **28** 870 (1962)
9. Landsberg L G *Usp. Fiz. Nauk* **173** 1025 (2003) [*Phys. Usp.* **46** 995 (2003)]; *Yad. Fiz.* **69** 771 (2006) [*Phys. At. Nucl.* **69** 743 (2006)]
10. Petcov S T *Yad. Fiz.* **25** 641, 1336 (1977) [*Sov. J. Nucl. Phys.* **25** 340, 698 (1977)]
11. Bilenky S M, Pontecorvo B *Phys. Rep.* **41** 225 (1978)
12. Ambrose D et al. (BNL E871 Collab.) *Phys. Rev. Lett.* **81** 5734 (1998)
13. Corcoran M (for the KTeV Collab.), Invited talk at *Workshop on e^+e^- in the 1 GeV to 2 GeV Range: Physics and Accelerator Prospects, Alghero, Italy, Sept. 2003; eConf C0309101 THWP003* (2003); hep-ex/0402033
14. Sher A et al. (BNL E865 Collab.) *Phys. Rev. D* **72** 012005 (2005); hep-ex/0502020; Appel R et al. (BNL E865 Collab.) *Phys. Rev. Lett.* **85** 2450 (2000)
15. Appel R et al. (BNL E865 Collab.) *Phys. Rev. Lett.* **85** 2877 (2000)
16. Rajaram D et al. (HyperCP Collab.) *Phys. Rev. Lett.* **94** 181801 (2005); hep-ex/0505025
17. Brooks M L et al. (MEGA Collab.) *Phys. Rev. Lett.* **83** 1521 (1999)
18. Bellgardt U et al. (SINDRUM Collab.) *Nucl. Phys. B* **299** 1 (1988)
19. Dohmen C et al. (SINDRUM II Collab.) *Phys. Lett. B* **317** 631 (1993)
20. Eidelman S et al. (Particle Data Group) *Phys. Lett. B* **592** 1 (2004)
21. Aubert B et al. (BaBar Collab.) *Phys. Rev. Lett.* **92** 121801 (2004); hep-ex/0312027; Abe K et al. (Belle Collab.) *Phys. Rev. Lett.* **92** 171802 (2004); hep-ex/0310029
22. Okada Y *J. Korean Phys. Soc.* **45** S467 (2004); hep-ph/0402077
23. Kuno Y, Okada Y *Rev. Mod. Phys.* **73** 151 (2001); hep-ph/9909265
24. Barkov L M et al., Research Proposal to PSI R-99-05.1 (Villigen, Switzerland: Paul Scherrer Institute, 1999); <http://www.icepp.s.u-tokyo.ac.jp>; Bachman M et al., MECO Proposal to BNL (1997); <http://meco.ps.uci.edu>; Machida S et al. "A letter of intent to the J-PARC 50 GeV proton synchrotron experiments" (2003), <http://www-ps.kek.jp/jhf-np/LOIlist/pdf/L26.pdf>
25. Cahn R N, Harari H *Nucl. Phys. B* **176** 135 (1980)
26. Libanov M V, Troitsky S V *Nucl. Phys. B* **599** 319 (2001); hep-ph/0011095; Frère J-M, Libanov M V, Troitsky S V *Phys. Lett. B* **512** 169 (2001); hep-ph/0012306; *J. High Energy Phys.* (JHEP11) 025 (2001); hep-ph/0110045; Frère J-M et al. *J. High Energy Phys.* (JHEP06) 009 (2003); hep-ph/0304117; *J. High Energy Phys.* (JHEP03) 001 (2004); hep-ph/0309014
27. Landsberg L G *Yad. Fiz.* **68** 1240 (2005) [*Phys. At. Nucl.* **68** 1190 (2005)]; hep-ph/0410261
28. Okun' L B *Leptony i Kvarki* (Leptons and Quarks) 2nd ed. (Moscow: Nauka, 1990) [Translated into English (Amsterdam: North-Holland, 1984)]
29. Finkemeier M, in *The Second DAΦNE Physics Handbook* (Eds L Maiani, G Pancheri, N Paver) (Frascati: LNF, 1995) p. 389
30. Bulanov S S, Graduation thesis (Moscow: Moscow Engineering Physics Institute, State Univ., 1999)
31. Ageev E S et al. "Eksperimenty s zaryazhennymi kaonami na separirovannom kaonnom puchke uskoritelya IFVE" ("Experiments with charged kaons on the separated kaon beam of the IHEP accelerator", <http://www.oka.ihep.su/Members/zopeadmin/oka-papers/pred.ps/view> (Protvino: RF State Research Center 'Institute for High Energy Physics', 2003) p. 89
32. Steiner H J et al. *Phys. Lett. B* **36** 521 (1971)
33. Chizhov M V *Phys. Lett. B* **381** 359 (1996); hep-ph/9511287; *Mod. Phys. Lett. A* **8** 2753 (1993)
34. Yushchenko O P et al. (ISTRA+ Collab.) *Phys. Lett. B* **589** 111 (2004)
35. Yushchenko O P et al. (ISTRA+ Collab.) *Phys. Lett. B* **581** 31 (2004)
36. Yushchenko O P "Issledovanie K_S -raspadov na ustanovke ISTRA+, poisk anomal'nykh raspadov kalibrovichnykh bozonov na ustanovke DELPHI" ("Investigation of K_S -decays at the ISTRA+ detector, searches for anomalous decays of gauge bosons at the DELPHI facility"), Thesis for Doctorate of Physicomathematical Sciences (Protvino: RF State Research Center 'Institute for High Energy Physics', 2004)
37. Alexopoulos T et al. (KTeV Collab.) *Phys. Rev. Lett.* **93** 181802 (2004); hep-ex/0406001
38. Shimizu S et al. (KEK-E246 Collab.) *Phys. Lett. B* **495** 33 (2000); Horie K et al. (KEK-E246 Collab.) *Phys. Lett. B* **513** 311 (2001); hep-ex/0106006; Levchenko A S et al. (KEK-E246 Collab.) *Yad. Fiz.* **65** 2294 (2002) [*Phys. At. Nucl.* **65** 2232 (2002)]; hep-ex/0111048
39. Tesarek R J (KTeV Collab.), hep-ex/9903069; Lai A et al. (NA48 Collab.) *Phys. Lett. B* **604** 1 (2004); hep-ex/0410065
40. Bijnens J, Colangelo G, Ecker G *Ann. Phys. (New York)* **280** 100 (2000); Post P, Schilcher K *Eur. Phys. J. C* **25** 427 (2002)
41. Grossman Y *Nucl. Phys. B* **426** 355 (1994); Bélanger G, Geng C Q *Phys. Rev. D* **44** 2789 (1991)
42. Peccei R, in *Kaon Physics* (Eds J L Rosner, B D Winstein) (Chicago: Univ. of Chicago Press, 2001) p. 23
43. Kiselev V V, Likhoded A K, Obratsov V F, hep-ph/0204066
44. Ecker G, Pich A, de Rafael E *Nucl. Phys. B* **291** 692 (1987)
45. Bergström L, Singer P *Phys. Rev. Lett.* **55** 2633 (1985); *Phys. Rev. D* **43** 1568 (1991)
46. Shabalin E P *Pis'ma Zh. Eksp. Teor. Fiz.* **22** 117 (1975) [*JETP Lett.* **22** 53 (1975)]
47. D'Ambrosio G et al. *J. High Energy Phys.* (JHEP08) 004 (1998)
48. Desande A L, Ph.D. Thesis (New Haven, Conn.: Yale Univ., 1995)
49. Alliegro C et al. *Phys. Rev. Lett.* **68** 278 (1992)
50. Appel R et al. *Phys. Rev. Lett.* **83** 4482 (1999)
51. Adler S et al. *Phys. Rev. Lett.* **79** 4756 (1997)
52. Ma H et al. *Phys. Rev. Lett.* **84** 2580 (2000)
53. Dukes E C, hep-ex/0205063
54. Burkhardt H et al. *Phys. Lett. B* **512** 317 (2001); hep-ph/0011345
55. Landsberg L G *Yad. Fiz.* **64** 1811 (2001) [*Phys. At. Nucl.* **64** 1729 (2001)]
56. Cheng C-H, Geng C Q, Hu I-L *Phys. Rev. D* **67** 074029 (2003); hep-ph/0302207
57. Bolotov V N et al. (ISTRA Collab.) *Phys. Lett. B* **243** 308 (1990)
58. Počanić D (for the PIBETA Collab.) *Int. J. Mod. Phys. A* **20** 472 (2005); hep-ph/0407198
59. Poblaguev A A et al. *Phys. Rev. Lett.* **89** 061803 (2002); hep-ex/0204006
60. Gabrielli E *Phys. Lett. B* **301** 409 (1993)
61. Voloshin M B *Phys. Lett. B* **283** 120 (1992)
62. Poblaguev A A *Phys. Lett. B* **238** 108 (1990)
63. Hardy J C, Towner I S *Phys. Rev. Lett.* **94** 092502 (2005); nucl-th/0412050
64. Shanker O *Nucl. Phys. B* **206** 253 (1982)
65. Davidson S, Bailey D, Campbell B A Z. *Phys. C* **61** 613 (1994)
66. Gershtein S S, Likhoded A A, Onishchenko A I *Phys. Rep.* **320** 159 (1999)
67. D'Ambrosio G, Isidori G *Int. J. Mod. Phys. A* **13** 1 (1998)
68. Shabalin E P *Usp. Fiz. Nauk* **171** 951 (2001) [*Phys. Usp.* **44** 895 (2001)]
69. Franzini P, in *The Second DAΦNE Physics Handbook* Vol. 1 (Eds L Maiani, G Pancheri, N Paver) (Frascati: INFN, 1992) p. 15
70. Ammosov V V et al., Preprint N98-2 (Protvino: Inst. for High Energy Phys., 1998)
71. Obratsov V F, Landsberg L G *Nucl. Phys. B: Proc. Suppl.* **99** (3) 257 (2001); Landsberg L G *Yad. Fiz.* **65** 1795 (2002) [*Phys. At. Nucl.* **65** 1747 (2002)]
72. Kekelidze V D, Talk at the session of IHEP Scientific-Technical Council, 22 December, 1999; Batley R et al., Proposal to CERN-SPSC-P-253 (1999); CERN/SPSC 2000-003
73. White C G et al. (Hyper CP Collab.) *Nucl. Phys. B: Proc. Suppl.* **71** 451 (1999); Leros N et al. *Nucl. Phys. B: Proc. Suppl.* **99** (3) 211 (2001)
74. Lee-Franzini J, in *The Second DAΦNE Physics Handbook* Vol. 1 (Eds L Maiani, G Pancheri, N Paver) (Frascati: INFN, 1992) p. 761; Maiani L, Paver N, in *The Second DAΦNE Physics Handbook* Vol. 1 (Eds L Maiani, G Pancheri, N Paver) (Frascati: INFN, 1992) p. 239
75. Dib C O, Peccei R D *Phys. Lett. B* **249** 325 (1990)
76. Bel'kov A A et al. *Phys. Lett. B* **232** 118 (1989); hep-ph/0010142
77. Shabalin E P, Preprint ITEP-8-98 (Moscow: Inst. of Theoretical and Experimental Phys., 1998)

78. Makulec I (for the NA48/2 Collab.), hep-ex/0505081
79. Choong W-S, Ph.D. Thesis (Berkeley: Univ. of California, 2000); Akopdzhanov G A et al. (TNF-IHEP Collab.) *Eur. Phys. J. C* **40** 343 (2005); hep-ex/0406008
80. Zhitnitsky A R *Yad. Fiz.* **31** 1024 (1980) [*Sov. J. Nucl. Phys.* **31** 529 (1980)]
81. Efrosinin V P et al. *Phys. Lett. B* **493** 293 (2000); hep-ph/0008199
82. Peccei R D, hep-ph/9909236
83. Braguta V V, Chalov A E, Likhoded A A *Phys. Rev. D* **66** 034012 (2002); hep-ph/0205203
84. Garisto R, Kane G *Phys. Rev. D* **44** 2038 (1991); Fabbrichesi M, Vissani F *Phys. Rev. D* **55** 5334 (1997); Wu G-H, Ng J N *Phys. Lett. B* **392** 93 (1997)
85. Bélanger G, Geng C Q *Phys. Rev. D* **44** 2789 (1991)
86. Kobayashi M, Lin T-T, Okada Y *Prog. Theor. Phys.* **95** 361 (1995)
87. Abe M et al. (KEK-E246 Collab.) *Phys. Rev. Lett.* **83** 4253 (1999)
88. Abe M et al. (KEK-E246 Collab.) *Nucl. Phys. A* **721** 445 (2003); hep-ex/0211049
89. Asano Y et al., in *Letters of Intent for Nuclear and Particle Physics Experiments at the J-PARC*, J-PARC 03-6, L19; <http://www-ps.kek.jp/jhf-np/LOIlist/pdf/L19.pdf>
90. Kudenko Yu G, Khotjantsev A N *Yad. Fiz.* **63** 890 (2000) [*Phys. At. Nucl.* **63** 820 (2000)]
91. Braguta V V, Likhoded A A, Chalov A E *Phys. Rev. D* **65** 054038 (2002)
92. Tchikilev O et al. (ISTRA+ Collab.), hep-ex/0506023
93. Braguta V V, Likhoded A A, Chalov A E *Phys. Rev. D* **68** 094008 (2003)
94. Arkani-Hamed N, Dimopoulos S, Dvali G *Phys. Lett. B* **429** 263 (1998); *Phys. Rev. D* **59** 086004 (1999)
95. Ellis J, Hagelin J S, Rudaz S *Phys. Lett. B* **192** 201 (1987); Ellis J, Hagelin J S *Nucl. Phys. B* **217** 189 (1983)
96. Adler S et al. (E787 Collab.) *Phys. Lett. B* **537** 211 (2002); hep-ex/0201037
97. Wilczek F *Phys. Rev. Lett.* **49** 1549 (1982)
98. Atiya M S et al. *Phys. Rev. Lett.* **70** 2521 (1993)
99. Giudice G F, Rattazzi R *Phys. Rep.* **322** 419 (1999); Gorbunov D S, Dubovskii S L, Troitskii S V *Usp. Fiz. Nauk* **169** 705 (1999) [*Phys. Usp.* **42** 623 (1999)]; Dubovsky S L, Gorbunov D S, Troitsky S V, hep-ph/9905466
100. Gorbunov D S, Rubakov V A *Phys. Rev. D* **64** 054008 (2001); Gorbunov D S *Nucl. Phys. B* **602** 213 (2001)
101. Tchikilev O G et al. (ISTRA+ Collab.) *Phys. Lett. B* **602** 149 (2004)
102. Adler S et al. (E787 Collab.) *Phys. Rev. D* **63** 032004 (2001)
103. Comfort J R et al., KOPIO Project Conceptual Design Report, BNL (August 2005)
104. Coleman S, Glashow S L *Phys. Rev. D* **59** 116008 (1999)
105. Kane G *Phys. Today* **50** (2) 40 (1997)
106. Kane G L *Nucl. Phys. B: Proc. Suppl.* **8** 469 (1989)
107. Trampetic J *Acta Phys. Pol. B* **33** 4317 (2002); hep-ph/0212309
108. Adler S et al. (E787 Collab.) *Phys. Rev. D* **65** 052009 (2002)
109. Artamonov A V et al. (E949 Collab.) *Phys. Lett. B* **623** 192 (2005); hep-ex/0505069
110. Alavi-Harati A et al. *Phys. Rev. Lett.* **83** 922 (1999)
111. Landsberg L G *Phys. Rep.* **128** 301 (1985)
112. Artamonov A V et al. (E949 Collab.) *Phys. Rev. D* **72** 091102 (2005); hep-ex/0506028
113. Prézeau G, Kurlov A *Phys. Rev. Lett.* **95** 101802 (2005); hep-ph/0409193
114. Atiya M S et al. (BNL E787 Collab.) *Phys. Rev. Lett.* **66** 2189 (1991)
115. Auerbach L B et al. *Phys. Rev. Lett.* **92** 091801 (2004)
116. Appel R et al. *Phys. Rev. Lett.* **85** 2450 (2000)
117. Wolfe M C, KTeV Note (2000)
118. Citron A et al. *Nucl. Instrum. Meth.* **155** 93 (1978); **164** 31 (1979)
119. Lengeler H, Plane D E, Preprint CERN SPS/EBP/79-16 (Geneva, 1979)
120. Landsberg L G, Obraztsov V F, in *Proc. of the Workshop on K-Physics: KAON-99, Chicago, June 21–26, 1999* (Eds J L Rosner, B D Winstein) (Chicago: Univ. of Chicago Press, 2000) p. 589; Landsberg L G, Obraztsov V F, Vavilov D V, Talk at *BNL Workshop on Future Kaon Experiments at the AGS, May 13, 2004*
121. Buras A J et al., hep-ph/0508165
122. Ambrosino F et al. (KLOE Collab.) *Phys. Lett. B* **632** 43 (2006)